

Cite this: *Biomater. Sci.*, 2025, **13**, 93

## Engineering considerations in the design of tissue specific bioink for 3D bioprinting applications†

Shivi Tripathi,<sup>a,b</sup> Madhusmita Dash,<sup>c</sup> Ruchira Chakraborty,<sup>d</sup>  
Harri Junaedi Lukman,<sup>e</sup> Prasoon Kumar,<sup>e</sup> Shabir Hassan,<sup>f,g</sup>  
Hassan Mehboob,<sup>e</sup> Harpreet Singh<sup>h</sup> and Himansu Sekhar Nanda<sup>i</sup>

Over eight million surgical procedures are conducted annually in the United States to address organ failure or tissue losses. In response to this pressing need, recent medical advancements have significantly improved patient outcomes, primarily through innovative reconstructive surgeries utilizing tissue grafting techniques. Despite tremendous efforts, repairing damaged tissues remains a major clinical challenge for bioengineers and clinicians. 3D bioprinting is an additive manufacturing technique that holds significant promise for creating intricately detailed constructs of tissues, thereby bridging the gap between engineered and actual tissue constructs. In contrast to non-biological printing, 3D bioprinting introduces added intricacies, including considerations for material selection, cell types, growth, and differentiation factors. However, technical challenges arise, particularly concerning the delicate nature of living cells in bioink for tissue construction and limited knowledge about the cell fate processes in such a complex bio-mechanical environment. A bioink must have appropriate viscoelastic and rheological properties to mimic the native tissue microenvironment and attain desired biomechanical properties. Hence, the properties of bioink play a vital role in the success of 3D bioprinted substitutes. This review comprehensively delves into the scientific aspects of tissue-centric or tissue-specific bioinks and sheds light on the current challenges of the translation of bioinks and bioprinting.

Received 11th September 2024,  
Accepted 19th October 2024

DOI: 10.1039/d4bm01192a

rsc.li/biomaterials-science

### 1. Introduction

3D bioprinting is cutting-edge technology in tissue engineering and regenerative medicine that enables the construction of

3D tissue structures with specific shapes and patterns.<sup>1</sup> This technology can create skin, muscle, cartilage, bone, nerve tissues, *etc.* The market size for 3D bioprinting was \$2.13 billion in 2022. It is expected to grow to \$8.3 billion by 2030, with a compound annual growth rate (CAGR) of 18.51%.<sup>2</sup> The bioprinting industry witnesses a yearly increase in the number of companies, including newcomers like Bico (CELLINK) and Poietis, as well as established players like GE Healthcare, venturing into the field. The market demand is driven by the increasing need for tissue and organ transplantation due to the rise in chronic diseases, which can damage tissues and organs, reduce quality of life, and resist treatment.<sup>3</sup> While organ transplantation can effectively address organ dysfunction, the availability of suitable donor organs is a considerable constraint. For example, a new name is added to the organ transplant waiting list every 15 minutes in the United States.<sup>4</sup> However, only one-third of patients on this list receive matched organs from donors. The stagnant supply of organs, meeting only 10% of global demand, highlights the urgent need for alternatives. In response, 3D bioprinting is advancing rapidly due to the demand for personalized treatments and alternatives to animal testing. While innovations currently position bioprinted tissues for medical research and drug development applications, their clinical adoption still faces

<sup>a</sup>Biomaterials and Biomanufacturing Laboratory, Discipline of Mechanical Engineering, PDPM Indian Institute of Information Technology Design and Manufacturing, Jabalpur 482005, MP, India. E-mail: himansu@iiitdmj.ac.in

<sup>b</sup>International Centre for Sustainable and Net Zero Technologies, PDPM-Indian Institute of Information Technology Design and Manufacturing Jabalpur, Madhya Pradesh 482005, India

<sup>c</sup>School of Minerals, Metallurgical and Materials Engineering, Indian Institute of Technology Bhubaneswar, Argul, Khordha, Odisha 752050, India

<sup>d</sup>Biodesign and Medical Device Laboratory, Department of Biotechnology and Medical Engineering, National Institute of Technology, Rourkela, 769008 Odisha, India. E-mail: kumarprasoon@nitrrkl.ac.in

<sup>e</sup>Department of Engineering and Management, College of Engineering, Prince Sultan University, Riyadh 12435, Saudi Arabia

<sup>f</sup>Department of Biological Sciences, Khalifa University, Abu Dhabi, United Arab Emirates

<sup>g</sup>Biotechnology Centre (BTC), Khalifa University, Abu Dhabi, United Arab Emirates

<sup>h</sup>Dr B R Ambedkar National Institute of Technology Jalandhar, Grand Trunk Road, Barnala Amritsar Bypass Rd, Jalandhar, Punjab 14401111, India

<sup>i</sup>Terasaki Institute for Biomedical Innovation, 21100 Erwin, St Los Angeles, CA 91367, USA

† Electronic supplementary information (ESI) available. See DOI: <https://doi.org/10.1039/d4bm01192a>

issues due to bioprinter incapacibilities, bioink concerns, and ethical and legal barriers.<sup>5</sup>

Among all the challenges, addressing bioink concerns, such as mechanical properties and biocompatibility, is crucial for fabricating functional 3D constructs that mimic actual tissues. Bioink is a blend of biomaterials, biomolecules, and living cells used as the input for a bioprinter to create solid structures that closely match the specific geometry of targeted tissues or organs.<sup>6</sup> Hydrogels, commonly used as bioinks in 3D bioprinting, replicate the extracellular matrix (ECM) to support cells and create tissue-like structures.<sup>6,7</sup> For example, a blend of alginate, gelatin, and hyaluronic acid is used to create cartilage-specific bioinks that replicate the cartilage ECM and promote chondrocyte differentiation and growth, producing accurate and detailed cartilage replicas.<sup>8</sup> Similarly, bone-specific bioinks are also being produced by amalgamating collagen, hydroxyapatite, and glycosaminoglycans.<sup>9</sup> These specialized bioinks are designed to mimic the composition of bone tissue, providing a biomimetic environment that supports the growth and maturation of bone cells. These bioinks, combining collagen for support, hydroxyapatite for mineralization, and glycosaminoglycans for cell signalling, create a specialized microenvironment that enhances osteoblast activity and enables the precise printing of complex bone structures.

Despite their benefits, biomaterials used in bioinks for 3D-printed tissue constructs intended for implantation can provoke immune responses by activating the immune cells.

For example, hyaluronic acid activates cells through CD44, and when used in hydrogel form, it can induce foreign body reactions within four to eight weeks after transplantation.<sup>10</sup> In certain cases, polyethylene glycol (PEG) triggers a significant immune reaction, resulting in the production of anti-PEG IgM and IgG antibodies, as well as the formation of memory T cells.<sup>11</sup> Likewise, polyglycolic acid (PGA) can trigger inflammatory responses from xenogeneic sources.<sup>12</sup> As a result, these materials should be approached with caution when used as bioink for bioprinting tissue intended for transplantation.

Tissue-centric or tissue-specific bioinks solve this issue of immune reactions by allowing the incorporation of decellularized extracellular matrix (dECM) from specific tissues in the bioink for 3D bioprinting applications.<sup>13</sup> dECM is created by removing the cells from the ECM of the tissue or organ while preserving the native composition and architecture of the ECM.<sup>14</sup> dECMs can promote cell proliferation and differentiation while preserving the distinct biochemical and mechanical characteristics of original tissues. dECMs from diverse tissues, such as the heart, liver, and lung, are being utilized by researchers to formulate bioinks that can be used to print functional tissue structures.<sup>15</sup> These bioinks could create complex tissue designs with high accuracy and fidelity by facilitating cell proliferation and differentiation. Kim *et al.*<sup>16</sup> created a liver-derived dECM bioink to enhance the biomimicry of 3D liver tissue models. The incorporation of dECM into the bioink offers a liver-specific microenvironment for hepatocytes that enhance the function of 3D liver tissue models, with



**Shivi Tripathi**

*Ms Shivi Tripathi is currently pursuing a PhD in Mechanical Engineering at the Indian Institute of Information Technology Design and Manufacturing (IIITDM), Jabalpur, India. She received her Master of Technology in Mechanical Engineering with a specialization in advanced production systems from Samrat Ashok Technological Institute, Vidisha, Madhya Pradesh, India. Her research interests include-*

*biomaterials, additive manufacturing, controlled drug delivery and guided bone regeneration for bone healing applications.*



**Madhusmita Dash**

*Dr Madhusmita Dash received a PhD in Energy from an interdisciplinary graduate school, School of Energy Sciences and Engineering, Indian Institute of Technology (IIT) Guwahati, India. She is currently a Council of Scientific and Industrial Research (CSIR) Research Associate (RA) under CSIR-HRDG New Delhi at the School of Minerals, Metallurgical and Materials Engineering, IIT Bhubaneswar,*

*India. She is interested in interdisciplinary design innovations for energy and environment using chemical sciences and bioengineering principles. Some of the key areas of her research include the extraction of sustainable biofuels and biomaterials from lignocellulosic biomass, the use of deep eutectic solvents (DES) and other green solvents for efficient recycling of E-wastes and the design of efficient energy storage systems for a better environment. She published her articles in high-impact journals of repute, such as Chemical Engineering Journal, Biomass and Bioenergy, Renewable Energy and Sustainable Energy Reviews, Biomaterials Science, etc.*

a 4.3-times increase in albumin secretion, a 2.5-times increase in urea secretion, and a 2.0-times increase in cytochrome enzyme activity compared to the tissue models without dECM. It also showed 1.8 times better drug responsiveness than the tissue model without dECM, highlighting its potential for developing functional *in vitro* liver models for drug toxicity testing. Similarly, Chae *et al.*<sup>17</sup> employed 3D cell-printing technology to create biomimetic tendon and ligament tissue constructs using stem cells and tissue-specific bioinks. The tissue-specific bioinks enabled prolonged cell culture with high cell viability and enhanced tendon formation, leading to better alignment of cells and structure with the progress of time. Apart from tissue specific cues, the ideal bioink should offer excellent printability, mechanical stability, insolubility in cell culture media, appropriate biodegradability, non-toxicity, non-immunogenicity, and support for cellular adhesion.<sup>18</sup> Therefore, it is crucial to simultaneously consider multiple factors for the successful transition of bioinks and bioprinting from research to clinical use. For example, Jia *et al.*<sup>19</sup> developed a set of 30 alginate solutions to study the effects of fundamental material properties, density, and viscosity of alginate solutions on their printability. This investigation aimed to identify an appropriate range of alginate material properties for bioprinting applications. However, the high expense of bioinks and the time-intensive nature of printing trials have stimulated increasing interest in computational simulations within this area. In response to these challenges, the existing literature highlights various strategies to overcome current limitations in 3D bioprinting for tissue engineering, demonstrating continued efforts to advance the field. However, the reliance on generic bioinks hinders the clinical application of this technology. These generic bioinks lack tissue-specific cues, provide inadequate cell support, suffer from poor vascu-

larization, and have mismatched mechanical properties, all affecting the quality of the printed tissue.<sup>20</sup>

Therefore, this review fills this gap of underexplored challenges in the existing literature by providing recent strategies used to create robust bioinks suitable for 3D bioprinting of bone, skin, cartilage, and liver tissues. It provides an overview of additive manufacturing techniques and the different considerations for developing bioinks tailored to specific methods, along with polymer-based bioinks, essential for understanding 3D bioprinting. The article covers tissue-specific bioinks for mimicking target tissues, computational methods, machine learning for predicting bioink properties, and discusses the challenges in advancing 3D bioprinting for healthcare applications. It also provides a future outlook on these developments.<sup>6,9,14,15,19–28</sup> Fig. 1 shows the entire biofabrication process, from MRI scanning to bioink formulation to 3D bioprinting.<sup>29</sup> This process forms the core framework for all applications discussed in this review and highlights its importance in bioprinting.<sup>30</sup>

## 2. Additive manufacturing techniques for bioprinting

Additive manufacturing (AM) offers extensive customization for printing structural components for medical applications based on patient-specific data. AM has shown its potential for a number of activities like medical device prototyping, surgical planning, tissue or organ printing, and so on.<sup>31</sup> The automated production of versatile 3D human tissues and organs could simplify organ transplantation and provide the solution for pre-clinical drug and biological testing.<sup>32</sup> Various methods have been devised to create 3D models from metals, ceramics,



**Ruchira Chakraborty**

*Ms Ruchira Chakraborty is currently pursuing a PhD in Biomedical Engineering in the Department of Biotechnology and Medical Engineering at the National Institute of Technology (NIT) Rourkela, India. She received her Master of Technology in Industrial Biotechnology in 2021 from Manipal Institute of Technology, Karnataka, India. Her research interests include in vitro models, biomaterials, and additive manufacturing.*



**Harri Junaedi Lukman**

*Dr Harri Junaedi Lukman earned his Bachelor of Engineering degree from the Materials Engineering Department at the Bandung Institute of Technology, Indonesia, in 2004 with a major in polymer materials. He then pursued a higher degree at King Saud University in Saudi Arabia, where he obtained his Master of Science in Mechanical Engineering in 2013, followed by a PhD in the same field in 2021.*

*Currently, he is a post-doctoral researcher in the Structures and Materials Lab., Prince Sultan University, Saudi Arabia. Harri's research focuses on composite materials, with a particular emphasis on polymer composites, nanocomposites, and fiber-reinforced polymers. He is also deeply involved in exploring the potential of 3D printing technologies.*

polymers, *etc.* The strategies and capabilities of AM vary depending on the materials employed, cross-linking mechanisms, and material deposition processes. Every procedure upholds a specific scope of control over model design, mechanical properties, and biodegradation.<sup>33</sup> 3D bioprinting, a subtype of AM, uses biological materials such as cells, biomaterials, and growth factors to create functional 3D living tissues and organ constructs.<sup>34</sup> Commonly used 3D bioprinting methods include extrusion-based printing, vat photopolymerization, and jetting-based techniques. Jetting-based bioprinting can be categorized into various types: laser-based printing, inkjet printing, microvalve bioprinting, and electrohydrodynamic printing. The desired bioinks and the specific properties of each printing method are discussed in subsequent sections.

### 2.1 Extrusion-based bioprinting

Extrusion-based bioprinting is increasingly popular because it is accessible, cost-effective, and does not use potentially harmful energy sources like lasers, making it an affordable method for printing a variety of bioinks with high cell viability.<sup>35</sup> A key advantage of this bioprinting technique is the flexibility of bioinks, which can incorporate various hydrogels, such as collagen and ECM proteins, allowing the replication of actual tissues. Additionally, enhancing these biomaterials with

growth factors or peptides can boost cell adhesion, proliferation, and differentiation, facilitating the creation of custom-designed tissues.<sup>36</sup> For fabricating tissue constructs, it involves a dispensing head and an automated three-axis robotic system.<sup>37</sup> The syringe with a nozzle filled with bioink is deposited on a stage either by a dispensing head that moves along three axes or by moving the stage while the head remains fixed.<sup>38</sup> Inside the syringe, cells experience different velocity gradients based on their positions from the center to the edge. The highest velocity gradient and maximum shear stress occur near the nozzle wall, where cells close to the wall move more slowly than those in the center, resulting in more significant cell deformation.<sup>39</sup> Shear stress, a mechanical force that deforms a material along a plane parallel to the stress direction, is regarded as the primary cause of cell damage or death in extrusion-based bioprinting. Theoretically, cell damage increases exponentially with the rising shear stresses, starting at zero in the absence of stress and reaching up to 100% under high-stress conditions.<sup>39</sup> However, different cell types vary in their sensitivity and response to shear stress, leading to variations in cell viability. Despite having cell viability issues, the versatility of the bioink used is one of the primary advantages of this bioprinting technique. Zhao *et al.*<sup>40</sup> utilized extrusion-based 3D printing technology to create chitosan ducts for soft tissue engineering applications. The prepa-



**Praseon Kumar**

*Dr Praseon Kumar received a PhD in Mechanical Engineering jointly from the Indian Institute of Technology, Bombay, India, and Monash University, Melbourne, Australia. He was a National Post-doctoral Fellow in the division of Materials Engineering, Indian Institute of Science, Bangalore. He worked as Assistant Professor at the Department of Medical Devices in the National Institute of Pharmaceutical Education and*

*Research (NIPER), Ahmedabad. Currently, he is working as an Assistant Professor Grade 1 at the National Institute of Technology (NIT) Rourkela, India. His current research interests include the biodesign of materials and devices for healthcare applications, additive manufacturing, and lab-on-chip devices.*



**Shabir Hassan**

*Dr Shabir Hassan received a PhD in Natural Sciences (Chemistry) from the University of Zurich, Switzerland. He did his post-doctoral training at Harvard University and MIT, USA, and is currently serving as an Assistant Professor of Biology at Khalifa University, Abu Dhabi, UAE. Before joining Khalifa, he was an Early Career Investigator at Harvard Medical School and Associate Bioengineer at Brigham and Women's Hospital,*

*USA. His main focus of research has been devising in vitro platforms for diseases such as cancer and different tissues for drug discovery and drug delivery applications. Additionally, his interests revolve around the 3D bioprinting of disease models to study genetic and rare diseases. He has won many awards for his academic and research excellence and published more than 55 research papers in international journals of repute. The mini microscope he developed was recognized as one of the Royal Society of Chemistry's Hot Papers. He has also been instrumental for innovations in fabricating 3D self-oxygenating artificial tissues for implants in volumetric tissue losses. Dr Hassan serves as an Associate Editor for *Frontiers in Biomaterials Science*. He served as *Founding Associate Editor for MIT Science Policy Review (MIT, USA)* in 2020.*

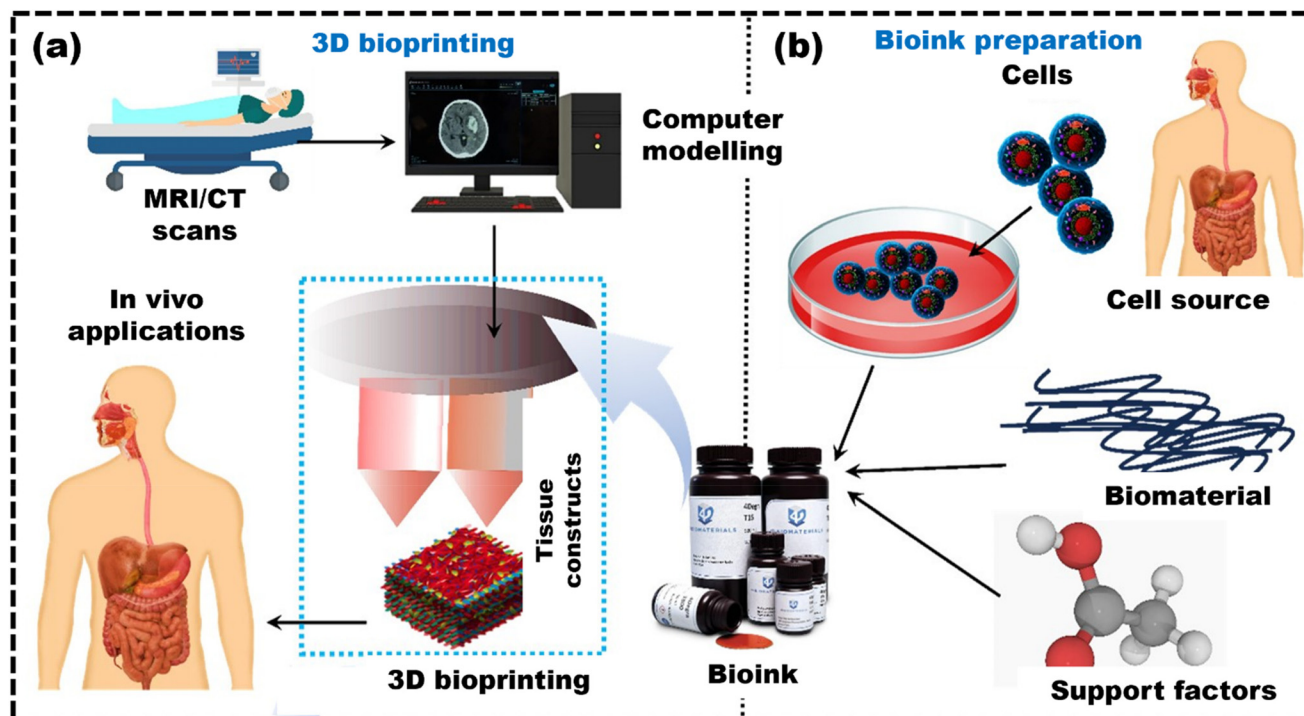


**Fig. 1** The diagram shows the overall process of 3D bioprinting, highlighting the key phases: (a) schematic shows the complex processing of data, reproduced from Ripley *et al.*<sup>29</sup> with permission from John Wiley and Sons, copyright (2016); (b) bioink preparation for 3D bioprinting and its applications, reproduced from Jose *et al.*<sup>30</sup> with permission from Elsevier, copyright (2024).

ration process can be refined using various acidic solutions, such as formic acid, acetic acid, glycolic acid, and lactic acid, to manufacture chitosan ducts. The optimal solvent for chitosan was 30 wt% glycolic acid solution.<sup>37</sup> The Young's

modulus, tensile strength, and fracture strain values for chitosan ducts were  $12.38 \pm 1.19$  MPa,  $10.98 \pm 0.61$  MPa, and  $146.03 \pm 15.05\%$ , respectively, similar to the soft tissue properties. These characteristics make chitosan ducts suitable for



**Hassan Mehboob**

*Dr Hassan Mehboob received a PhD in Mechanical Engineering from Chung-Ang University, Seoul, South Korea, in 2015. Afterward, he worked at Qatar University as a postdoctoral research fellow from 2016 to 2019. Then he joined Prince Sultan University in 2019 as an Assistant Professor and currently he is working as an Associate Professor at the same university. His research interests include additive manufacturing, composite biomaterials, biomechanics, implant design, and finite element analysis. Dr Mehboob has published several of his articles in specialized high impact journals on composites such as Composite Structure, Composites Part B: Engineering, Composite Science and Technology and so on.*



**Harpreet Singh**

*Dr Harpreet Singh received a PhD from the Indian Institute of Technology Roorkee, India. He is currently working as an Assistant Professor at the Dr B R Ambedkar National Institute of Technology Jalandhar. His research interests are broadly related to the advancement of precision machining processes, nano finishing science and technology, green manufacturing methods, microwave processing of metals and composites, polymer processing and PMCs, bio-materials, material processing and characterization studies. He has published several research papers in international peer reviewed journals of repute and presented at national and international conferences in India and abroad. He has been a resource person and delivered invited lectures at several national and international conferences, STTPs, and QIP programs.*

soft-tissue restoration.<sup>41</sup> However, like other biological structures, chitosan ducts need an appropriate microenvironment to support cell adhesion, proliferation, and differentiation. Cell-laden micro-scaffold-based bioinks can tackle these challenges by offering a more physiologically relevant microenvironment for cells to further support tissue regeneration.

Tan *et al.*<sup>42</sup> utilized a micropipette extrusion-based 3D bioprinting method to fabricate living multicellular tissues using cell-laden micro-scaffold-based bioinks. The bioink consists of poly(lactic-co-glycolic acid) (PLGA) porous microspheres with a thin encapsulation of agarose-collagen (AC) hydrogel. L929 mouse fibroblasts were cultured to assess the biocompatibility of the printed construct. The bioprinted construct demonstrated excellent biocompatibility, with more than 90% cell viability maintained over the 2 days, 7 days, and 14 days of cell culture. Furthermore, compared to the AC hydrogel, the mechanical strength of the construct was significantly improved, exceeding it by more than 100 times. However, single-component bioinks typically lack essential traits like cell-specific bioactivity and optimal rheological properties. This limitation results in a narrow bio-fabrication window, restricting the applicability of extrusion bioprinting in tissue engineering and regenerative medicine. Selecting specific additional polymers, micro-, or nanoparticles for existing single-component bioinks enables the design of multicomponent bioinks. Xin *et al.*<sup>43</sup> investigated the hydrogel microparticle dissipation process during printing, analyzing both exter-

nal resistance from the apparatus and the internal physico-chemical properties of the hydrogel microparticles through experimental and computational methods. These offer a broader bio-fabrication window, enabling enhanced functionality and mechanical stability to mimic targeted physiological tissues.<sup>44</sup> Overall, 3D extrusion bioprinting is poised to make significant advancements with novel bioinks and improved printing techniques, paving the way for promising medical applications.

## 2.2 Vat photopolymerization-based bioprinting

Vat photopolymerization (VP) has been widely used in tissue engineering and regenerative medicine due to its superior spatiotemporal control over bioresin.<sup>45</sup> This capability enables the fabrication of intricate 3D hierarchical structures that closely resemble human tissues and organs.<sup>46</sup> VP bioprinting technology uses the curing properties of photocurable materials by directing a light beam onto the precursor solution, allowing for on-demand material curing. This method enables the creation of various 3D structures by controlling where and how long the light beam is projected.<sup>47</sup> Among them, stereolithography (SLA), digital light projection (DLP), and volumetric bioprinting technology are commonly used VP techniques. SLA technology uses photosensitive liquid resin as bioink, which solidifies upon exposure to ultraviolet light.<sup>48</sup> A computer-controlled laser traces each layer, solidifying the resin, and the process is repeated layer-by-layer to create 3D constructs. DLP uses a UV lamp or laser with a digital mirror device to cure resin layer-by-layer, forming 3D constructs. Unlike SLA, which uses a moving laser, DLP employs a dynamic mask for light exposure.<sup>49</sup> Both methods demonstrate the versatility of VP techniques, allowing for the accurate creation of complex shapes in various applications. For instance, Guillaume *et al.*<sup>50</sup> developed photo-cross-linkable poly(trimethylene carbonate) (PTMC) resins containing 20% and 40% hydroxyapatite (HA) nanoparticles and employed SLA technology to fabricate scaffolds with precise macro-architecture. The results indicated that rabbits implanted with PTMA-MA scaffolds containing 40% nano-HAP showed the most significant degree of vascularization at the lesion site, effectively promoting the formation of new bone tissue. Likewise, Ma *et al.*<sup>51</sup> employed the DLP technique of VP to fabricate a gelatin methacrylate/methacrylated hyaluronic acid hydrogel liver model, matching the stiffness of actual liver tissue. The hepatic model provided a 3D environment for hiPSC-derived hepatic cells cocultured with supporting cells (human umbilical vein endothelial cells) in a hepatic lobule-like structure. It enabled *in vitro* maturation and helped maintain the functional integrity of hiPSC-derived hepatic cells within a biomimetic setting. Although extensive studies have reported on VP-based bioprinting of human tissues such as the liver, skin, and bone, achieving the complete fabrication of transplantable tissues remains elusive. Human organs have complex structures composed of various cell types and materials. Therefore, utilizing multiple materials is essential to replicate human tissue in VP bioprinting accurately.<sup>52</sup> However, the vat storage of bioresin



**Himansu Sekhar Nanda**

*Himansu Sekhar Nanda, Ph.D. received a PhD in Materials Science and Engineering from the International Joint Graduate School of the National Institute for Materials Science (NIMS) and the University of Tsukuba, Japan. He was a post-doctoral fellow at King Abdullah University of Science and Technology (KAUST), Saudi Arabia, and a postdoctoral research fellow at Nanuang Technological University (NTU),*

*Singapore. Currently, he is working as an Assistant Professor Grade 1 at the Indian Institute of Information Technology Design and Manufacturing (IIITDM), Jabalpur, India. He was a Visiting Scholar at the College of Materials Science and Engineering, Beijing University of Chemical Technology (BUCT), Beijing and a Senior Visiting Scholar at Fudan University, China. He was a Research Scientist at the Terasaki Institute for Biomedical Innovation (TIBI), Los Angeles, USA, and now he is an affiliate faculty member at TIBI. His primary research interests include biomaterials and advanced biomanufacturing for regenerative engineering. He is also interested in emerging material technologies for a clean and sustainable environment.*

in VP poses more challenges for multimaterial printing than extrusion and inkjet bioprinting. The bioresin used in VP-based bioprinting must have low viscosity, as higher viscosity can cause the sedimentation of encapsulated cells. Furthermore, bioresins for VP need to be transparent to enable light penetration and initiate photopolymerization.<sup>47</sup> However, there is a limited availability of highly transparent biomaterials suitable for bioresins.<sup>53</sup> Therefore, more research is needed to address these challenges and create universal bioresin toolboxes that effectively manage viscosity while allowing for cell encapsulation.

## 2.3 Jetting-based bioprinting

**2.3.1 Laser-assisted bioprinting.** Laser-assisted bioprinting (LAB) technology is promising for fabricating artificial tissues.<sup>54,55</sup> Its high resolution and precision enable the creation of a suitable ECM microenvironment. LAB is a direct-write method that employs the laser-induced forward transfer (LIFT) principle. A laser pulse is concentrated on a thin film of bioink, which absorbs the laser energy and generates a bubble. The expansion of this bubble generates a high-speed jet of liquid bioink. Upon hitting the substrate, this jet gives rise to tiny liquid droplets. Then, the laser is moved to another spot on the surface of the bioink, and the process is repeated to create a pattern or a structure of interest. LAB bioprinting provides multiple advantages, such as enabling high cellular densities of approximately  $1 \times 10^8$  cells per mL with fine printing resolution ( $\sim 40 \mu\text{m}$ ).<sup>56</sup> It also accommodates a wider range of viscosities (1–300 mPa s) compared to other drop-on-demand bioprinting techniques.<sup>57</sup> It maintains cell survival rates above 90%. This high cell density printing, with this nozzle-free printing method, removes nozzle clogging problems. High viability suggests limited damage caused by the printing process, but it does not mean zero cell damage or death.<sup>58</sup> Although LIFT experiences lower shear stress compared to nozzle-based systems, it still impacts cell integrity. Increased laser fluence raises shear stress, reducing cell viability by damaging membranes and possibly altering stem cell differentiation. This presents a significant challenge for LAB. Additionally, during the initial cell transfer, the laser heats the bioink by interacting with the absorbing matrix, potentially causing thermal damage to cells.<sup>59</sup> The high laser fluence and focused spot size can deactivate enzymes and denature proteins within the cells. Exposure to a high-energy density short-wavelength laser, such as the UV laser, may also be one of the causes of cell damage since UV light can destroy living cells by damaging DNA double strands.<sup>60</sup> Optimizing the LAB process requires investigating the causes of cell injury, such as physical stress from acceleration and deceleration, laser exposure, rapid temperature shifts causing thermal damage, chemical changes in the bioink, and nutrient shortages. Despite this, its sub-micron resolution makes it particularly useful for printing small-scale tissues and organs, such as blood vessels and neural tissues.<sup>61,62</sup> Sorkio *et al.*<sup>63</sup> explored the feasibility of using LAB with human stem cells to fabricate layered 3D-printed tissues that mimic the structure of native corneal tissues. The 3D

corneal structures showed robust mechanical properties without the need for additional bioink crosslinking following LAB. 3D stromal bioprinted structures were implanted into porcine corneal organ cultures to evaluate their functionality and integration with the host tissue.

The 3D bioprinted stromal structures adhered to the host tissue, indicating successful tissue integration potential. This highlights the potential of LAB 3D bioprinting for creating functional tissue constructs that integrate with native tissues and contribute to their regeneration.<sup>64</sup> Similarly, Keriquel *et al.*<sup>54</sup> demonstrated the utilization of LAB technology for on-site bone regeneration by precisely printing specific biological components (nHA collagen material) and mesenchymal stromal cells (MSCs) within a defect in the calvaria (upper part of the skull) of mice (Fig. 2a). Different cell geometries, with distinctive cellular repartitions (such as disc and ring), were also tested to show their impact on bone regeneration. The results showed that one month after printing, the nHA-collagen and nHA-collagen + MSC cells printed in a ring shape showed only marginal tissue reconstruction, mainly at the periphery of the defect. In contrast, the nHA-collagen + MSC cells printed in a disk shape showed significant new bone formation, well distributed throughout the defect. Hence, LAB proves effective at printing mammalian cells with minimal impact on their viability and functionality, presenting a promising avenue for *in situ* bioprinting of the tissues. However, a key challenge is developing functional blood vessels to improve the integration and effectiveness of synthetic bone grafts. Kédanet *et al.*<sup>65</sup> employed LAB to directly print endothelial cells within a mouse calvaria bone defect. The defect was pre-filled with collagen-containing vascular endothelial growth factor (VEGF) and mesenchymal stem cells (MSCs). This approach aims to establish pre-vascularization with a well-defined architecture and promoting *in vivo* bone regeneration. The influence of different cellular arrangements (disc, crossed, and random) on bone regeneration (br) and vascular organization (vr) was examined *in vivo*. After two months, vr and br showed statistically significant improvements in the 'disc' pattern (vr: +203.6%, br: +294.1%) and 'crossed circle' pattern (vr: +355%, br: +602.1%) compared to the 'random seeding' conditions.

In addition to its use in calvaria bone defect repair, LAB technology is gaining attention in treating pancreatic ductal adenocarcinoma (PDAC). Hakobyan *et al.*<sup>66</sup> used LAB to create 3D pancreatic cell spheroid arrays and monitored their phenotypic changes over time through image analysis and phenotypic characterization for PDAC. The results showed that the 3D model of spheroids containing various combinations of acinar and ductal exocrine pancreas cells was suitable for studying the early stages of PDAC development. As LAB enables precise control over cell placement, shape, and production speed, this high-throughput spheroid array model holds significant promise as a substitute for standard 2D cultures or more intricate and time-consuming 3D methods.<sup>67–69</sup>

Despite having various advantages like precision and resolution enabling the creation of intricate structures, LAB

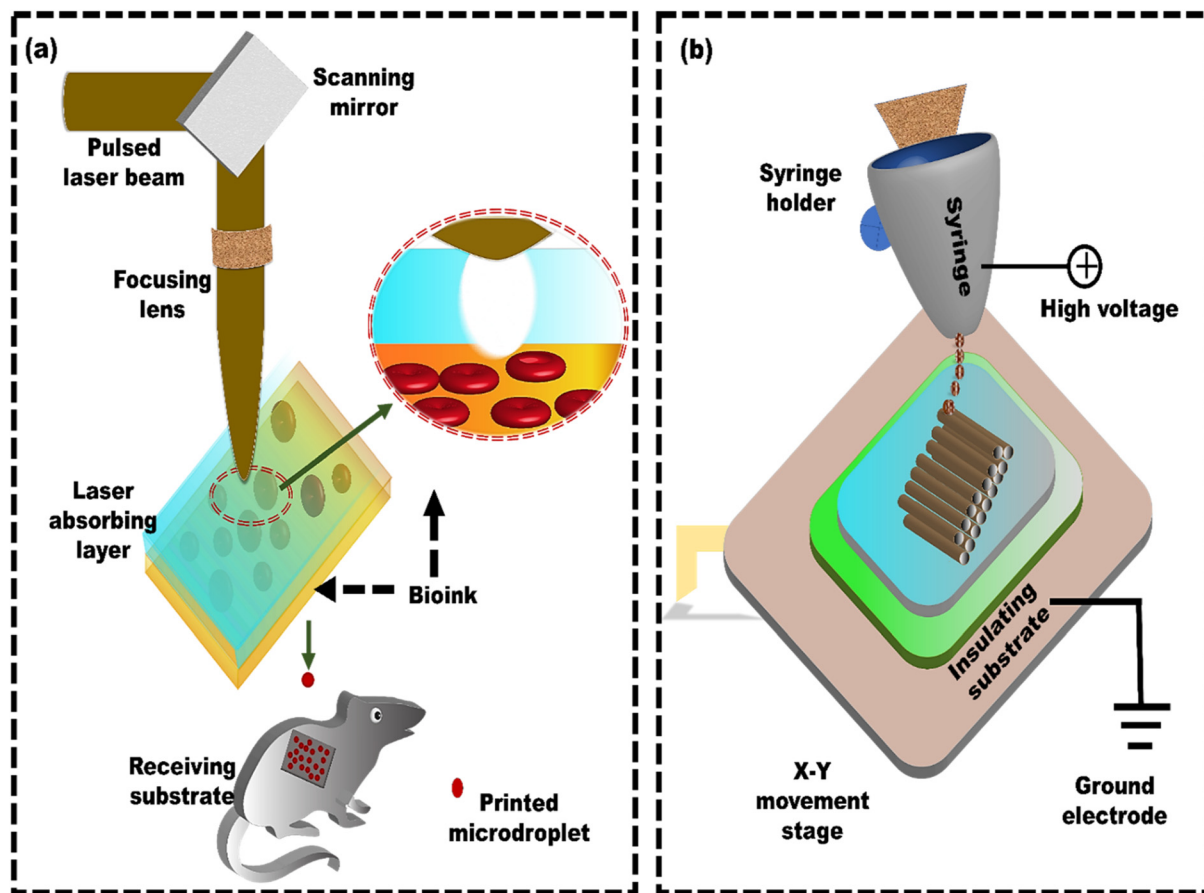


Fig. 2 Schematic of laser-assisted bioprinting (LAB) and electrohydrodynamic printing: (a) a standard LAB setup consists of a pulsed laser beam, a focusing system, and a ribbon that generates microdroplets, reproduced from Keriquel *et al.*<sup>54</sup> with permission from Elsevier, copyright (2017), and (b) electrohydrodynamic printing using a coaxial nozzle for creating microscale constructs with embedded cells, reproduced from Liang *et al.*<sup>94</sup> with permission from Elsevier, copyright (2018).

also faces several technical challenges. A support bath or environment is often needed to print complex 3D structures to maintain their shape and prevent deformations because the viscosities accommodated in the LAB are often too low to construct a stable structure without support.<sup>64</sup> Scaling from the laboratory benchtop to factory production poses another challenge. The current printing speeds of LAB technology need to be faster to efficiently produce large-scale bioproducts.<sup>64,70</sup> Regarding commercial availability, laser-based bioprinters are relatively expensive and require significant expertise. Thus, more investigations and advancements are required to tackle these technological obstacles to increase the use of LAB in both academic and industrial settings.

**2.2.2 Inkjet bioprinting.** Inkjet-based bioprinting provides an effective solution for tissue engineering and regenerative medicine by facilitating the precise placement of sub-nanoliter droplets at specified locations without contact, using a drop-on-demand (DOD) approach.<sup>71</sup> This leads to improved accuracy and higher ink utilization efficiency. Inkjet printing can work with a range of biological materials and enables structures to be created with varying cell densities by modifying the

density or size of the droplets.<sup>72</sup> Nayak *et al.*<sup>73</sup> utilized direct inkjet writing (DIW) to print polymer–ceramic composites for bone tissue regeneration and to evaluate their behaviour under thermomechanical loading. The rheological properties of the colloidal gels were assessed to establish shear-thinning capabilities, which enabled extrusion through a custom-built DIW printer. The polymer–ceramic composite gels exhibited effective shear-thinning during extrusion, with a significant increase in cellular viability observed when  $\beta$ -TCP particles were incorporated into the polymer matrix compared to pure PLA. Kang *et al.*<sup>74</sup> demonstrated the use of automated high-resolution inkjet printing to place alveolar cells, creating a 3-layered alveolar barrier model with an impressive thickness of approximately 10  $\mu\text{m}$ . The study demonstrated that this 3D structured model more accurately replicated lung tissue structure, morphology, and functions compared to a traditional 2D cell culture model and when evaluated against an unstructured 3D model made of a homogeneous mixture of alveolar cells and collagen. The findings indicated that this thin, multi-layered model accurately simulated tissue-level responses to influenza infection. Although inkjet-based bioprinting enables

accurate drop-on-demand cell deposition in 3D tissue constructs and fosters important cell–cell and cell–matrix interactions, it faces challenges such as insufficient cell homogeneity and low cell viability.

Shear stress in inkjet bioprinting primarily develops during two key phases, which include the ejection of cell-laden droplets from the nozzle and their landing on the substrate. Extended exposure to mechanical shear stress can affect the phenotype and viability of biological cells, potentially leading to cell lysis.<sup>75</sup> Inkjet bioprinting exposes cells to significantly higher shear stress levels, reaching up to 500 Pa, but only for about 100  $\mu$ s.<sup>75</sup> The response to shear stress is strongly influenced by the type of cell, the shear stress's magnitude, and the exposure time. Increasing the concentration of cells in the DOD inkjet bioprinting system causes the droplets to jet out at a slower impact velocity. This slower droplet speed helps protect the cells by reducing splashing, improving the overall quality of the printed material. Additionally, it is essential to limit the printing time for each layer to prevent the droplets from evaporating too much, which helps maintain cell viability.<sup>76</sup> For example, Ng *et al.*<sup>77</sup> used a thermal inkjet system to dispense sub-nanoliter cell-laden droplets, identifying two critical factors, droplet impact velocity and droplet volume, which significantly affected the viability and proliferation of printed cells. The results demonstrated that under the optimal conditions, with a concentration of 4 million cells per mL and a printing time of less than 2 minutes, the cells showed elongation by day 1 and proliferated efficiently, covering almost 90% of the surface area by day 7. Therefore, it is crucial to optimize the magnitude of shear stress and the exposure time to enhance the benefits of inkjet bioprinting.

**2.2.3 Microvalve bioprinting.** Microvalve bioprinting is drop-on-demand (DOD) printing, similar to inkjet and laser-based bioprinting.<sup>78</sup> This system offers several advantages over other methods, including high cell viability (over 86%), consistent cell distribution, and high-speed printing.<sup>79</sup> A typical microvalve printhead comprises a pneumatic pressure source, plunger, and solenoid coil. The coil acts as a magnetically activated pump, where adjusting the electric current alters the magnetic field, moving the plunger to regulate the nozzle opening for dispensing. In this entire process, the wall shear stress in the nozzle increased during the microvalve opening phase, reaching its highest point just before the valve closed.<sup>79</sup> Following that point, the wall shear stress inside the nozzle abruptly decreased and remained very low due to the ligament retraction effect until the dispensing process was completed. It may adversely affect cell viability until the dispensing process is complete.<sup>80</sup> However, microvalve bioprinting, as an automated robotic platform, is increasingly recognized as a vital tool for tissue engineering and regenerative medicine.<sup>81</sup> Lee *et al.*<sup>82</sup> employed microvalve-assisted coaxial 3D bioprinting to fabricate functional skeletal muscle tissue. The artificial muscle fascicle (AMF) consists of a core filled with C2C12 myoblast aggregates, mimicking muscle fibers, and a photo-cross-linkable hydrogel shell that acts as connective tissue. A multi-printed artificial muscle tissue (AMT) was

implanted into an immunocompromised rat's anterior tibia muscle defects. The AMT fabricated *via* microvalve-assisted coaxial 3D bioprinting responded to electrical stimulation and exhibited histological characteristics of regenerated muscle tissue, marking a significant advancement in mimicking native skeletal muscle. The Biofactory, a commercial microvalve bioprinter from regenHu Ltd (Switzerland), has also proved to be effective for lung tissue engineering.<sup>83</sup> It was used to bioprint a human air–blood tissue barrier composed of endothelial cells, epithelial cells, and a basement membrane. These lung models are beneficial for drug testing and regulatory toxicology research.

Still, the resolution is an issue in microvalve bioprinting that needs attention because microvalves offer lower resolution ( $\sim$ 150  $\mu$ m) compared to inkjet printing ( $\sim$ 20  $\mu$ m).<sup>84</sup> Additionally, the impingement shear stress is comparable to the nozzle wall shear stress. It may even exceed it in some instances. Therefore, minimizing impingement shear stress is essential in microvalve bioprinting to reduce process-induced cell death. Nasehi *et al.*<sup>80</sup> showed that the distance between the nozzle and the platform influenced the amplitude of impingement shear stress. Consequently, this important factor should be addressed by adjusting the nozzle-to-platform distance to optimize cell viability in the case of microvalve bioprinting. Overall, this technique is better suited for co-printing larger volumes of biomaterials, such as cells, genes, hydrogels like collagen and alginate, and growth factors, which require a larger nozzle size.

**2.2.4 Electrohydrodynamic bioprinting.** Electrohydrodynamic (EHD) printing is a promising method integrating layer-by-layer AM with electrohydrodynamics to fabricate precise micro/nano-scale 3D structures.<sup>85</sup> In EHD bioprinting, a high voltage is applied between the nozzle and the collecting substrate to facilitate the electrical ejection of material flow. The conductive bioink is placed in the needle. The ink is drawn toward the substrate as the electric field is applied, forming the desired structure. The electric field can be adjusted to control the size and shape of the printed structures, as well as the orientation and alignment of the cells within the structure.<sup>86</sup> Applied voltage mainly influences droplet shape, which indirectly affects cell viability. As long as the voltage remains below a specific limit, it has no significant impact on cell viability.

EHD bioprinting typically involves minimizing the nozzle-to-collector distance to a few millimeters. This modification ensures a singular material flow, facilitating stable and controlled deposition of minute fibers.<sup>87</sup> EHD offers several advantages over other bioprinting techniques, including its ability to print various biomaterials (hydrogels, biopolymers, and living cells), creating functional tissues and organs that closely mimic the actual tissues. It also offers a precision of approximately 50 nm high-resolution and creates heterogeneous, gradient structures.<sup>88</sup> These structures are achieved by controlling the electric field and the flow rate of the bioink, which can be used to create structures with varied cell densities, stiffness, and porosity.<sup>89</sup> These heterogeneous and gradient structures are essential for creating tissues with complex

functions, such as muscles and organs, which require different cell types and environments to function correctly.<sup>90</sup>

It simplifies transferring micro/nano-architectures from photomasks to biologically relevant materials, demonstrating flexibility in producing tiny 3D architectures.<sup>91</sup> Similarly, in contrast to light-based micro/nanoscale 3D printing techniques like projection micro-stereolithography and two-photon polymerization, EHD bioprinting is a cost-effective method.<sup>92</sup>

Cell printing is extensively utilized in biomedical fields because it creates living tissue constructs with precise control over the cell arrangements. However, producing cell-laden 3D structures with high cell viability and high resolution is still difficult. EDH bioprinting is increasingly recognized as a method to address the challenge of achieving high resolution and cell viability in 3D constructs.<sup>93</sup> Liang *et al.*<sup>94</sup> developed a coaxial nozzle-assisted EHD cell printing strategy to fabricate 3D cell-laden constructs (Fig. 2b). The results demonstrated that the proposed strategy could print 3D hydrogel structures with uniform filament dimensions (around 80  $\mu\text{m}$ ) and consistent cell distribution, with more than 90% cell viability. Still, the fabrication of complex, heterogeneous 3D living constructs with multiple cell types and diverse hydrogel compositions remains challenging. Altun *et al.*<sup>95</sup> used the EHD strategy to fabricate a bacterial cellulose/polycaprolactone (BC/PCL) composite scaffold for tissue engineering applications. The BC/PCL composite scaffold fibers were spaced approximately 100  $\mu\text{m}$  apart, and the depth of the fibers was  $4.7 \pm 1.03 \mu\text{m}$ . The BC/PCL composite scaffold demonstrated over 155% cell viability compared to the PCL scaffold, indicating its strong potential for tissue engineering applications with improved bioactivity. Despite their advantages, most scaffolds in the literature feature a single pore size or porosity. However, native biological tissues, like cartilage and skin, have a layered architecture with zone-specific pore sizes and mechanical properties. As a result, functionally graded materials are becoming increasingly popular for addressing these challenges by incorporating zones with different pore sizes and mechanical properties. Vijayavenkataraman *et al.*<sup>96</sup> used the EHD technique to develop PCL-based functionally graded scaffolds (FGS) with various gradient patterns, such as radial, sectional, diagonal, concentric, and axial directions for interfacial tissue engineering, and *in vitro* cancer metastasis. The FGS patterns were tested for mechanical properties under tensile loading and compared with simulated results. The computational analysis aligns with experimental observations in all cases. Mechanical testing confirmed that all the FGS had a mean yield stress from 6 MPa to 8 MPa, whereas the mean yield strain was between 3% and 9%. He *et al.*<sup>97</sup> explored the potential of utilizing solution-based EHD 3D printing to produce microscale scaffolds made of PCL, including multi-walled carbon nanotubes (MWCNTs) (Fig. 3a). The solution-based strategy aimed to overcome the challenges of uniformly incorporating functional or bioactive nanomaterials into printed microfibers in viscous melted polymers. When the printing process used 8 wt% PEO and 5 wt% PCL concentrations, 3D fibrous structures with fibers measuring 10  $\mu\text{m}$  in diameter,

like the size of living cells, were developed (Fig. 3b and c). The results revealed that although MWCNTs have a detrimental effect on cell attachment, the developed PEO–PCL–MWCNT scaffolds promoted cell alignment (Fig. 3d). Cells adhered and aligned along the microfibers of the PEO–PCL–MWCNT scaffolds (Fig. 3e). Similarly, Choe *et al.*<sup>98</sup> employed electrohydrodynamic jetting (EHDJ) to fabricate a PCL/cellulose composite scaffold consisting of coil-shaped struts and controllable macro/micropores. This coil-shaped framework demonstrated substantial cell migration of  $79 \pm 1.7\%$ , whereas the control (PCL coil-shaped scaffold) showed a lower cell movement of  $51 \pm 2.4\%$ . The uniform distribution of cellulose within coil-shaped PCL/cellulose composite scaffolds directly contributes to their high cell proliferation rates, indicating their potential application in hard tissue regeneration.

Apart from several advantages of EDH, specific challenges hinder the broader implementation of EHD bioprinting, and addressing these challenges is crucial to unlocking its full potential. The key issues include the limited height of 3D micro/nanofibrous structures, reaching approximately 5 mm due to variations in electrical force during stacking.<sup>99</sup> Strategies such as dynamic voltage adjustments and using paper substrates have been explored to overcome these challenges. While EHD bioprinting offers high resolution, precisely depositing tiny fibers for intricate microstructures and efficiently fabricating large tissue scaffolds with EHD bioprinting are significant challenges. These issues have been addressed using electrostatic forces to control filament paths, achieving printing speeds of up to  $0.5 \text{ m s}^{-1}$  horizontally and  $0.4 \text{ m s}^{-1}$  vertically.<sup>100</sup> This electrostatic deflection technique shows great promise for ultrafast printing. It significantly enhances the scalability of EHD bioprinting, especially for large and complex tissue scaffolds.<sup>101</sup> Despite these advancements, several challenges persist, such as biomaterial scarcity, particularly for high-resolution EHD bioprinting.<sup>102</sup> This emphasizes the need for innovative, material-independent solutions to broaden the application of EHD in biomedical engineering.

Overall, the detailed overview of 3D bioprinting methods covers every aspect, from materials to capabilities and applications in tissue engineering. The most widely used 3D bioprinting technologies adapted for fabricating tissue constructs and their resolution, materials, and possible applications are summarized in Table 1.

### 3. Considerations for developing bioinks for 3D bioprinting

Bioinks play a fundamental role in 3D bioprinting, serving as the foundation for the process and ensuring the desired printability and structural stability of the printed structure.<sup>122</sup> This stability is crucial for the success of the bioprinting process, as it directly impacts the capability to create intricate tissue structures with exceptional resolution and reproducibility.<sup>123</sup> Wettability, rheological properties, crosslinking methods, and

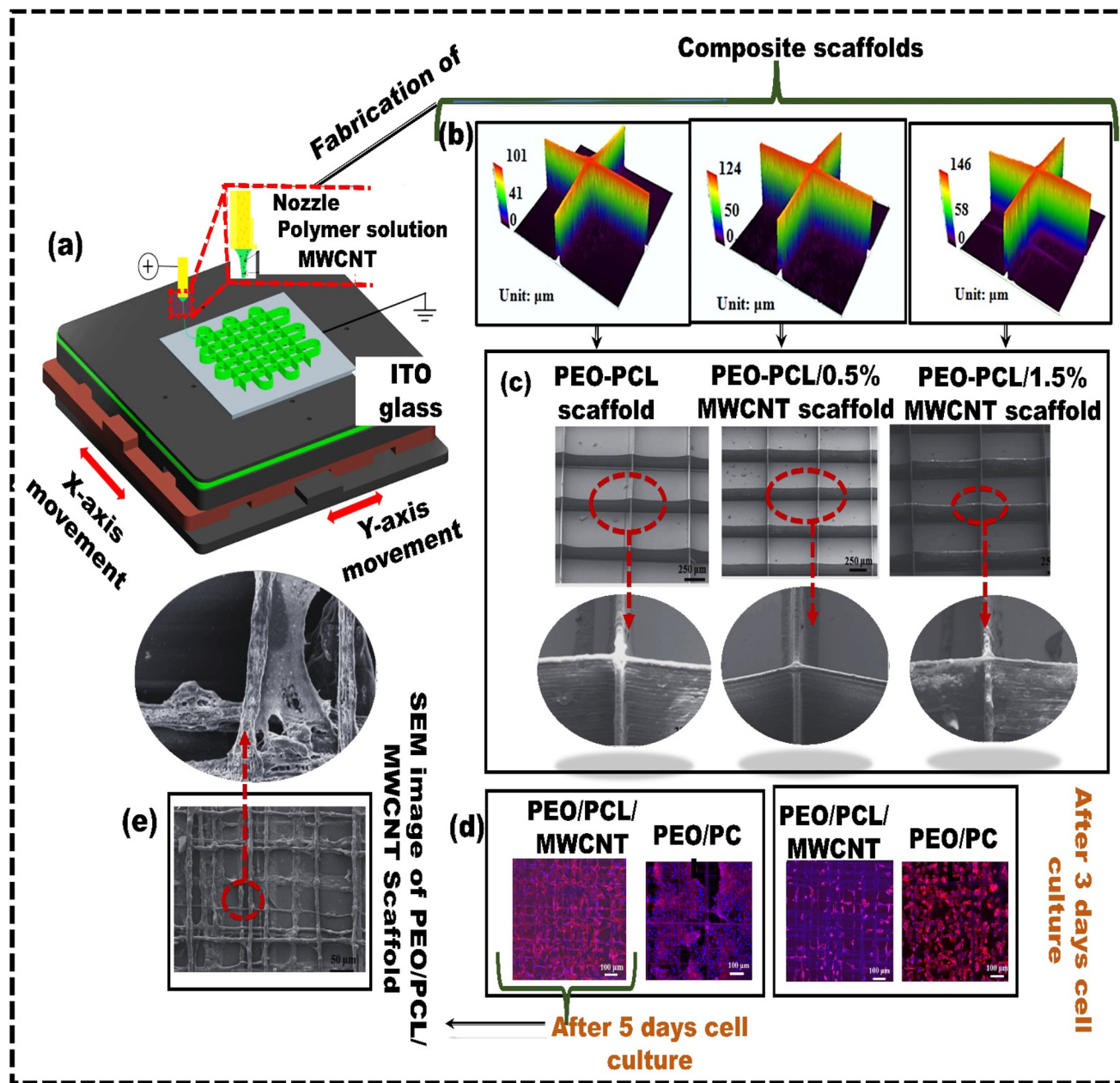


Fig. 3 Solution-based electrohydrodynamic 3D printing: (a) schematic representing the electrohydrodynamic method used for preparing micro-scale PEO–PCL–MWCNT composite scaffolds; (b) profiles of 3D composite scaffolds with varying MWCNT content; (c) SEM images; (d) fluorescent microscopy images showing cellular structures on PEO–PCL–MWCNT and PEO–PCL scaffolds; (e) SEM images depicting cell morphology on PEO–PCL–MWCNT scaffolds following a five-day cell culture period, reproduced from Jiankang et al.<sup>97</sup> with permission from IOP Publishing, Ltd, copyright (2017).

Table 1 Various printing techniques and their properties

Printing technique	Resolution	Material	Application
Extrusion based	150–600 $\mu\text{m}$ (ref. 103)	Hydrogels, thermoplastics	Cartilage, <sup>104</sup> adipose, <sup>105</sup> a cellular scaffold, <sup>106</sup> cell-free scaffold <sup>107</sup>
Laser based	20–100 $\mu\text{m}$ (ref. 108 and 109)	Hydrogels, ceramics, etc.	Bone, <sup>55</sup> vascular, <sup>110</sup> adipose, <sup>111</sup> organoid, <sup>112</sup> cornea, <sup>63</sup> skin <sup>68</sup>
Electrohydrodynamic	50 nm (ref. 113 and 114)	PCL, chitosan, GelMA	Bone, <sup>115</sup> blood vessel, <sup>116</sup> tendon/ligament, corneal stroma, <sup>117</sup> cartilage, <sup>118</sup> cardiac patch <sup>119</sup>
Inkjet bioprinting	<50–75 $\mu\text{m}$ (ref. 120)	Hydrogel-based materials such as alginate, calcium chloride and, acrylated PEG, etc.	Skin (dermo-epidermal skin constructs), <sup>121</sup> DNA microarray, <sup>71</sup> pharmaceutical development <sup>71</sup>

immunogenicity are interconnected factors significantly impacting bioprinting success. Wettability affects bioink adhesion to the print bed; a smaller contact angle improves stability during layer deposition, which is essential for vertical fidelity and preventing displacement.<sup>124–127</sup> Rheological properties, such as viscosity and shear-thinning behaviour, influence the flow of bioink during printing, balancing the stabilization of encapsulated cells with ease of extrusion to ensure cell viability and high-resolution prints.<sup>128</sup> Crosslinking methods like thermal, ionic, enzymatic, and photo-crosslinking create stable structures, with the choice affecting both mechanical strength and cytocompatibility. Lastly, minimizing immunogenicity is crucial for long-term success, as materials should reduce immune responses to avoid inflammation and promote biodegradability and biocompatibility for cell growth and function.<sup>129</sup> In extrusion-based bioprinting, the choice of bioink and its properties is vital for achieving structural stability and maintaining shape fidelity during printing. While, in inkjet bioprinting, where cells are suspended in low-viscosity fluids, the impact of bioink properties on stability may be less pronounced due to inherent characteristics of the fluid. Therefore, by optimizing bioink formulations tailored to the specific bioprinting method, it is possible to enhance the stability of the printed constructs, leading to improved cell viability, tissue regeneration, and functional outcomes. Besides the properties of the bioink, for translation purposes, bioinks must be sterile, free from endotoxins, and not induce pyrogenicity.<sup>130</sup> So, it is vital to consider these bioink aspects and the challenges that must be addressed for successful commercialization and clinical adoption.<sup>131</sup>

### 3.1 Designing bioink for extrusion-based 3D bioprinting

Choosing a suitable bioink material for extrusion bioprinting requires establishing a thorough performance index to assess its suitability.<sup>126</sup> Bioinks must satisfy different performance requirements in extrusion bioprinting at each stage—before, during, and after extrusion.<sup>103</sup> In the pre-extrusion stage, key characteristics of bioinks include viscosity, cell distribution, and biocompatibility, while during extrusion, shear-thinning is crucial as it helps reduce shear stress.<sup>132</sup> Shear-thinning relies on the reversible breaking of crosslinked bonds within hydrogel materials, primarily formed by non-covalent interactions. When subjected to high shear forces, these non-covalent bonds break, causing a reduction in the bioink's viscosity.<sup>133</sup> Once the shear forces are removed, the bonds reform through molecular non-covalent forces, increasing viscosity and preserving the bioink's shape stability.<sup>134</sup> The minimal force needed for the bioink to begin flowing is known as yield stress, and too much of it can harm cells and 3D printing apparatus.<sup>135</sup> Static viscosity and yield stress provide an initial basis for evaluating a material's suitability for bioink preparation in extrusion-based printing. A material is not suitable for extrusion bioprinting if its viscosity barely changes with shear force or the yield stress is too high.<sup>44</sup>

In the second stage, known as the shear-thinning phase following extrusion, the viscosity of the bioink decreases with

increasing shear rate. This enables continuous extrusion, the creation of uniform filaments, and enhances cell survival during the process.<sup>136</sup> But there is a threshold below which viscosity reduction causes the bioink to extrude as a droplet instead of a homogeneous filament. The third stage is the post-print recovery stage. In this stage, the post-print curing capability of the bioink is assessed by examining the relationship between viscosity and time, which is linked to the stability of size and cell dispersity.<sup>137</sup> For example, slow viscosity recovery may result in the sedimentation of cells.<sup>125</sup> Additionally, temperature is also critical in extrusion-based bioprinting in managing bioink rheology and crosslinking. Biomaterials like gelatin and collagen, which are temperature-sensitive, shift from liquid to gel at around 37 °C, allowing for smooth extrusion and proper solidification.<sup>138</sup> Hence, crosslinking methods such as ionic, thermal, or photochemical require precise temperature control to ensure optimal printability and adequate bonding after extrusion. Among various cross-linking materials, thermally crosslinked hydrogels are becoming increasingly popular because they enable flexible crosslinking through adjustments to the temperature and duration.<sup>139</sup> For instance, Moncal *et al.*<sup>140</sup> designed a novel thermally-controlled extrusion unit for the bioprinting of collagen/Pluronic composite bioinks. The rat bone marrow-derived stem cells (rBMSCs) were incorporated into the composite bioink, and their viability and proliferation were assessed over a week *via in vitro* cell culture. The formulated bioink showed promising performance for bioprinted cells. The cells could attach, spread, and increase within the collagen fibers. Due to its capability to regulate the alignment of collagen fibers, this composite bioink holds potential promise for future applications in cartilage,<sup>141</sup> skin,<sup>142</sup> or corneal<sup>143</sup> tissue engineering. Additional research is necessary to create extrudable biomaterial bioinks that possess suitable mechanical properties and bioactivity, specifically adapted to the requirements of different organs and tissue elasticity.

### 3.2 Designing bioink for jetting-based 3D bioprinting

Surface tension, inertia, and viscosity are the main forces influencing the jetting phenomena in bioprinting.<sup>144</sup> The relative importance of these forces in basic jetting phenomena can be evaluated using Reynolds and Weber dimensionless numbers.<sup>126</sup> Droplet dispensing is effective only at a specific ratio of these forces. The Reynolds number (Re) indicates the ratio of inertial forces to viscous forces, as shown below in eqn (1).

$$\text{Re} = \frac{\rho V d}{\eta} \quad (1)$$

where  $\rho$  and  $\eta$  are the fluid density and viscosity, respectively,  $V$  is its characteristic velocity, and  $d$  is the characteristic length scale, typically the diameter of the jet, nozzle, or droplet. The Weber number (We) in eqn (2) represents the ratio of inertial forces to surface tension.<sup>145</sup>

$$\text{We} = \frac{\rho V^2 d}{\gamma} \quad (2)$$

where  $\gamma$  is the surface tension. For droplets, the Weber number also reflects the ratio of the droplet's kinetic energy to its surface energy. For a droplet to be dispensed effectively, its kinetic energy must exceed the surface energy to keep the droplet intact. Practical dispensing occurs when  $We > 4$ .<sup>146</sup> When the droplet's inertia or kinetic energy is excessively high, it can result in undesirable splashing upon hitting the surface. Splashing occurs when  $We^{1/4}Re^{1/4} > 50$  for simple Newtonian fluids on flat smooth surfaces.<sup>147</sup>

The Ohnesorge number (Oh) effectively summarizes the physical properties of the bioink and the characteristic length scale as follows in eqn (3).

$$Oh = \frac{\sqrt{We}}{Re} \quad (3)$$

These properties are sometimes represented as the inverse of the Ohnesorge number ( $Z = Oh^{-1}$ ) or as the Laplace number ( $La = Oh^{-2}$ ). The value of the Ohnesorge number is independent of the driving conditions, *i.e.*, fluid velocity.<sup>148</sup> When the Ohnesorge number exceeds 1 ( $Oh > 1$ ), viscous forces dominate and obstruct the separation of droplets from the nozzle.<sup>149</sup> When the Ohnesorge number is too low ( $Oh < 0.1$ ), the viscous forces are unable to stabilize the breaking jet, causing it to break apart into several unwanted satellite droplets.<sup>150</sup> Satellite droplets have much less momentum than a single large droplet, making them more prone to being altered by air currents between the droplet and the medium. This results in uncertainty in their placement.<sup>151</sup> Hence, designing an effective bioink for jetting-based bioprinting necessitates thoroughly understanding the above-mentioned physical factors. Optimizing these parameters is crucial for improving the performance of jetting-based technologies and thereby advancing the field of tissue engineering.

### 3.3 Designing bioink for VAT photopolymerization-based 3D bioprinting

In VP, several important factors impact the quality and performance of the printed constructs, with viscosity playing a crucial role.<sup>152</sup> It affects multiple elements of the printing process and the final product, including the polymerization rate, oxygen inhibition, cure depth, green strength, and the forces applied to the construct during the peeling process. Most importantly, viscosity affects the resin's printability by controlling the recoating process between layers. As mentioned earlier, each printed layer requires a new resin coating before photopolymerization can continue. When the resin flows more slowly, this step takes longer, increasing the time between layers and extending the print duration.<sup>153</sup> Resins with high viscosity can cause bubbles or result in an incomplete recoating. Therefore, high-viscosity polymers should be avoided, and low-viscosity resins are preferred to improve the efficiency of the recoating process.<sup>154</sup> Viscosities appropriate for VP typically vary from 1 Pa s to 10 Pa s, depending on the molecular weight.<sup>155</sup> The resin's viscosity affects the cure rate by influencing monomer mobility. Generally, lower viscosity enhances

monomer mobility, allowing reactive functionalities to interact more quickly and speeding up cure rates.<sup>156</sup> Accelerating the conversion from liquid resin to solid construction leads to reduced overall construction times. Higher viscosity increases cross-linking near the surface, improving the green strength of the construct.<sup>157</sup> However, it also raises capillary forces during layer separation, negatively impacting low-modulus hydrogels used in tissue engineering. Therefore, it is crucial to understand how viscosity influences the printing process when developing new bioresins for VP.

### 3.4 Sterilization techniques

Sterilization eradicates all types of microbial life, including bacteria, yeast, and viruses.<sup>158</sup> According to guidelines like ISO 11737, medical equipment must be sterilized to guarantee that no pathogens are present on it.<sup>158</sup> Thus, while using 3D bioprinted constructs in clinical settings, it's essential to consider practical measures that lower the risk of implantation-related infections. The commonly used sterilization methods include chemical and physical methods.<sup>159</sup> Irradiation, autoclaving, steam treatment, plasma, and syringe filtration are examples of physical sterilizing techniques, whereas using peracetic acid (PAA), ethanol, and ethylene oxide (EtO) are the chemical methods.<sup>160</sup> For example, microorganisms are made inactive in EtO through the alkylation of nucleic acid groups, including hydroxyl, carboxyl, phenolic, and amino groups. As a result, the microbes suffer damage or die, which stops their ability to replicate and metabolize. Rizwan *et al.*<sup>161</sup> studied the impact of different sterilizing techniques like autoclaving, EtO treatment, and gamma ( $\gamma$ ) irradiation on GelMA-based bioinks. The findings suggested that sterilization using EtO reduced the viability of the encapsulated cells. Both autoclaved GelMA samples and samples treated with EtO showed a notable decrease in compressive modulus.  $\gamma$  irradiation compromised the printability of GelMA, likely due to its detrimental effect on the sol-gel transition. Overall, autoclaving showed no cytotoxic effects and did not affect printability, indicating its suitability for GelMA-based bioinks. Similarly, Hodder *et al.*<sup>162</sup> examined the impact of different sterilization methods on alginate/methyl cellulose (alg/MC) bioinks containing bovine primary chondrocytes for 3D bioprinting. The investigation suggested exposing the bioink to  $\gamma$  irradiation at a dose of 25 kGy notably decreased the stability and viscosity of alginate/methyl cellulose (alg/MC) after bioprinting compared to other sterilization methods. This indicates that  $\gamma$  irradiation might not be appropriate for 3D bioprinting using alg/MC bioinks. To date, bioinks that contain cells cannot be sterilized without causing any damage to the cells. Therefore, new sterilization methods are needed to prevent cytotoxic effects, material deterioration, discoloration, and embrittlement. These methods should preserve the mechanical properties of materials used in bioink and be less damaging to cells and other biological factors. This challenge introduces a new research area with the potential for significant advancements in translational research. Hence, future studies in 3D bioprinting should explore the impact of sterilization on rheology,

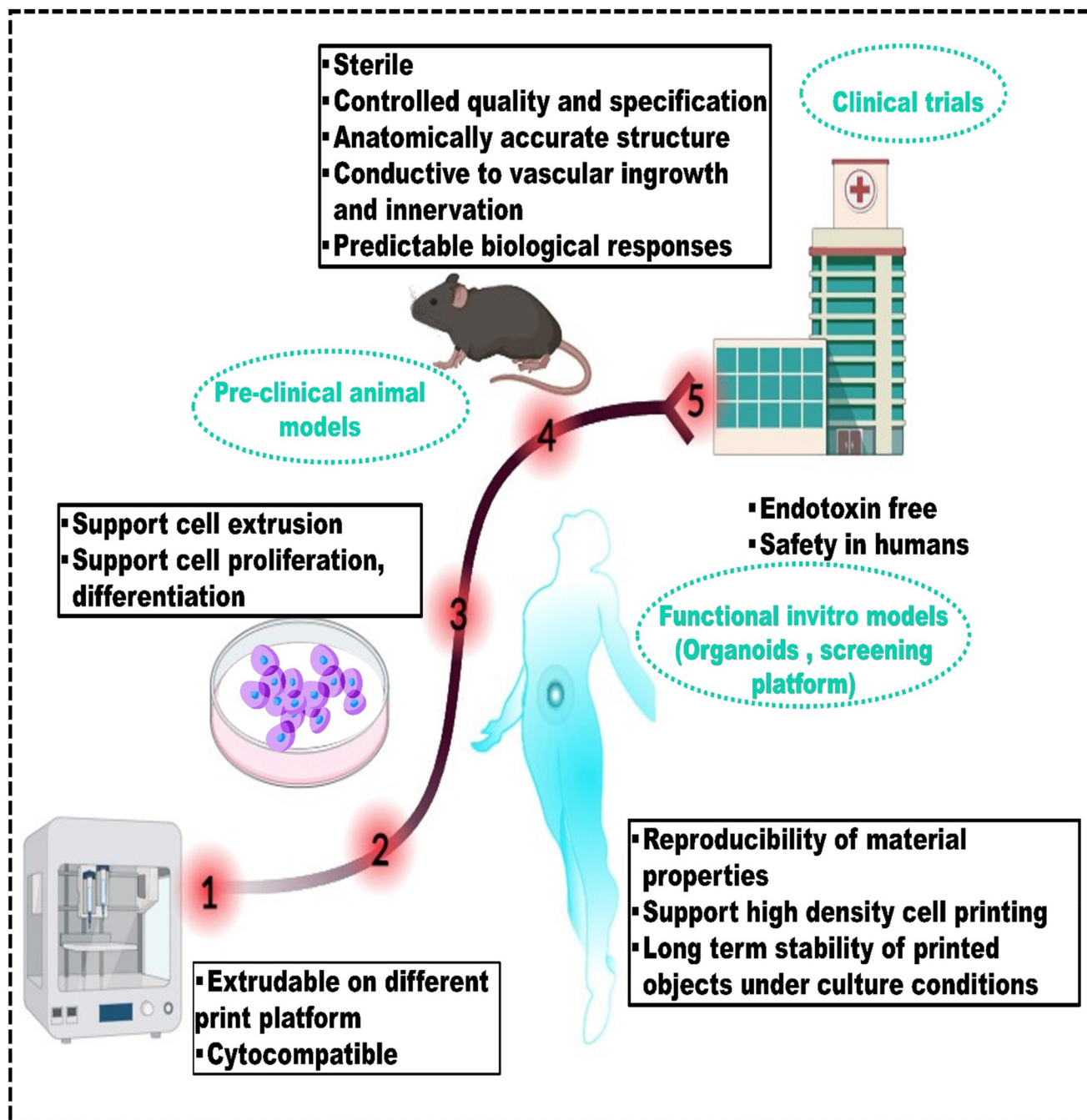


Fig. 4 Navigating the bioinks' translational path to the clinic: standardizing properties through performance criteria, reproduced from Gu *et al.*<sup>163</sup> with permission from Wiley-VCH GmbH, copyright (2021).

printability, and the mechanical and biological properties of the printed constructs.

For successful clinical application of bioprinted structures, it is crucial to maintain their structural integrity, ensure sufficient mechanical strength, and guarantee long-term viability. This necessitates developing bioinks with specific properties and investigating sterilization methods that minimize damage to the bioprinted materials. Hence, there is a need to standardize the properties of bioink using specific criteria and

tools for measuring performance at different stages of development, as shown in Fig. 4.<sup>163</sup>

#### 4. Synthetic and natural polymer-based bioinks

Polymers are commonly used as bioink materials in 3D bioprinting because their diverse and attractive features comp-

lement the 3D printing process. Natural polymers, such as alginate, collagen, gelatin, and hyaluronic acid (HA), have gained popularity due to inherent biocompatibility and similarity to human tissue ECM.<sup>164</sup> Collagen is a significant component of the ECM and has been used in bioinks to regenerate cartilage and skin.<sup>165</sup> HA is a major component of synovial fluid and is widely used in bioinks for cartilage and bone regeneration.<sup>166</sup> Gelatin, derived from collagen, has been used as a bioink for cell encapsulation and the regeneration of various tissues, including bone, cartilage, and skin.<sup>167</sup> In recent developments of natural polymer bioinks, the integration of growth factors and cell signaling molecules has become a notable trend for promoting tissue regeneration.<sup>168</sup> Simultaneously, the application of 3D printing techniques is utilized to construct hierarchical structures and gradients within the printed tissues.

Similarly, synthetic polymers such as polycaprolactone (PCL) and polyethylene glycol (PEG) are commonly used as bioinks due to their well-demonstrated biocompatibility and tunable mechanical properties.<sup>169</sup> PCL has excellent mechanical properties and can be processed into various structures, making it an ideal material for bone tissue engineering.<sup>170</sup> Due to the high water solubility, biocompatibility, and ease of modification of PEG, it can also be widely used as a bioink.<sup>171</sup> It can also be modified to include specific functional groups to enhance cell adhesion and proliferation.<sup>172,173</sup> The polymeric bioinks should align with the 3D printing process and create a

biocompatible environment that closely mimics actual tissue. Ideally, these bioinks should degrade in a controlled manner without producing any harmful by-products.<sup>174</sup> Both synthetic and natural polymers have advantages and disadvantages, and the choice of polymer depends on the specific application and desired properties of the printed tissue or organ. However, most polymeric bioinks initiate gelation after extrusion, typically requiring high polymer fraction solutions (>5 wt%) for sufficient printing viscosity.<sup>39</sup> These dense matrices can impede *in vivo* matrix remodelling and vascularization, making them not suitable for tissue engineering. Moreover, high polymer fractions in cell-encapsulating bioinks can restrict cell activities, limiting their use in cell-laden structures. Rutz *et al.*<sup>175</sup> introduced a single bioink method to generate extrudable, gel-phase bioinks from various synthetic and natural materials (Fig. 5a). While gels typically behave as solids and do not flow, careful control of chemical cross-linking enables gel bioinks to be extruded through fine nozzles (200  $\mu\text{m}$ ) while maintaining their integrity (Fig. 5b). Bioinks were printed layer-by-layer to create well-defined, self-supporting structures where each layer remained stable without collapsing (Fig. 5c). PEGX-fibrinogen and PEGX-gelatin were successfully co-printed, demonstrating the ability to spatially organize multiple ECM types within a single 3D construct (Fig. 5d). Cell viability in PEGX-gelatin and PEGX-fibrinogen bioinks was qualitatively assessed using the live/dead assay, confirming the method's ability to support human

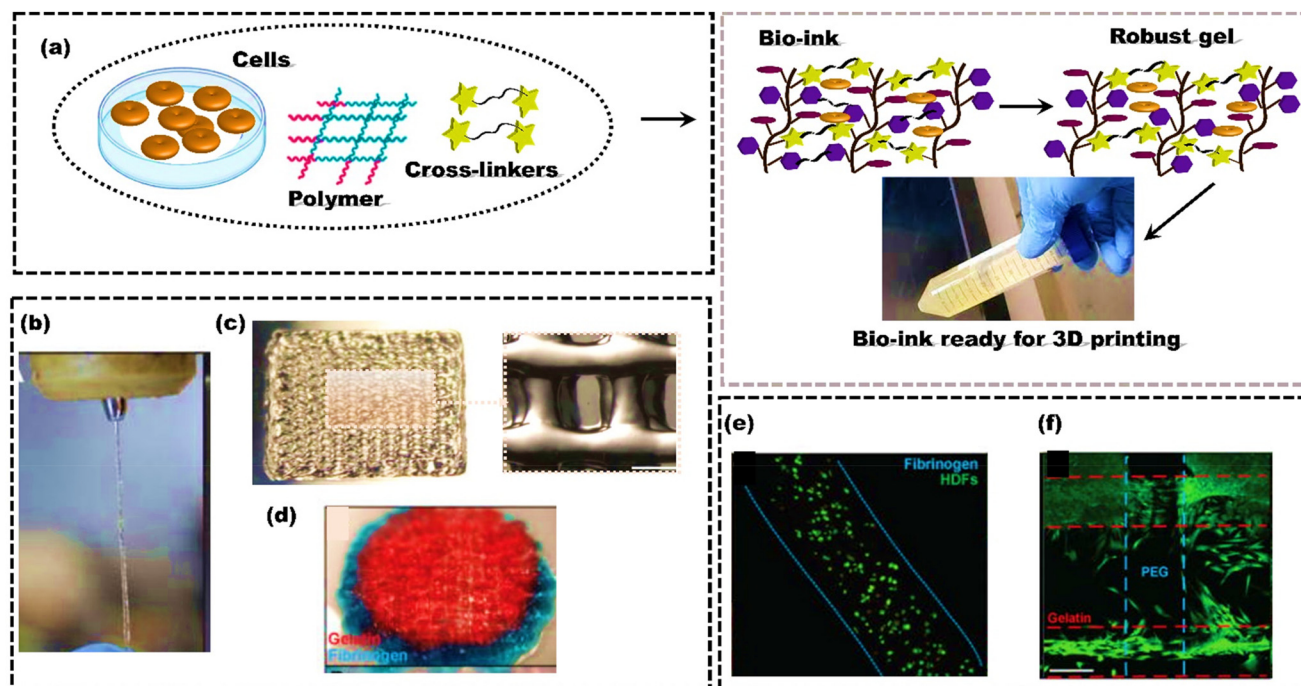


**Fig. 5** Schematic representing the formulation of bioink to form high-strength scaffolds; (a) Polymer, cells and cross-linkers are mixed to form robust gel through cross-linking; (b) extrusion through a 200  $\mu\text{m}$  tip; (c) 15  $\times$  15 mm<sup>2</sup> printed, 4 layers; (d) PEGX-gelatin (red) and PEGX-fibrinogen (blue) co-printed cylinder, 15 mm diameter; (e) cell viability using a live/dead assay at one-day post-printing using 3 w/v% fibrinogen at a 0.2 PEG ratio, scale bars 200  $\mu\text{m}$ ; (f) PEGX-PEG and PEGX-gelatin co-printed structure seeded with HDFs (green, Calcein AM). Cells preferentially adhere to PEGX-gelatin, reproduced from Rutz *et al.*<sup>175</sup> with permission from Wiley-VCH, copyright (2015).

dermal fibroblast (HDF) and human umbilical vein endothelial cell (HUVEC) viability after the printing process (Fig. 5e). PEGX-PEG and PEGX-gelatin were co-printed into a single construct, where HDFs selectively adhered to the gelatin struts, showing the ability to direct cell adhesion to specific areas of the scaffold (Fig. 5f).<sup>176,177</sup>

Polymeric bioinks derived from supramolecular assemblies are increasingly used in biomedical applications, especially for injectable systems delivering therapeutics and cells.<sup>178</sup> Heterogeneity impacts drug release profiles and cellular interactions, emphasizing the importance of biochemical and biophysical signal scales, while controlling microstructural evolution in bioinks enhances methods for introducing structural heterogeneity. Rodell *et al.*<sup>179</sup> modified hyaluronic acid (HA) with  $\beta$ -cyclodextrin ( $\beta$ -CD) or adamantane (Ad) to create CD-HA and Ad-HA, which formed supramolecular assemblies through host-guest interactions. These mechanisms resulted in pore diameters spanning three orders of magnitude and void fractions of up to  $93.3 \pm 2.4\%$ . The findings enhance the understanding of polymer assembly and microstructure in supramolecular hydrogels, facilitating the development of structurally complex systems. However, network relaxations after printing prevent covalent cross-linking from producing highly durable structures. Employing dual cross-linking can mitigate this issue, resulting in improved stability and durability of the printed constructs. Ouyang *et al.*<sup>180</sup> used a dual crosslinking strategy to stabilize printed HA filaments with supramolecular bonds immediately after extrusion. This initial stabilization ensured short-term stability, further strengthened by covalent crosslinking. The printed structures stayed stable for up to a month during incubation. On the other hand, HA-based hydrogel inks that used only single crosslinking, either supramolecular interactions or covalent cross-linking, lost their filament structure or became unstable after just a few layers. The dual-crosslinking approach eliminates the need for additional support materials like gelatin or alginate. Likewise, Hong *et al.*<sup>181</sup> developed a tough hydrogel composed of PEG and sodium alginate, suitable for cell encapsulation. The product hydrogel of covalently cross-linked PEG and ionically cross-linked alginate possesses a high fracture toughness of  $1500 \text{ J m}^{-2}$  (more than the articular cartilage's toughness value<sup>182</sup>). High cell viability, ranging from  $86.0 \pm 3.8\%$  to  $75.5 \pm 11.6\%$ , was observed consistently throughout the 7 day culture period. The resulting hydrogel promotes the long-term viability of cell culture by facilitating nutrient diffusion and waste transport.

Ying *et al.*<sup>183</sup> developed a bioink by combining poly(ethylene oxide) (PEO) and gelatin methacryloyl (GelMA) in an aqueous two-phase emulsion, resulting in bioprinted structures with well-connected pores. The stiffness of the GelMA-PEO hydrogel increased from  $0.9 \pm 0.3$  to  $1.4 \pm 0.1$  kPa as the PEO concentration increased from 0.5% to 1.6%. With a constant PEO concentration, increasing the GelMA-to-PEO ratio from 1 : 1 to 4 : 1 raised the Young's modulus from  $2.3 \pm 0.4$  to  $9.8 \pm 1.6$  kPa. Live/dead assays with different mammalian cells (HepG2, HUVECs, NIH/3T3 fibroblasts) showed that the emul-

sion bioink and resulting porous hydrogels enhanced cell growth and spreading compared to the non-porous hydrogels. Raphael *et al.*<sup>184</sup> described a new methodology for 3D bioprinting of cell-laden constructs with high geometrical definition, mechanical stability, and cell viability. The idea revolves around using a new commercial self-assembling peptide-based hydrogel. This hydrogel forms a nanofibrous bioink through the self-assembly of synthetic peptides when subjected to ionic strengths like those found in the human body. Optimizing the printing parameters enables the system to print both soft and stiff bioinks without compromising the viability of encapsulated cells. This 3D printing method allowed for stacking individual droplets of soft matter bioink to develop larger structures. It was also used to print branched alginate microvasculature.<sup>185</sup> Similar to peptide-based hydrogels, Pluronic also has good printing properties due to shear thinning behaviour and good shear recovery, which are crucial for accurate 3D extrusion printing.<sup>186</sup> Though Pluronic has demonstrated promising *in vivo* outcomes as a material for cartilage tissue engineering, *in vitro* studies have demonstrated that long-term cell viability is low in the presence of more than 5% Pluronic.<sup>187</sup> Unfortunately, significant concentrations of Pluronic are needed to display gelation and the necessary rheological behaviour for extrusion printing. Therefore, the "nanostructuring" method was employed by Müller *et al.*<sup>188</sup> with the aim of enhancing the long-term survival of encapsulated cells while maintaining superior printing qualities. Diacrylate Pluronic F127 (PF127-DA) was mixed with regular Pluronic F127 for 3D bioprinting of bovine chondrocytes. After printing, photocrosslinking stabilized PF127-DA, and washing out PF127 created a nanostructured network. This nanostructuring improved the long-term viability of bioprinted chondrocytes to 86%, compared to 62% for pure acrylated Pluronic hydrogel.

Overall, the studies mentioned above highlight the benefits of composite bioinks formed by blending natural and synthetic polymers or different synthetic polymers. This approach leverages their complementary properties to overcome individual advantages and disadvantages.<sup>189</sup> Still, there is a need to include tissue-specific cues to replicate the native ECM and biomimetic environment to support cell adhesion, proliferation, and differentiation.

## 5. Tissue-specific bioinks

More recently, the quest for a suitable bioink to create a conducive microenvironment for cellular activities has been emphasized. This is because conventional bioinks struggle to replicate or inherit the intrinsic cues present in a native ECM.<sup>190</sup> Therefore, bioinks must be designed to mimic the specific properties of the target tissue, such as biocompatibility, mechanical strength, and appropriate degradation rates to replicate or inherit the intrinsic cues present in a native ECM. For example, bioinks created for skin tissue printing must imitate the unique traits of skin, such as stretchability and flexibility. Conversely, bioinks used for bone tissue printing

must replicate the ability of the bone to endure mechanical stress. The ongoing progress in biomaterials science is anticipated to further refine the development of tissue-specific bioinks for 3D bioprinting.

### 5.1 Bioinks for skin tissue engineering

Skin, the largest organ of the human body, has a multidimensional architecture with three distinct layers: the epidermis, dermis, and hypodermis.<sup>191</sup> The epidermis acts as a barrier against pathogens and UV radiation. The dermis provides structural support, contains nerve endings for sensation, and maintains the vascular network for thermoregulation. The hypodermis is crucial for temperature regulation, serving as an insulating layer. The adipose tissue within it traps heat and helps maintain the core temperature of the body by minimizing heat loss to the environment. The interaction of these layers and their microstructures ensures the essential function of skin tissue.<sup>192</sup> The protective function of the skin is crucial for preventing injuries and maintaining integrity. However, skin injuries or burns and damage significantly impact global healthcare spending, accounting for over half of annual expenditures.<sup>193</sup> This emphasizes the importance of understanding and addressing the function of skin and vulnerabilities to prevent and treat skin-related health problems effectively. Skin tissue engineering offers a promising solution for treating skin injuries and disorders, using grafts from the patient or donors.<sup>194</sup> However, traditional methods like skin grafts and flaps have limitations such as donor site morbidity and availability issues. The limitations of traditional methods in creating precise microarchitecture and replicating native skin can be overcome by 3D bioprinting.<sup>195</sup> However, one of the main challenges in bioprinting skin substitutes is accurately depositing layers to replicate the complex structure of skin tissue.<sup>196</sup> Thus, achieving success in this field necessitates selecting an appropriate bioink with biomaterials, cell sources, and the growth factors that support cell proliferation, differentiation, and tissue regeneration.<sup>197</sup> The bioprinted skin grafts must replicate the composition and properties of native skin layers to encourage *de novo* tissue formation with functional characteristics.<sup>198</sup> Recently, dECM has paved the way for innovative therapeutic products in skin tissue engineering and advanced biomimetic *in vitro* systems for skin modeling. It offers significant potential and has shown promising results for wound healing and *in vitro* skin modeling. dECM derived from the porcine dermis can be used to create a printable bioink containing human dermal fibroblasts. Jang *et al.*<sup>199</sup> created a skin-like structure using a bioink containing skin-derived dECM, keratinocytes, and fibroblasts with 3D bioprinting technology for surgeries involving skin transplantation and extensive burns.

The 3D-printed skin showed rapid re-epithelialization and superior tissue regeneration in histological and immunohistochemical analyses of the animal experiment.

Likewise, Lee *et al.*<sup>200</sup> developed a soft tissue-specific bioink using decellularized porcine skin powder (PSP) (Fig. 6a). The study showed that higher PSP concentrations increased the vis-

cosity, making the bioink suitable for 3D printing (Fig. 6b). Cell viability was approximately 75%, and there was notable preservation of elastin, suggesting that PSP-inks could be a viable option for skin dermis bioink in 3D bioprinting (Fig. 6c).

Ramakrishnan *et al.*<sup>201</sup> developed a multicomponent bioink system comprising gelatin, alginate, dECM, and fibrinogen for 3D printing skin tissues with dermal and epidermal histology. This bioink exhibited excellent shape fidelity, shear-thinning properties, and muscular mechanical strength. Histological studies revealed collagen-I and CK14 markers, indicating maintained cellular phenotype and functionality. The cells expressed skin-specific genes and secreted proteins, with regulated ECM deposition supporting effective tissue regeneration, making it suitable for wound healing applications. Despite these advantages, some challenges still need to be addressed that are quite complex, such as fabricating skin constructs with features like hair follicles, sweat glands, and sebaceous glands.<sup>202</sup> Achieving the accurate colour and texture to imitate natural skin can be challenging.<sup>203</sup> Despite challenges, skin-specific bioinks hold immense potential in skin tissue engineering, offering a promising path for advanced skin substitutes in wound healing, cosmetics, and disease modeling.<sup>204</sup>

### 5.2 Bioinks for bone tissue engineering

The available methods for restoring bone defects, like allografts and autografts, face several challenges.<sup>206</sup> These include limited donor tissue supply, the risk of complications, transplant rejection, and biocontamination.<sup>207</sup> Bone tissue engineering has gained traction as a promising approach involving replacing bone tissue with a 3D scaffold containing cells.<sup>208,209</sup> 3D scaffolds are designed to mimic bone ECM and can also contain bioactive factors to stimulate bone regeneration.<sup>210</sup> Numerous fabrication methods for bionic 3D scaffolds have been developed, such as phase separation,<sup>211</sup> electrospinning,<sup>212</sup> and salt leaching, *etc.*<sup>213</sup> These methods create porous matrices with controlled surface morphology and adjustable processing variables. However, they may occasionally result in less controlled structures. In contrast, 3D bioprinting uses bioink to create scaffolds with complex geometries, evenly distributing cells and releasing signaling factors in an orderly manner.<sup>214</sup> Establishing a complex 3D structure with a personalized and enriched ECM composition in bone tissue regeneration is a fundamental initial step.<sup>215</sup> This requires cytocompatible and osteoinductive bioink for successfully regenerating functional bone tissue.<sup>216</sup> Synthetic self-assembling peptides, with a nanofibrous structure resembling the native ECM, are an excellent component of bioinks. Amorphous magnesium phosphates (AMPs) are synthetic self-assembling peptides that demonstrate enhanced resorption efficacy while maintaining elevated biocompatibility, osteoinductive properties, and mitigated inflammatory response.<sup>217</sup> Dubey *et al.*<sup>218</sup> developed a bioink made of ECM hydrogel and AMP encapsulated with dental pulp stem cells (DPSCs) for 3D bioprinting of craniomaxillofacial bone tissue (Fig. 7a and b). The ECM/AMP bioink showed improved osteogenic differen-

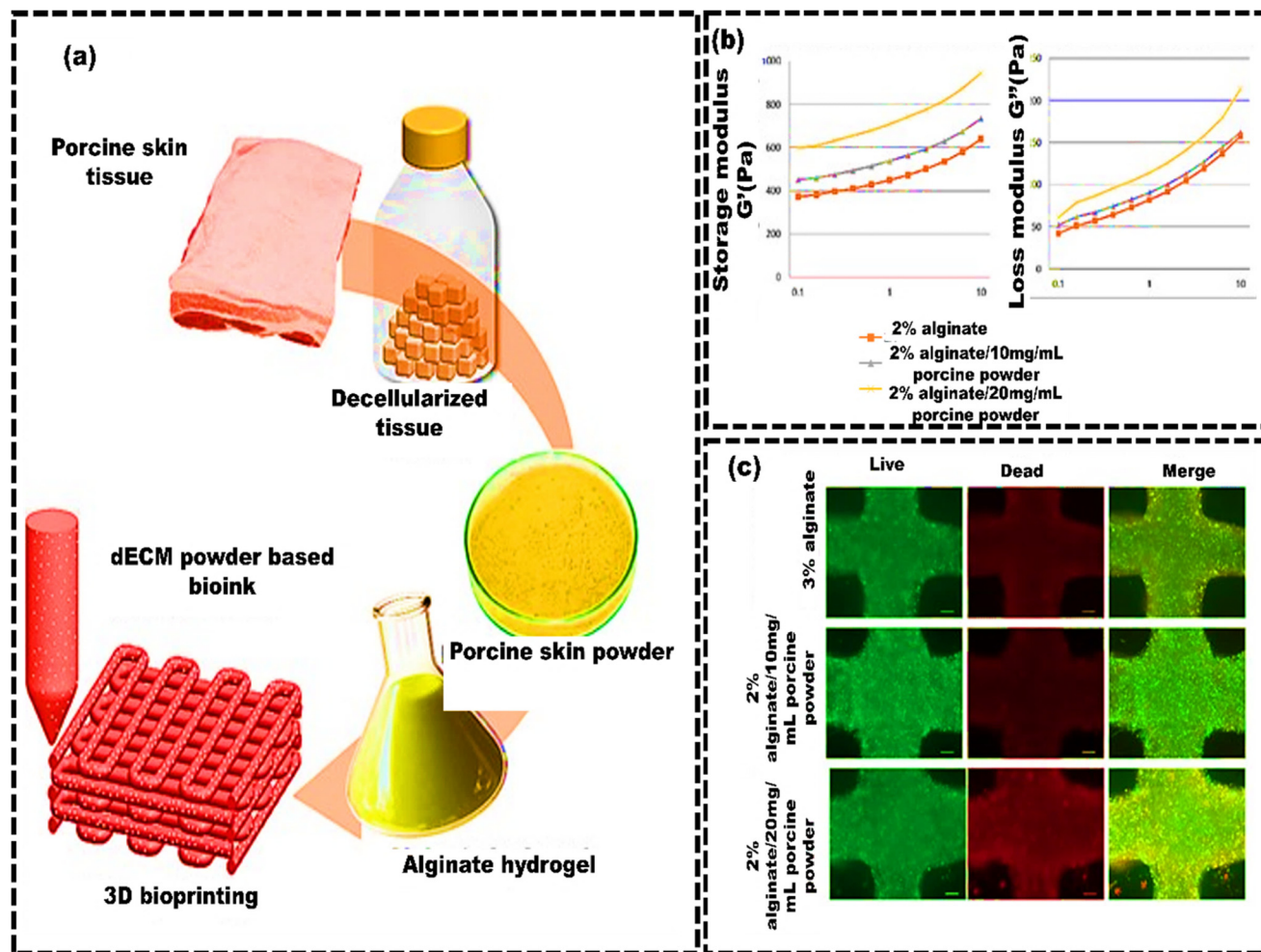


Fig. 6 Skin decellularized bioink for soft tissue engineering. (a) Schematic of the manufacturing process of porcine skin powder (PSP)-based inks, which involves decellularized porcine skin tissue for bioprinting; (b) mechanical properties of PSP-inks: logarithmic plots of storage modulus  $G'$  and loss modulus  $G''$  against frequency (0.1–10 Hz at 24 °C); (c) cellular metabolic activity and viability assessment of printed cells in PSP inks using fluorescence imaging of live/dead staining. Scale bars represent 200  $\mu\text{m}$ , reproduced from Lee *et al.*<sup>205</sup> with permission from MDPI, copyright (2020).

tiation compared to the ECM bioink without requiring chemical inducers (Fig. 7c). This bioink enables the fabrication of 3D constructs with good shape fidelity and osteogenic potential, suggesting that AMP can trigger osteogenic differentiation in encapsulated DPSCs. Compared to the ECM group, the ECM/AMP formulation had 1.7 times higher bone volume at 4 weeks and 1.4 times higher at 8 weeks. Bone density in ECM/AMP increased significantly from 4 to 8 weeks (Fig. 7d). This demonstrates that AMP in the bioink significantly enhanced bone formation, supporting its potential for *in situ* bioprinting. Similarly, the concept of nanoengineered ionic covalent entanglement (NICE) for 3D bone bioprinting can also be used to further enhance the osteogenic differentiation of the stem cells without the need for any osteogenic medium. The NICE bioinks provide precise control over printability, mechanical properties, and degradation, allowing customized 3D biofabrication of resilient, cellularized structures. Chimene D *et al.*<sup>219</sup> developed a NICE bioink to address the issues of developing a bioink compatible with cells and featuring excellent printabil-

ity to repair craniomaxillofacial bone defects. The study showed that the osteoinductive bioink stimulated the production of osteo-related mineralized ECM by encapsulating hMSCs without the need for growth factors. These NICE bioinks offer a precise method to reconstruct bone structures from CT scans of actual patients. They serve as a customizable and user-friendly alternative to autografts, providing surgeons with more options for bone surgery. Although these reconstructed structures using NICE bioink provide anatomical resemblance, additional bone-specific cues are needed to imitate the complex environment of native bone tissue more effectively. Lee *et al.*<sup>220</sup> developed a process to generate bioactive alginate-based bioink with dECM obtained from porcine bone. The bone derived dECM was modified through the methacrylate (Ma) reaction, referred to as Ma-dECM, to avoid the issue of low printability of the dECM. Ma-dECM was incorporated into alginate to create a composite bioink. The printability and cell viability were then assessed using human adipose-derived stem cells. The developed alginate-based cell-

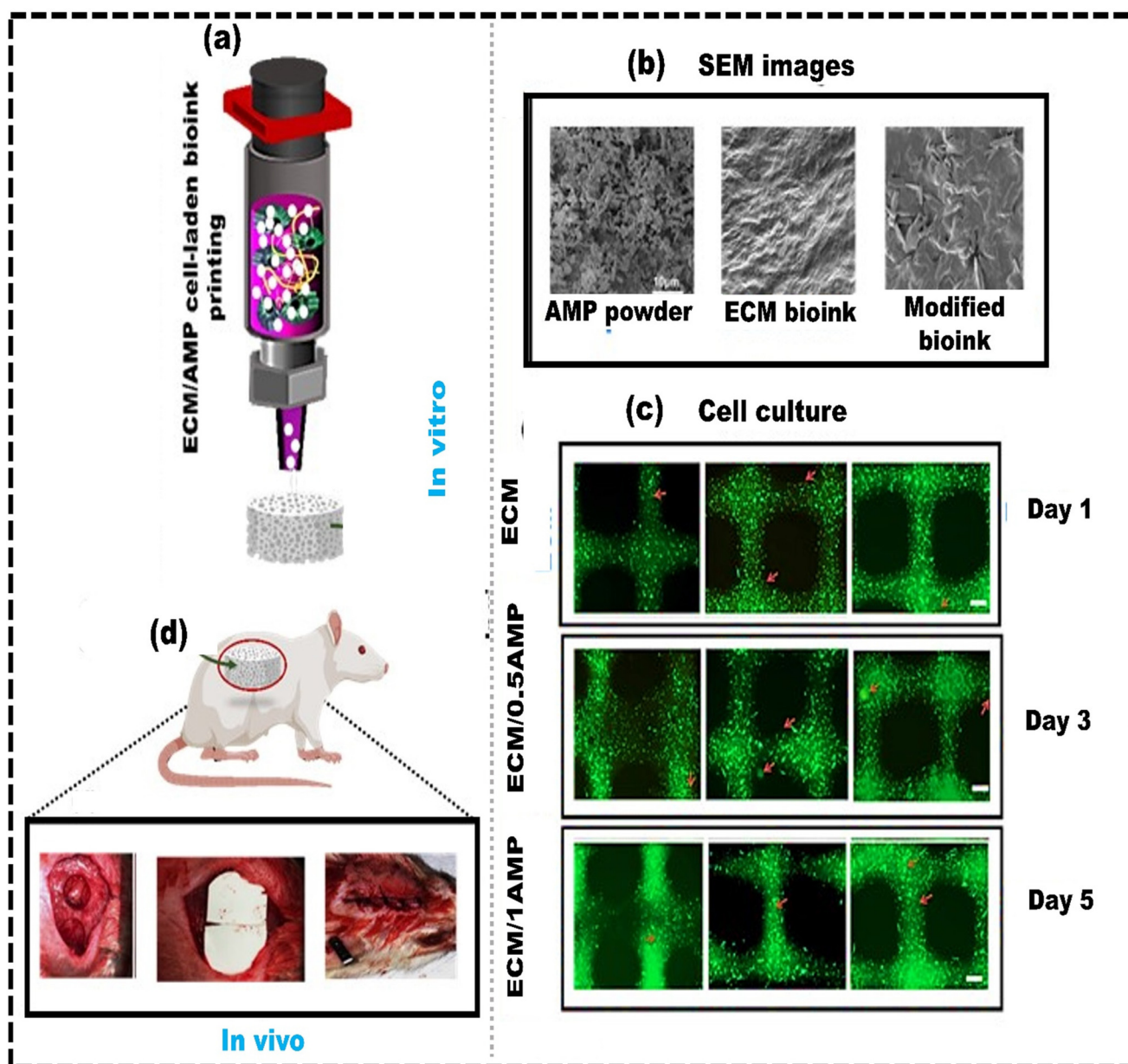


Fig. 7 Development of a bone-specific bioink for 3D constructs with high shape fidelity and osteogenic potential: (a) 3D bioprinting of ECM/AMP cell-laden bioink; (b) SEM images of AMP powder, ECM bioink, and AMP modified bioink; (c) Calcein AM (green) and PI (red) staining assay for live and dead cell analysis showing the elongated morphology in AMP modified constructs; (d) image showing the defect after wound cleaning, implantation and suture performed in rats, reproduced from Dubey *et al.*<sup>218</sup> with permission from American Chemical Society, copyright (2020).

laden structures significantly affected the ability of human adipose-derived stem cells to differentiate into bone-forming cells when incorporated into the bioink. The composite bioink showed high *in situ* cell viability of more than 90%, suggesting that the polysaccharide-based biomaterial composite bioink had potential for bone tissue engineering applications. Kim *et al.*<sup>221</sup> proposed a novel bioink comprising bioceramic ( $\beta$ -TCP), fibrillated collagen and cells to create a 3D porous cell-laden composite structure. The composite structures demonstrated good mechanical stability and substantial cell viability ( $\sim$ 90%) in both preosteoblasts (MC3T3-E1) and

human adipose stem cells (hASCs). Furthermore, compared to the pure collagen bioink (control), the composite structure showed a considerable increase in osteogenic activity. Moreover, the hASC-loaded composite structure exhibited elevated levels of osteogenic gene expression even without an osteogenic medium, indicating that  $\beta$ -TCP enhanced the osteogenic differentiation of hASCs.

Overall, reconstructing defective bone tissue is complex, but bioprinting offers significant benefits for creating biomimetic implants. Significant progress has been made in selecting bioink components and formulating hydrogel-based

bioinks containing cells and dECM. These bioinks promise to improve scaffold compatibility and mechanical properties, which are essential for successfully fabricating tissue-engineered constructs. However, bionic scaffolds do not yet possess the same level of intelligence as actual tissues.

Therefore, improving bioink formulations for bone tissue engineering requires the careful selection and combination of materials replicating the native ECM, optimizing mechanical properties, and ensuring high cell viability and proliferation. The key strategies include incorporating a decellularized bone matrix and using hydrogels with tunable properties to enhance interactions between printed tissues, cells, and their microenvironment. Ongoing research and development on optimization in these areas is essential for advancing 3D bioprinting in bone tissue engineering applications.

### 5.3 Bioinks for cartilage tissue engineering

Articular cartilage is smooth white tissue with the primary role of offering a seamless, lubricated surface for movement and enabling the transfer of loads with minimal friction.<sup>222</sup> It consists of a compact ECM with a limited number of highly specialized cells known as chondrocytes. The ECM mainly consists of water, collagen, and proteoglycans, with smaller amounts of non-collagenous proteins and glycoproteins. These components collectively retain water, which is crucial for preserving the distinctive mechanical properties of ECM. Articular cartilage lacks blood vessels, nerves, or lymphatic channels, which makes it different from other tissues. Due to this, cartilage tissue exhibits a limited capacity for self-repair to the damage caused by congenital conditions, trauma, cancer, or age-related diseases.<sup>223</sup> Traditional cartilage repair methods (e.g., grafts, microfracture, and autologous chondrocyte implantation) have limitations like donor-site issues and tissue integration. Despite various advancements in repairing cartilage defects, the restricted spatial complexity of tissue-engineered implants, particularly in terms of cell types, materials, and active factors, has hindered the overall success of engineered cartilage.

The utilization of bioprinting technology in cartilage tissue engineering holds the potential to tackle cartilage defects and regeneration methods.<sup>224</sup> Selecting a bioink with a suitable composition and mechanical properties is essential for developing adequate cartilage substitutes. Antich *et al.*<sup>225</sup> developed a composite bioink with HA and alginate, co-printed with polylactic acid (PLA), using 3D bioprinting. The hydrogel in bioink forms cross-linked gels in the presence of calcium as a cross-linker, creating a hybrid construct for AC regeneration. The HA-based bioink and 3D hybrid construct exhibited compression and shear modulus values like those in healthy human articular cartilage. Live/dead staining showed over 85% cell viability before and after printing, demonstrating effective cell preservation due to the shear-thinning properties of bioink. Genomic stability of chondrocytes, assessed by G banding, revealed no karyotype changes, confirming a typical diploid karyotype and stable chromosomal integrity post-bioprinting. However, using chemical cross-linkers can result in

adverse effects like cell toxicity, structural alterations in polymers, and increased costs, emphasizing the importance of crosslinker-free alternatives.<sup>226</sup> Singh *et al.*<sup>227</sup> created a bioink without crosslinkers, which is ideal for extrusion and promotes cartilage repair. This ink combines *B. mori* and *P. ricini* silk, initiating self-gelling. Gelatin is then added to form a viscoelastic ink suitable for bioprinting. Porcine chondrocytes were encapsulated in this bioink and evaluated for printability, fidelity, biological function, and compatibility *in vitro* and *in vivo*. Optimal concentrations for cell-laden bioprinting were 5%–9% gelatin and 1%–2% silk fibroin. The bioink had the lowest viscosity between 25 and 35 °C, exhibiting gel-like properties at 4–25 °C and 35–45 °C and more liquid-like behaviour at 25–35 °C. Calcein-AM staining confirmed chondrocyte viability with a spherical morphology. *In vivo* testing by implanting the construct fabricated from that bioink under mouse skin showed cellular distribution within the construct, supporting its use in cartilage tissue engineering.

Rathan *et al.*<sup>228</sup> developed a hybrid construct for treating focal articular cartilage defects using a 3D-printed PCL network and cartilage-ECM (cECM)-functionalized bioink and evaluated its mechanical properties and biocompatibility. The biofabricated constructs demonstrated mechanical properties that closely mimicked the native articular cartilage. The bioinks are 3D printable, support MSC viability post-printing, and promote robust chondrogenesis *in vitro*. Enhanced chondrogenesis in cECM-functionalized bioinks is linked to a pathway resembling natural cartilage development, as seen through increased RUNX2 expression and calcium deposition *in vitro*. However, single-layer scaffolds cannot replicate the depth-dependent zonal structure of native cartilage, which is crucial for articular cartilage regeneration. Kang *et al.*<sup>229</sup> developed a trilayer scaffold using poly(ethylene glycol)-diacrylate-co-6-aminocaproic acid copolymers (bioink) to support the continuous differentiation of donor cells into cartilage tissue and to stimulate bone formation by recruiting endogenous cells. The trilayer scaffold consists of a biom mineralized bottom layer mimicking the calcium phosphate (CaP)-rich bone microenvironment, a cryogel middle layer with anisotropic pore architecture, and a hydrogel top layer. When the trilayer scaffold was implanted *in vivo*, these scaffolds promoted osteochondral tissue development with a cartilage surface rich in lubricin.

Despite these accomplishments, enhancing the mechanical properties of engineered cartilage constructs is crucial because joints experience tension, shear, and compression loads during daily activities.<sup>230</sup> So, the artificial cartilage replacements must be strong enough for appropriate joint reconstruction and capable enough to restore their properties after being exposed to changing external factors such as pH, temperature, shear stress, *etc.* Therefore, the research communities are more attracted to self-healing hydrogels for the formulation of bioinks to restore damaged cartilage tissues.<sup>231</sup> Overall, the cartilage-specific bioinks for fabricating the cartilage tissue equivalents are currently in the initial stages of preclinical trials. For example, over the past five years, only a few clinical trials evaluating cartilage tissue equivalents have been regis-

tered on ClinicalTrials.gov.<sup>232</sup> Therefore, more development is needed in bioinks designed explicitly for cartilage tissue engineering, which will likely increase the preclinical and clinical trials on cartilage-specific bioinks.

#### 5.4 Bioinks for liver tissue engineering

The liver is pivotal in facilitating over 500 distinct biochemical processes like metabolic activities, bile synthesis, detoxification, coagulation, immunological functions, thermogenesis, the regulation of water and electrolyte levels, and so on.<sup>233</sup> The liver houses several types of resident cells, including hepatocytes, hepatic stellate cells, liver sinusoid endothelial cells, Kupffer cells, and biliary epithelial cells. Liver conditions like acute liver failure (ALF),<sup>234</sup> chronic liver condition (CLD),<sup>235</sup> fibrosis, viral hepatitis,<sup>236</sup> and cancer are causing higher mortality. Hence, the global burden of liver disease is rising, leading to around 2 million deaths annually and resulting in substantial economic costs and decreased quality of life.<sup>237</sup> Essential surgeries like hepatectomy and liver transplants are crucial. For patients with severe liver dysfunction, transplantation is the only effective treatment.

However, due to limited donors, immune rejection, and surgical complications, liver transplants face challenges in clinical practice.<sup>238</sup> Liver tissue engineering holds promise in addressing the aforementioned challenges, and 3D bioprinting is an innovative approach to improve these procedures.<sup>239</sup> Bioinks for liver tissue engineering are formulated using readily available biomaterials like gelatin, collagen, alginate, etc.<sup>240</sup> However, these bioinks cannot replicate the ideal biological environment for liver tissue regeneration because they lack liver-specific biochemical components. When liver-derived material serves as a bioink, achieving uniform printing often involves enhancing it with poly(ethylene glycol) diacrylate (PEGDA) and UV cross-linking. However, UV light or radicals from the photoinitiator can unexpectedly affect cell behaviour, potentially causing toxicity in the bioink. Lee *et al.*<sup>241</sup> developed a liver-dECM bioink for 3D cell printing and compared its performance with widely available commercial collagen bioink for different biomedical applications (Fig. 8a and b). The liver dECM bioink effectively preserved the essential ECM components of the liver. It demonstrated excellent printability, with minimal cell death observed during printing, indicating its non-toxic nature. The study evaluated stem cell differentiation and HepG2 cell function in the liver dECM bioink. The results showed that the liver dECM bioink promoted stem cell differentiation and improved HepG2 cell function compared to a commercial collagen bioink. However, the pepsin digestion process, employed to solubilize decellularized tissue for these conventional dECM bioink preparations, degrades the native structure and mechanical strength of the tissue.<sup>242</sup> Furthermore, various researchers have reported that the process of digestion may denature specific biochemical constituents of dECM, such as growth factors and proteins.<sup>243</sup> As a result, the main obstacles to the application of conventional dECM bioink in 3D bioprinting are its weak mechanical properties, inconsistent physical pro-

erties, slow crosslinking speed, and reduced biochemical components. Therefore, improving the 3D printability and mechanical properties of conventional dECM bioink is gaining tremendous attention. In this regard, Kim *et al.*<sup>244</sup> created a dECM bioink with improved 3D printability and mechanical properties using dECM micro-particles (approximately 13.4  $\mu\text{m}$ ) prepared from decellularized porcine liver *via* freeze-milling. These dECM microparticles were incorporated into a gelatin mixture to develop a novel bioink named dECM powder-based bioink (dECM pBioink) (Fig. 9a). The conventional dECM bioink and the dECM pBioink both exhibited a micro-fibril network, with the conventional dECM bioink showing a more compact fibril structure than the dECM pBioink (Fig. 9b). The results demonstrated significant improvement in its printability and mechanical properties. In contrast to conventional dECM bioink, it exhibited a maximum increase in elastic modulus by 9.17 times. Micro-patterns containing viable cells were successfully fabricated with 93% cell viability (Fig. 9c and d). Moreover, the dECM pBioink exhibited better performance in layer stacking for 3D printing than the conventional bioink, which had difficulty in maintaining its shape. These advancements have led to the creation of clinically relevant liver scaffold constructs that are decellularized and recellularized with intact vascular linings, showing promising applications in regenerative medicine. However, despite these advancements, the immunogenicity of decellularized liver scaffolds made from dECM bioink is a concern due to potential antigenic molecules remaining even after cellular removal, which can trigger immune responses upon implantation, leading to scaffold rejection and failure of engineered liver tissue. To address this concern, it is essential to repopulate the parenchymal area within decellularized scaffolds with functional hepatocytes. This approach aims to create a biocompatible environment that integrates well with host tissue, reducing the risk of immune rejection. While primary hepatocytes have consistently maintained their properties, their function has initially demonstrated capabilities such as temporarily stabilizing serum ammonia levels. However, further research is needed to optimize the functionality of repopulated hepatocytes within decellularized scaffolds for achieving long-term, stable liver-specific functions.

Overall, the bioinks derived from decellularized tissues for skin, bone, cartilage, and liver tissue engineering create a biomimetic microenvironment closely resembling the native ECM of the target tissue. By incorporating tissue-specific biochemical cues and preserving the native ECM composition and structure, dECM bioinks support cell adhesion, proliferation, and differentiation. This leads to the formation of complex and heterogeneous tissue constructs that mimic the cellular organization and microenvironment of native tissues. However, controlling compositional changes during decellularization is challenging, leading to batch-to-batch variations due to the differences in tissue composition.<sup>243</sup> Due to variations in the amounts of ECM proteins and cues present in each bioink formulation, these differences influence cell behaviour in bioprinting applications.<sup>245</sup> To address this concern, one poten-

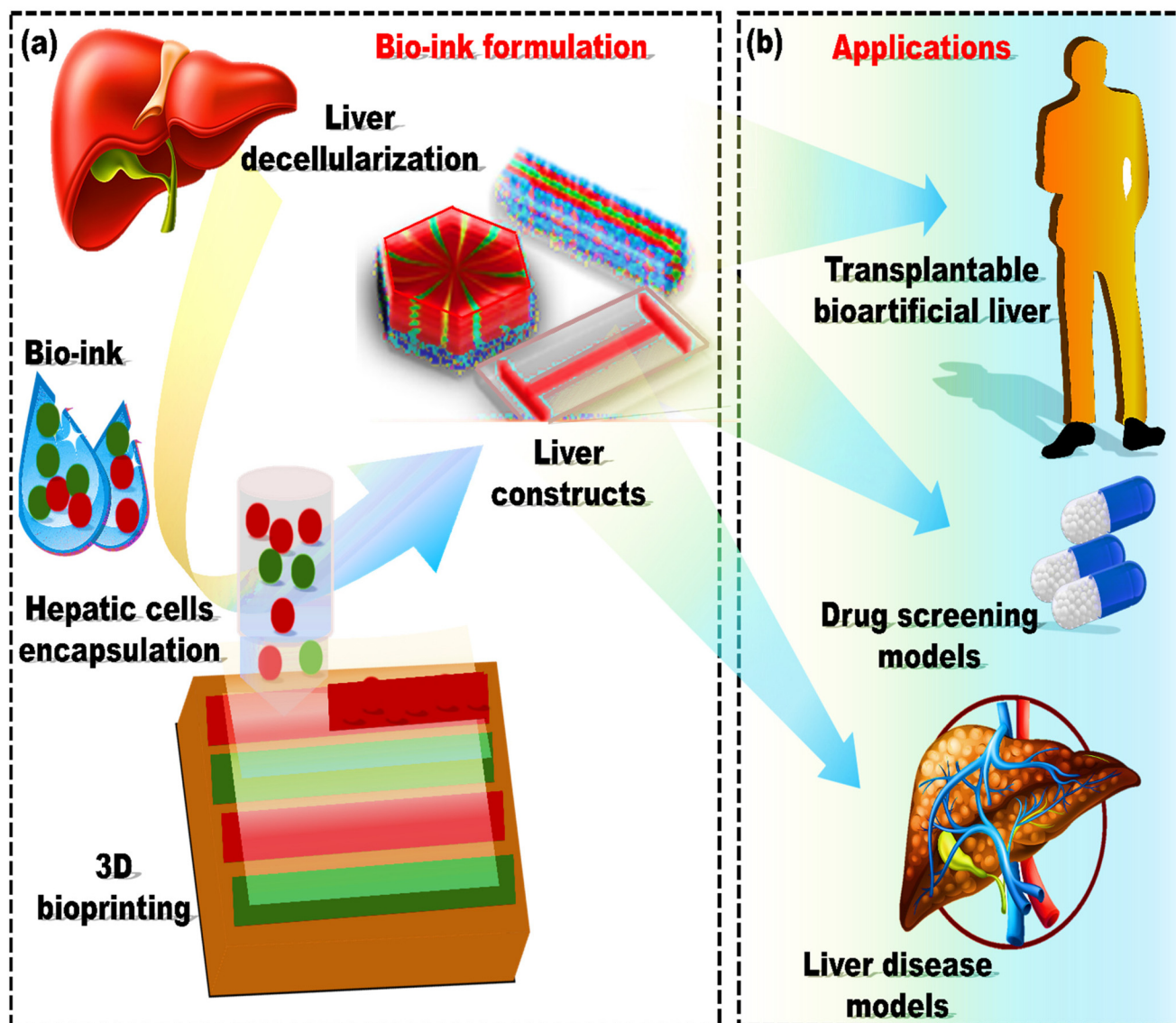


Fig. 8 Diagram depicting (a) the formulation of liver dECM bioink and (b) the utilization of liver dECM bioink in 3D cell printing for liver tissue engineering, reproduced from Lee et al.<sup>241</sup> with permission from American Chemical Society, copyright (2017).

tial solution is to decellularize tissues in larger quantities and then blend them for use in dECM-based bioink formulations. Further investigation is required to overcome these challenges because dECM-based bioinks exhibit considerable potential as viable options for *in situ* bioprinting in various applications, owing to their superior biochemical properties.<sup>246</sup> Table 2 presents several kinds of bioinks that are currently employed in the construction of different tissue constructs.

## 6. Computational methods for predicting bioink properties

The thrust for high-performance bioink in 3D bioprinting opens up new possibilities for designing functional tissue constructs replicating the complex geometries and properties of

native tissues.<sup>265</sup> Extensive research offers experimental support for the notion that different geometric characteristics and tunable material attributes of bioinks can greatly influence cell viability and appropriate development of the target tissue architecture. For example, in the case of drop-on-demand 3D bioprinting, loss of cell viability is impacted by shear stress.<sup>266</sup> Cell viability is a crucial parameter of cell behaviour that can be influenced by the injection process and droplet impact during DoD printing. During the impact process, cell damage is mainly caused by von Mises stress and surface area strain.<sup>267</sup>

Shear stress is a critical factor to consider for cell survival during the injection process.<sup>268</sup> Furthermore, shear stress has a significant impact on cell biology. For example, moderate shear stress has been shown to promote stem cell differentiation,<sup>269</sup> whereas excessive shear stress can damage the cell

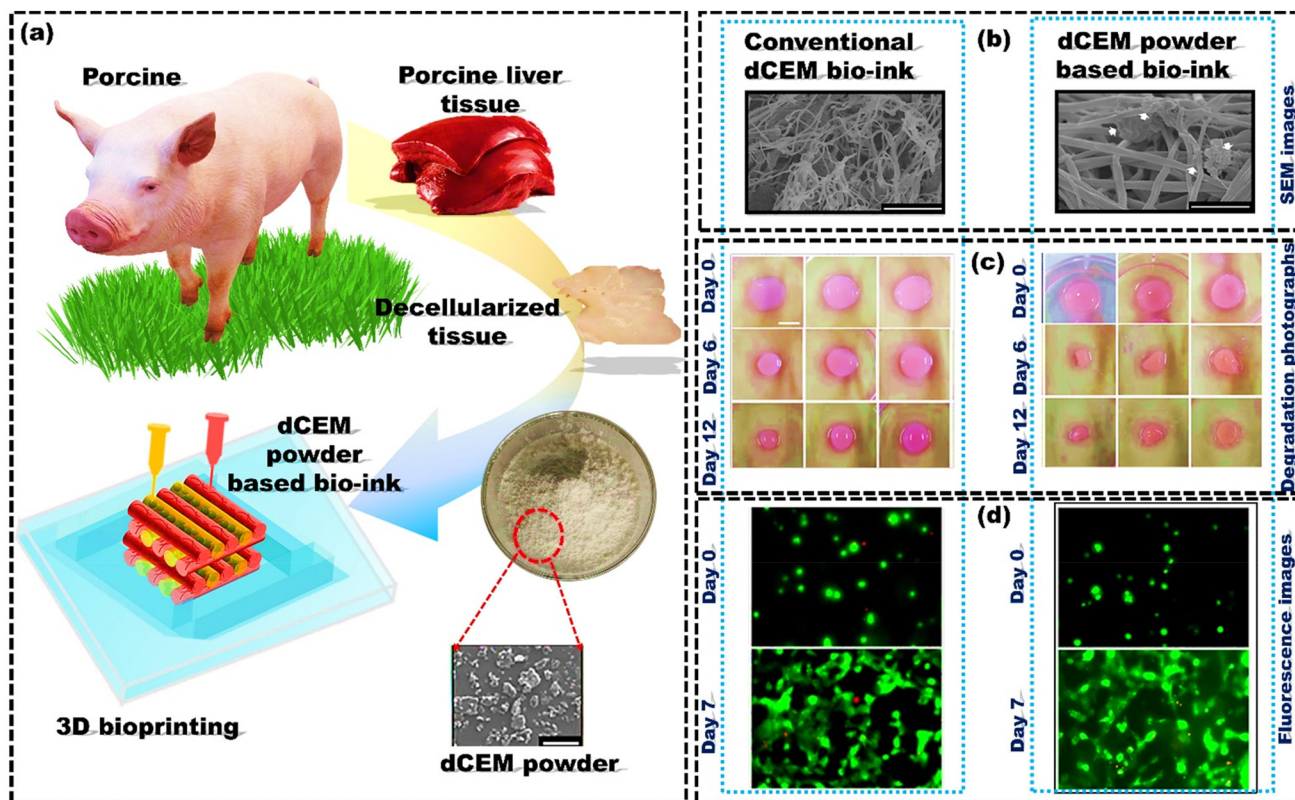


**Fig. 9** Development of liver derived powder based dECM bioink for enhanced printability and mechanical properties: (a) porcine liver tissue is decellularized, powdered, and incorporated into a gelatin mixture to create dECM powder-based bioink (dECM pBioink) for 3D bioprinting; (b) SEM pictures of crosslinked bioinks. The presence of loaded dECM micro-particles is highlighted by white arrows (scale bar: 2  $\mu\text{m}$ ). (c) The degradation of conventional dECM bioink and dECM pBioink (1, 2, and 3 wt%); (d) fluorescence images depicting cell viability on day 0 and day 7, reproduced from Kim *et al.*<sup>244</sup> with permission from IOP Publishing, Ltd, copyright (2020).

membrane, leading to cell rupture.<sup>270</sup> Hence, optimizing shear stress is essential for improving cell viability and ensuring that cellular behaviours, such as proliferation and differentiation, occur correctly. However, to mitigate the issue of shear stress to some extent, microgels are emerging as a star player as a new bioink in 3D bioprinting.<sup>271</sup>

Microgels are water-based particles with micrometer-scale diameters organized similarly to hydrogels, often through dense packing or jamming.<sup>272</sup> The unique rheological characteristics of a microgel can safeguard encapsulated cells from shear forces during the printing process.<sup>273</sup> Due to their distinctive dynamic structure, excellent biocompatibility, and adjustable mechanical properties, microgels hold substantial potential in tissue engineering.<sup>274</sup> However, sometimes cells are encapsulated in an asymmetrical position within the microgel, resulting in partial encapsulation and possible cell escape during gelation and subsequent culturing.<sup>275</sup> Furthermore, incomplete encapsulation or off-center cells in a microgel expose cells unevenly to biochemical and biomechanical stimuli, which can negate the intended functions of the microgel, such as immunoprotection.<sup>276</sup> Therefore, there is a need to overcome these challenges of shear stress during irregular cell distributions and limited cell density for the successful implementation of this 3D bioprinting in regenerative medi-

cine and for effectively addressing organ shortages.<sup>58</sup> Computational simulation has emerged as a valuable resource in this optimization process, effectively reducing the need for extensive experimental trials and the associated costs.<sup>277</sup> Numerous research studies have utilized simulation and modeling in conjunction with experimental methods to improve and predict the mechanical, biological, and rheological behaviour of bioinks.<sup>278,279</sup> One example was the coaxial printing of sodium alginate along with the crosslinking agent calcium chloride by Sun *et al.*<sup>280</sup> to fabricate vascular scaffolds. Finite element simulation helped analyze bioink flow behaviour and the extrusion process, thereby optimizing the printing parameters to control cross-linking to obtain the desired cellular distribution and proliferation within the vascular scaffold. Additionally, by predicting how the crosslinking process affects the mechanical environment within the bio-printed scaffold, finite element modelling simulation enables the optimization of printing parameters, leading to improved cell viability and differentiation. Likewise, using computational fluid dynamics (CFD), a powerful tool that simulates material behaviour *via* parametric modifications to rheological parameters, can reduce the requirement for thorough testing and iterations. Göhl *et al.*<sup>281</sup> utilized a CFD simulation tool (IPS IBOFlow) to investigate the effect of different printing para-

**Table 2** Various types of bioink are used for the construction of bio-printed tissue constructs

Bioink	Printing technique	Tissue	Reference
Cryo bioink	Extrusion based	Vasculature	El Assal <i>et al.</i> <sup>247</sup>
Magnetic iron oxide nanoparticles	Hybrid nano-printing system	Vasculature networks	Yildirim Ö <i>et al.</i> <sup>248</sup>
AgNPs in hydrogels	Extrusion-based printing	Cyborg organs/cartilage	Hassan <i>et al.</i> <sup>249</sup>
Au NPs with thiol-modified hyaluronic acid and gelatin (AuNP-sECMs)	Extrusion-based printing	Vascular	Skardal <i>et al.</i> <sup>250</sup>
Poly(vinyl alcohol) (PVA)	Extrusion-based 3D printing	Artificial cartilage re-constructs	Meng <i>et al.</i> <sup>251</sup>
ECM/AMP hydrogel containing 2% octapeptide FEFEFKFK	Microvalve bioprinting	Cranio-maxillofacial bone tissue	Dubey <i>et al.</i> <sup>252</sup>
Graphene–polyurethane composite	Conventional bio-printer	Neural tissue constructs	Huang <i>et al.</i> <sup>253</sup>
Matrigel with alginate	Pneumatic dispensing system enabled	Human endothelial progenitor cells (EPCs) laden constructs	Poldervaart <i>et al.</i> <sup>254</sup>
Ru/SPS with dECM	DLP bioprinting system and extrusion-based printing	Various tissues	Kim <i>et al.</i> <sup>255</sup>
dECM-based bioink	Bio-architect 3D bioprinter	3D primary ovarian cell-laden	Zheng <i>et al.</i> <sup>256</sup>
GelMA with liver dECM.	DLP (digital light processing)	Liver tissue	Mao <i>et al.</i> <sup>257</sup>
Silk-dECM construct + TGF- $\beta$ encapsulated	Extrusion-based bioprinting system	Cartilage tissue	Zhang <i>et al.</i> <sup>258</sup>
Hyaluronic acid methacrylate (HAMA)	Extrusion-based bioprinting system	3D-printed islet organoid	Wang <i>et al.</i> <sup>259</sup>
Hyaluronic acid (hyaluronan, HA)	Extruder and microvalve-based print	Cartilage tissue constructs	Hauptstein <i>et al.</i> <sup>260</sup>
fibrinogen with PEG or a PEG–gelatin mixture	Thermal inkjet printing technology	Micro-vasculature networks	Cui <i>et al.</i> <sup>261</sup>
Fibrinogen	Laser-based 3D bioprinters	3D assembly of multi-cellular arrays	Gruene <i>et al.</i> <sup>111</sup>
Fibrin and alginate	Inkjet bioprinter	Cartilage tissue	Nakamura <i>et al.</i> <sup>262</sup>
Gelatin–alginate composite	Extrusion-based bioprinter	Cell-laden aortic valve conduits	Duan <i>et al.</i> <sup>263</sup>
Collagen	Laser-based 3D bioprinters	3D skin tissue	Koch <i>et al.</i> <sup>264</sup>

meters on a bioprinting process. IPS IBOFlow imitates the final structure of printed material and the deposition of bioink by utilizing a unique surface tension model and a viscoelastic rheology model. The ability of the simulation tool to replicate 3D bioprinting using ink with diverse viscoelastic properties indicated its potential applicability across various viscoelastic solutions and hydrogels. Choe *et al.*<sup>282</sup> developed a 3D solid mechanics model to investigate the effect of shear stress on the hydrogel scaffold. First, the simulation examined the distribution of stress and deformation of composite scaffolds made from materials used for osteochondral tissue regeneration. Assessments were conducted on four PCL/polyethylene glycol diacrylate (PEGDA) and four PCL/GelMA interface scaffolds (PCL alone, 1 PCL:1 PEGDA, 2 PCL:1 PEGDA, and 3 PCL:1 PEGDA). Second, the simulation examined the distribution of stress and the deformation of several different biphasic interface scaffolds. Shear stresses were applied to these bioink scaffolds with varying moduli (high and low). The scaffolds made up of only PCL demonstrated the uniform distribution of von Mises stress across the interface and exhibited the lowest average von Mises stress values (PCL/PEGDA: 103.31 kPa; PCL/GelMA: 103.42 kPa) (Fig. 10a). Conversely, interface scaffolds with mechanical interlocking designs experienced an elevated von Mises stress at the interface, primarily due to stress concentration within the hydrogel struts forming the interface layer (Fig. 10b). von Mises stress values were highest for PCL/GelMA and PCL/PEGDA interface scaffolds (139.19 kPa and 137.78 kPa, respectively) out of all interface scaffolds with 1:1 interlocking patterns. The 1:1 PCL/GelMA and 1:1 PCL/PEGDA scaffolds with mechanically interlocking interfaces exhibited a notable increase in an average von Mises stress

(PCL/PEGDA: 33%; PCL/GelMA: 35%) compared to their respective PCL scaffolds. In all PCL/GelMA and PCL/PEGDA scaffolds, the cartilage layer showed the highest displacement, while the bone layer exhibited the lowest displacement (Fig. 10c and d).

Cells subjected to mild shear stress (<5 kPa) showed excellent cell viability (up to 96%), while cells subjected to higher shear pressures (5–10 and >10 kPa) had decreased cellular vitality (91% and 76%, respectively).<sup>283</sup> Similarly, CFD can also predict the effect of the temperature of the CELLINK Bioink (commercial bioink) on the velocity and shear stress to optimize the cell viability of the bioprinted constructs. In most bioinks, there are specific functionalities, and their properties can vary significantly with changes in temperature. Therefore, Gómez-Blanco *et al.*<sup>284</sup> used CFD analysis to investigate bioink behaviour at different temperatures (15, 25, and 37 °C) and three conical tip geometries (20, 22, and 25G) as inlet parameters. The study examined the effects of these variables on shear stress, pressure, and velocity in CELLINK Bioink. The simulation results showed that pressure, velocity, and shear stress combinations were almost constant. Using this bioink at 37 °C is recommended to not only reduce shear stress but also enhance the volumetric flow. Increased volumetric flow results in higher bioprinting speeds, which in turn reduces the time for which the cells are subjected to pressure. Moreover, the shear stress predicted by simulations suggested that cell viability remained adequate at all temperatures as long as the values of shear stress were below 5 kPa. Consequently, computational modelling can effectively reduce the need for trial-and-error in 3D printing while improving the results of tissue engineering. So far, most of the studies reported in the litera-

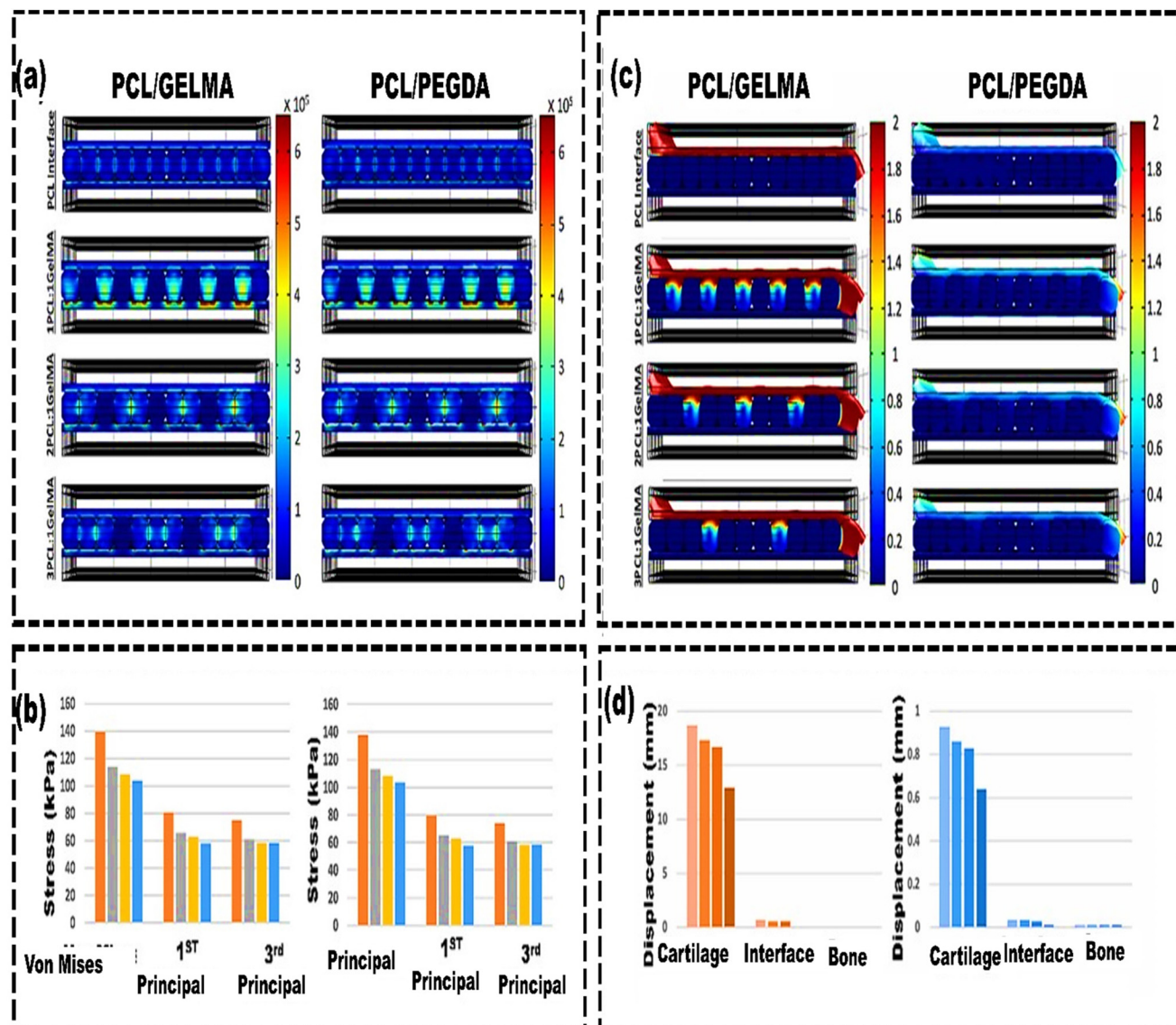


**Fig. 10** Stress and displacement distribution in various hydrogel scaffolds: (a) von Mises stress contours for PCL/GelMA and PCL/PEGDA interface scaffolds. Stress is uniform in PCL-only scaffolds. The greatest stress is at the ends of GelMA struts. (b) Comparing stresses in PCL/GelMA and PCL/PEGDA interface scaffolds. Scaffolds with mechanical interlocking patterns show higher interface stresses than PCL-only scaffolds. 1 PCL:1 GelMA and 1 PCL:1 PEGDA scaffolds have the highest von Mises and principal stresses among the four types. (c) Comparison of displacement contours: PCL/GelMA vs. PCL/PEGDA interface scaffolds. GelMA scaffolds with mechanical interlocking exhibit higher interface displacement than PEGDA, while PCL-only scaffolds show minimal displacement upon shear. (d) Comparing vertical displacement along the y-axis in the cartilage, interface, and bone layers of PCL/GelMA scaffolds. Mechanical interlocking patterns increase displacement compared to PCL-only scaffolds. 1 PCL:1 GelMA scaffolds show the highest displacements. PCL/GelMA scaffolds exhibit about ten times more displacement in cartilage and interface layers than PCL/PEGDA scaffolds, reproduced from Choe *et al.*<sup>282</sup> with permission from IOP Publishing Ltd, copyright (2022).

ture are focused on optimizing the properties of bioink, probably because 3D bioprinted constructs for tissue engineering depend on the behaviour of the bioink.<sup>285</sup> However, there are a few limitations that hinder accurate computational simulation. For example, simulations often assume conditions such as using cell-free bioinks and no interaction between the printing substrate and filaments in extrusion-based printing. These assumptions can lead to discrepancies between the simulated model and the actual 3D-printed construct.<sup>286</sup> Despite being in the early stages, utilizing computational modelling inte-

grated with experimental data could mitigate processing errors or facilitate real-time error management.

## 7. Machine learning to accelerate bioink development

Recent developments in bioprinting methods, biofabrication strategies, and innovations in materials and chemistries have significantly improved the replication of physiologically rele-

vant tissue structures.<sup>5</sup> This advancement facilitates incorporating multiple cell types and diverse material properties within a single structure. For bioprinting to succeed, an ideal bioink must enable efficient printing, preserve cell viability, and create an environment that supports cell proliferation and differentiation and mimics natural cellular behaviour after printing.<sup>287</sup> The material requirements for pre- and post-printing can be drastically different. Many bioinks demonstrate excellent pre-printing properties but have insufficient post-printing performance, mainly when providing the environment for effective cell and tissue development.<sup>288</sup> For example, structures printed with sodium alginate, Pluronic F-127, or gelatin demonstrate strong structural integrity and maintain high shape fidelity, creating filaments.<sup>289</sup> However, sodium alginate and Pluronic F-127 do not contain cell binding sites for attachment unless they undergo further modification. On the other hand, gelatin includes binding sites for cell attachment; however, it turns into a liquid solution at 37 °C. This requires a modification to transform it into a more stable, permanent form. In situations where post-printing crosslinking is needed for lasting shape stability and mechanical strength, highly crosslinked hydrogels can reduce oxygen and nutrient diffusion, compromising the survival of encapsulated cells. Traditional computational simulations are helpful in optimizing processes, reducing the need for extensive experiments, and lowering costs. However, they often rely on oversimplified assumptions, which may not fully represent the complexity of biological materials.<sup>290</sup> Additionally, modelling theories have limited utility because only a few can accurately predict material properties, and those that do are generally applicable only to single-component inks within a narrow concentration range.<sup>291</sup>

Analytical techniques such as machine learning, a subset of artificial intelligence, and multiple regression can be used to identify and predict the complex relationships among ink formulations, ink properties, and printability.<sup>292</sup> For example, Lee *et al.*<sup>293</sup> identified a 3D-printable bioink through machine learning. The first step was selecting suitable rheological characteristics of biomaterials and then modifying them through ink composition design. Multiple regression was utilized to confirm the machine learning results and predict printability according to the composition of collagen and fibrin in the bioink. Eqn (4) presents the prediction algorithm that facilitated achieving a high storage modulus ( $G'$ ) and low yield stress ( $\tau_y$ ) through multiple regression, resulting in a printable ink with high shape fidelity

$$\begin{aligned} NV = & a + bC - cH - dF + (C - e)(C - e)f \\ & + (C - e)(H - g)h - (H - g)(H - g)i \\ & + (C - e)(F - j)k - (H - g)(F - j)l \\ & + (F - j)(F - j)m \end{aligned} \quad (4)$$

where NV is the normalization value to obtain a high  $G'$  and low  $\tau_y$ ,  $C$  is the concentration of collagen,  $H$  is the concentration of HA, and  $F$  is the concentration of fibrin. The lower-

case letters ( $a$  to  $m$ ) are constants corresponding to the following values:  $a = 0.4290567362$ ,  $b = 0.0051813811$ ,  $c = 0.001484911$ ,  $d = 0.037698223$ ,  $e = 6.210563158$ ,  $f = 0.0018163108$ ,  $g = 1.1842105263$ ,  $h = 0.0013134514$ ,  $i = 0.00722503$ ,  $j = 4.3157894737$ ,  $k = 0.0004778907$ ,  $l = 0.006967951$ , and  $m = 0.0018847494$ . Overall, the produced bioink demonstrated high shape fidelity and good biocompatibility, allowing for the application and cultivation of various cells. Apart from this first study of using ML in bioprinting, there are many studies in the literature that depend significantly on the collection of large amounts of data to build a ML model.<sup>294</sup> To mitigate this issue of dependence on large data, Bayesian optimization (BO), a modern ML technique, is especially effective at adjusting the various printing process variables that require modification.<sup>295</sup> BO can build a black-box function model using fewer experimental data than other optimization methods. In contrast, methods like derivative-free local optimizers and genetic algorithms require a larger number of samples, which makes BO advantageous.<sup>296</sup> Amir Hashemi *et al.*<sup>297</sup> used ML to develop a chitosan–gelatin–agarose biomaterial ink. The optimized ink was evaluated for its printability, rheological properties, degradability, hydrophilicity, and biological response. The results suggested that a combination of 27% agarose, 53% chitosan, and 20% gelatin (ACG) might be the most suitable biomaterial ink for 3D extrusion bioprinting in terms of both printability and cell viability.

ML provides a systematic approach for identifying uncontrollable factors, improving the reliability of the bioprinting process, and optimizing biomaterials, bioinks, and process parameters. Various studies have shown the potential to customize bioprinted constructs and control their cell culture responses as expected.<sup>298</sup> However, the limited size and quality of datasets for ML pose significant challenges. The costly and labor-intensive nature of data collection means that only a small dataset of adequate quality is currently available for ML applications in bioprinting, particularly for material optimization and cell performance analysis.<sup>299</sup> Although ML is still in its infancy, integrating ML for biomaterial ink optimization provides significant advantages, making multi-component biomaterial ink potentially suitable for tissue engineering applications.<sup>300</sup>

## 8. Challenges and future outlook

3D bioprinting enables the accurate placement of cells and materials within constructs, making it well-suited for complex tissue engineering applications.<sup>61</sup> However, despite considerable advancements, several unresolved issues must be addressed before 3D-printed tissues and organs can be effectively used in clinical settings. Important considerations in 3D bioprinting include minimizing cell damage, developing optimal bioinks, ensuring the quality of 3D-printed constructs, hybrid bioprinting, and navigating various regulatory aspects. These factors highlight the necessity for further advancements in the field, which are discussed in detail below.

### 8.1. Printing-induced cell damage

The difficulty of accurately placing cells and constructing intricate structures needs to be resolved before the use of 3D bio-printed tissues in regenerative medicine.<sup>283</sup> To date, there is no single technique used to address this issue. For instance, extrusion-based 3D printing requires a small nozzle diameter to achieve maximum cell resolution. However, it significantly increases shear stress on the printed cells and reduces cell viability.<sup>301</sup> Although laser-based technology avoids the extrusion process and focuses on the 2D patterning of cells, its high cost and inability to construct complex 3D architectures have hindered its wider adoption. Similarly, the applications of droplet technologies to tissue creation are restricted to cartilage structures, fibro-cartilage interfaces, and bone tissues. High cell survivability and sub-100  $\mu\text{m}$  droplet widths are among the benefits of inkjet bioprinters.<sup>302</sup> Nevertheless, they also have drawbacks, such as clogging, restricted biopolymer compatibility, and very low cell density.

Although many studies have investigated DOD bioprinting, most have concentrated on the droplet formation process (printability) while giving minimal attention to the post-impact viability of the printed cells.<sup>58</sup> According to a study, shear stress during printing is not as harmful as droplet impact or substrate stiffness. There is still a need to fully understand how the droplet formation process affects the viability of cells after printing. The adverse effects of droplet impact on the substrate surface can be lessened by lowering the pressure in the printing chamber to 0.3 atm.<sup>267</sup> Under this reduced atmospheric pressure, the released droplet spreads gently on the substrate without causing any splashing.<sup>303</sup>

### 8.2 Bioink development

Advancements in bioprinting are restricted by the limited availability of suitable bioinks, which need to satisfy rigorous standards for both printability and biocompatible cross-linking methods.<sup>304</sup> The interaction between cells and their surrounding environment is vital for replicating cell–biomaterial dynamics. However, challenges such as inadequate tissue formation and limited cell–biomaterial connections remain significant concerns in bioprinted cell-encapsulated structures.<sup>305</sup> These polymeric materials do not adequately mimic the intricate structure of natural ECMs, which is crucial for directing tissue development and replicating important cell-to-cell interactions.<sup>306</sup> This review emphasized the importance of tissue specificity in preserving essential cellular functions and phenotypes by utilizing cells and ECMs derived from specific tissues and organs, providing detailed insights. While a dECM is a promising biomaterial, incomplete removal of cellular remnants can lead to potential pro-inflammatory responses.<sup>306</sup> One potential solution is to recreate the unique ECM niche by arranging specific biomaterials in designated regions. This approach focuses on developing a biomimetic microenvironment that better replicates the actual conditions required for specific cell types.<sup>307</sup> To measure its effectiveness, cytometry can be employed to analyze the physical and chemical

characteristics of the suspended cells, providing insights into their health within these bioinks. By evaluating cell viability (live/dead assay using propidium iodide and Calcein-AM),<sup>308</sup> apoptosis (by Annexin V and 7-AAD detection, prevalent in case of apoptosis),<sup>309</sup> proliferation (Ki-67 and BrdU in actively dividing cells)<sup>310</sup> differentiation before and after printing.<sup>311</sup> Cytometry can ensure that the cells within the bioink remain healthy, leading to more successful and reliable bio-printed tissues and organs. This technique enables researchers to optimize bioink formulations and refine printing processes, minimizing cell stress and death.<sup>312</sup> Cytometry also enables the development of tailored bioinks that meet the specific needs of different cell types, which is essential for creating complex, multicellular structures that closely mimic natural tissues. For instance, a 3D-printed annular ring-like scaffold was printed with a cellular mixture of human cardiac AC16 cardiomyocytes, fibroblasts, and microvascular endothelial cells.<sup>312</sup> Moreover, integrating cytometry into the bioprinting workflow enhances the consistency and reproducibility of bio-printed products, making it easier to scale up production and meet regulatory standards.<sup>308</sup> This is especially important for bioprinting to advance toward clinical applications, where maintaining cell health is critical for the functionality of bio-printed tissues.

### 8.3 3D bioprinted constructs

The absence of adequate vascularization in the designed structures is among the most pertinent concerns.<sup>313</sup> Cartilage, skin, and bladder grafts have been successfully employed in clinical practice because they can rely on the blood vessels of the host to meet their oxygen and nutrient requirements. However, vascularization takes a longer time for larger tissue grafts. The delay in delivering sufficient nutrients to cells within the large 3D scaffolds poses challenges in tissue engineering, as it leads to limitations in mass transport. This issue arises because of the restricted diffusion of oxygen and nutrients from the scaffold surface to deeper layers, which can result in cell death after a few hundred microns.<sup>314</sup> Hence, the huge 3D printed structures get damaged without a perfusable circulatory system, which restricts the dimensions of these constructs that are clinically relevant. Therefore, several techniques, such as the creation of a vascular network by using the sacrificial template approach, have been developed to combat these vascularization concerns. For instance, Tocchio *et al.*<sup>315</sup> proposed a flexible sacrificial molding technique for the creation of a robust vascular network in large, porous scaffolds. Highly resilient thermoplastic sacrificial templates made of poly(vinyl alcohol) were used to create these embedded fluidic systems. One major benefit of this technology is that it only requires filling the space surrounding the template and cross-linking the matrix to generate the vascularized scaffold. Another distinctive feature is the ability to create a perfusable matrix with regulated porosity and adjustable fluidic characteristics to create a scaffold that closely mimics the biological environment. Due to this, it may be possible to produce large-scale vascularized scaffolds, paving the way for a wide range of clinical uses.

Additionally, when trying to replicate a tissue or cellular and extracellular components of an organ very precisely, the resulting tissue construct often does not function exactly like the native tissues. Therefore, innovative design approaches may be necessary to prioritize both the function and fabrication efficiency of the construct. This could involve 3D-printed constructs that efficiently support tissue function, even if they do not precisely mimic the original size or shape of the tissue. For example, constructs like sheets or patches could assist in liver or pancreas function.<sup>316</sup> This method can significantly enhance biomanufacturing efficiency and decrease production expenses. However, it may require identifying suitable implantation sites, promoting connection with existing blood vessels, and ensuring sustained long-term integration and function. Likewise, utilizing automated designs in personalized biomanufacturing can regulate control mechanisms for predictable outcomes. 3D imaging and modelling software enable precise computational procedures, producing customized structures that align with the anatomy of a patient. This method assigns predefined hatching patterns, cell types, and materials to specific areas of the bioprinted structure using a 3D model derived from medical imaging (*e.g.*, CT or MRI).<sup>317</sup> A comprehensive understanding of biomaterial design, the successful integration of engineered tissue constructs with surrounding host tissue, and the biological processes involved in tissue healing and repair are crucial for meeting patient needs and advancing the clinical application of bioprinted product tissue engineering solutions.

#### 8.4 Need for hybrid bioprinting

Despite various reports on bioprinted cell-encapsulated constructs, the primary concerns still need to improve tissue formation and limited cell-biomaterial interactions.<sup>59</sup> Surface topography significantly affects cellular behaviour. Microscale features can impact cell shape and movement, while nanoscale textures can influence the differentiation and proliferation of stem cells.<sup>318</sup> When it comes to producing these nanoscale structures, which are essential for controlling cellular differentiation, the bioprinting method has its limitations. To overcome these limitations, hybrid systems that combine bioprinting and electrospinning can be employed to create complex constructs with detailed nanoscale structures while accurately depositing highly viable cells in designated areas.<sup>319</sup> For example, Graham *et al.*<sup>302</sup> presented a highly accurate cell printing technique with a 1 nL droplet resolution. High-resolution 3D constructs, including a branching cell junction, a slanted junction, and a bone–cartilage interface, were printed with a resolution smaller than 200  $\mu\text{m}$ . The printed constructs were cultured for a period of 35 days, demonstrating more than 90% cell viability. The study demonstrates that ovine mesenchymal stem cells can differentiate into cartilage cells and create cartilage-like structures rich in type II collagen, suggesting their promise for cartilage regeneration. Still, more improvement in scientific and technological platforms is needed to use 3D bioprinting in a hybrid manner with other printing techniques for fabricating bone, skin, liver, and carti-

lage constructs.<sup>320</sup> These technologies serve as reference points for assessing the current state of bioprinting with tissue-specific bioinks. Manufacturing speed is crucial for achieving large-scale tissue and organ fabrication. Combining microvalve and extrusion-based bioprinting methods enables precise drop-on-demand cell placement while continuously extruding hydrogel filaments, allowing for the creation of large, heterogeneous 3D cell-laden structures at high throughput.<sup>78</sup>

#### 8.5 Regulatory challenges

Despite the evolution of diverse manufacturing methods, the FDA currently evaluates conventionally manufactured products and 3D-printed healthcare devices using the same guidelines. However, some guidelines are specifically for 3D bioprinting, like the “21st Century Cures Act”.<sup>321</sup> This act outlines regenerative medicine treatments that could qualify for the “regenerative medicine advanced therapy (RMAT)” designation. These treatments include tissue-engineering products, human cells and tissue products, combined therapies or products, gene therapies, and cell therapies that permanently affect human cells and tissues, often through genetic changes.<sup>322</sup> Hence, to shape the future of tissue-specific bioink in 3D bioprinting, the FDA has provided extensive guidance to 3D printer manufacturers. Still, numerous regulatory challenges remain relevant for functional 3D-bioprinted constructs, including bioactive materials and living cells. For example, bioprinted constructs with living cells and bioactive materials pose unique regulatory challenges due to their intricate mechanisms and unknown long-term effects. Defining their potency is complex due to the multiple active components. Even minor manufacturing changes can lead to significant and unpredictable alterations in product characteristics. Hence, it is important to outline how existing laws and regulations governing device manufacturing will apply to emerging creators, like academic institutions and medical facilities producing personalized 3D-printed devices.<sup>323</sup> Apart from this, no established standards exist for 3D bioprinting technology, materials, or the overall process. While there are some guidelines for additive manufacturing technologies (ISO/DIS 17296-1)<sup>323</sup> and 3D printer manufacturers, there is a critical need for increased production guidelines and standardization for tissue specific bioink in 3D bioprinting.

Along with regulatory constraints, establishing standards for bioprinting materials like standardized cell-expansion basal media would streamline product development.<sup>324</sup> This standardization would also expedite clinical application and enable manufacturers to refine the processes for specific constructs, reducing the resource needs for base materials and technical processes. Logistics also become intricate when producing custom tissues or organs for individual patients. Patient-care facilities are unlikely to have 3D printing or the capacity for producing medical-grade materials. The existing cold storage, shipping methods, *etc.*, were designed many years ago and did not meet the precise requirements for transporting living biological products.<sup>325</sup> A novel logistic system

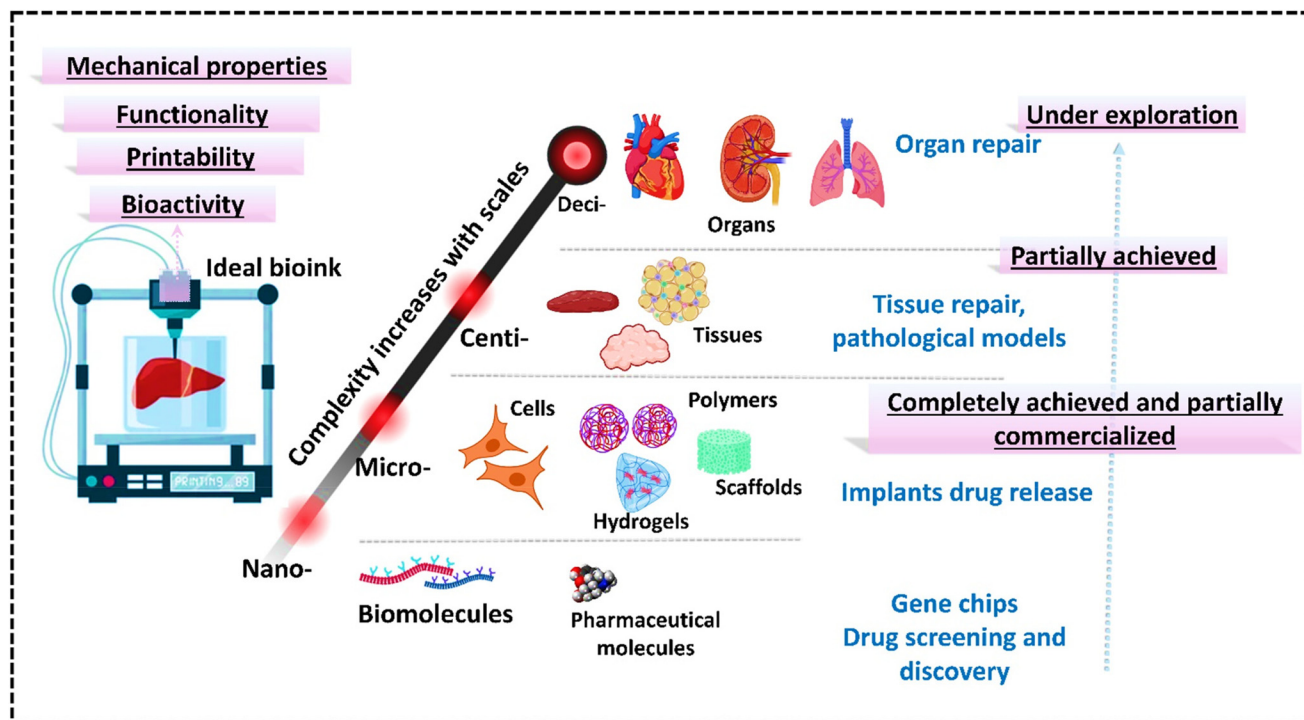


**Fig. 11** Properties of an ideal bioink and the roadmap for bioprinting. The items in the lower stages are components that contribute to the stages above them, and the complexity of assembly increases as the scale becomes larger. The right side shows typical bioprinting applications for each stage and their levels of completion, reproduced from Compaan *et al.*<sup>326</sup> with permission from American Chemical Society, copyright (2017).

that guarantees the necessary communication, data collection, stability, and documented compliance needs to be developed for emerging bioinks.

Overall, the roadmap of 3D bioprinting illustrates its hierarchical structure (Fig. 11).<sup>326</sup> It starts with nanoscale molecules and biomacromolecules, advances to microscale cell manipulation, and progresses to the assembly of centimeter-scale tissue pieces. Ultimately, these tissues can be combined into decimeter-scale organs designed to replicate the essential functions of natural organs for potential implantation.

## 9. Conclusion

Bioinks have attracted worldwide attention in tissue engineering because of their capability to create biomimetic, complex, and functional tissue constructs. This review explores existing and emerging bioinks and bioprinting methods. It covers up-to-date developments in fabricating tissue constructs that closely mimic native tissues, aiming to address the organ shortage crisis through advancements in 3D bioprinting. Polymeric materials are widely used as bioinks in 3D bioprinting due to their diverse properties, effectively supporting the printing process. However, these materials are insufficient for fully replicating the native ECM and biomimetic environment needed for optimal cell adhesion, proliferation, and differentiation. To enhance the performance of 3D bioprinting, the review emphasizes developing tissue-specific bioinks that

incorporate cues for bone, skin, cartilage, and liver tissue engineering. Furthermore, computational modeling can substantially reduce the time and cost of experimental trial-and-error optimizing a bioink formulation. The properties of bioink before, during, and after gelation are vital for its printability, affecting shape fidelity, structural resolution, and cell survival. By utilizing computational modeling, these properties can be effectively optimized. Machine learning is also documented as a method to enhance the reliability of the bioprinting process and to optimize biomaterials, bioinks, and process parameters. This review also discussed the complex challenges of utilizing 3D bioprinted tissues in regenerative medicine, particularly the critical issue of nutrient and oxygen diffusion, which can lead to cell death. It emphasizes the importance of developing vascular networks to improve nutrient delivery and the precision needed in placing cells within complex structures. Additionally, cytometry is recognized as an effective method for monitoring cell health in bioinks, decreasing cell mortality, and boosting the viability of bioprinted structures. Moreover, it discusses the regulatory hurdles associated with the multifaceted nature of bioprinted materials and the lack of established standards in the field. Therefore, with the rise of personalized medicine, it is necessary to develop bioinks that incorporate bioactive factors specific to each patient. Additionally, new regulatory frameworks may be necessary to address the challenges of bioprinting and other advanced medical products. 'Process-based' frameworks could be more beneficial than traditional 'product-based' approaches, as they

are better suited to handle product variability and customization. Hence, further research is required to overcome the current constraints of tissue-specific bioinks and develop personalized bioinks that can effectively support the growth, differentiation, and function of cells tailored to individual patients.

## Author contributions

All the authors listed have made a substantial, direct, and intellectual contribution to the work and approved its publication. More details on the specific contributions from each author are available in the ESI† under CRediT contributor roles.

## Data availability

No primary research results, software or code have been included and no new data were generated or analysed as part of this review.

## Conflicts of interest

The authors declare no conflicts of interest in the publication of this article.

## Acknowledgements

This work was supported by start-up research grants (SRG/2019/001504 and SRG/2021/000859) from the Science and Engineering Research Board (SERB), Department of Science and Technology (DST), Government of India. The authors acknowledge the support from Faculty Initiation Grant and International Centre for Sustainable and Net Zero Technologies, PDPM-IIITDM Jabalpur and teaching assistantship from Ministry of Education (MOE), Government of India. The authors would like to thank Prince Sultan University for their support.

## References

- Z. Xie, M. Gao, A. O. Lobo and T. J. Webster, *Polymers*, 2020, **12**, 1717.
- S. Vijayavenkataraman, *J. 3D Print. Med.*, 2023, **7**, 3DP8.
- B. Giri, S. Dey, T. Das, M. Sarkar, J. Banerjee and S. K. Dash, *Biomed. Pharmacother.*, 2018, **107**, 306–328.
- G. M. Abouna, *Transplant. Proc.*, 2008, **40**, 34–38.
- S. Tripathi, S. S. Mandal, S. Bauri and P. Maiti, *MedComm*, 2023, **4**, e194.
- P. Ramiah, L. C. du Toit, Y. E. Choonara, P. P. D. Kondiah and V. Pillay, *Front. Mater.*, 2020, **7**, 1–13.
- W. Fang, M. Yang, L. Wang, W. Li, M. Liu, Y. Jin, Y. Wang, R. Yang, Y. Wang, K. Zhang and Q. Fu, *Int. J. Bioprint.*, 2023, **9**, 759.
- J. Huang, J. Xiong, D. Wang, J. Zhang, L. Yang, S. Sun and Y. Liang, *Gels*, 2021, **7**, 144.
- N. Li, R. Guo and Z. J. Zhang, *Front. Bioeng. Biotechnol.*, 2021, **9**, 630488.
- M. Y. Kwon, C. Wang, J. H. Galarraga, E. Puré, L. Han and J. A. Burdick, *Biomaterials*, 2019, **222**, 119451.
- H. Wang, Y. Wang, C. Yuan, X. Xu, W. Zhou, Y. Huang, H. Lu, Y. Zheng, G. Luo, J. Shang and M. Sui, *npj Vaccines*, 2023, **8**, 169.
- K. Ceonzo, A. Gaynor, L. Shaffer, K. Kojima, C. A. Vacanti and G. L. Stahl, *Tissue Eng.*, 2006, **12**, 301–308.
- W. Park, G. Gao and D.-W. Cho, *Int. J. Mol. Sci.*, 2021, **22**, 7837.
- X. Zhang, X. Chen, H. Hong, R. Hu, J. Liu and C. Liu, *Bioact. Mater.*, 2022, **10**, 15–31.
- M. Zhe, X. Wu, P. Yu, J. Xu, M. Liu, G. Yang, Z. Xiang, F. Xing and U. Ritz, *Materials*, 2023, **16**, 3197.
- M. K. Kim, W. Jeong, S. Jeon and H. W. Kang, *Front. Bioeng. Biotechnol.*, 2023, **11**, DOI: [10.3389/fbioe.2023.1305023](https://doi.org/10.3389/fbioe.2023.1305023).
- S. Chae, Y.-J. Choi and D.-W. Cho, *Biofabrication*, 2022, **14**, 025013.
- J. Kim, *Bioengineering*, 2023, **10**, 457.
- J. Jia, D. J. Richards, S. Pollard, Y. Tan, J. Rodriguez, R. P. Visconti, T. C. Trusk, M. J. Yost, H. Yao, R. R. Markwald and Y. Mei, *Acta Biomater.*, 2014, **10**, 4323–4331.
- Y. Zhao, Y. Li, S. Mao, W. Sun and R. Yao, *Biofabrication*, 2015, **7**, 045002.
- Z. Xie, M. Gao, A. O. Lobo and T. J. Webster, *Polymers*, 2020, **12**, 1717.
- A. S. Theus, L. Ning, B. Hwang, C. Gil, S. Chen, A. Wombwell, R. Mehta and V. Serpooshan, *Polymers*, 2020, **12**, 1–19.
- Z. Wang, W. Kapadia, C. Li, F. Lin, R. F. Pereira, P. L. Granja, B. Sarmento and W. Cui, *J. Controlled Release*, 2021, **329**, 237–256.
- A. M. Shabbirahmed, R. Sekar, L. A. Gomez, M. R. Sekhar, S. P. Hiruthyaswamy, N. Basavegowda and P. Somu, *Biomimetics*, 2023, **8**, 16.
- J. R. Fuchs, B. A. Nasser and J. P. Vacanti, *Ann. Thorac. Surg.*, 2001, **72**, 577–591.
- S. J. Forbes and N. Rosenthal, *Nat. Med.*, 2014, **20**, 857–869.
- E. Jacques and E. J. Suuronen, *Clin. Transl. Sci.*, 2020, **13**, 440–450.
- M. Hospodiuk, M. Dey, D. Sosnoski and I. T. Ozbolat, *Biotechnol. Adv.*, 2017, **35**, 217–239.
- B. Ripley, D. Levin, T. Kelil, J. L. Hermsen, S. Kim, J. H. Maki and G. J. Wilson, *J. Magn. Reson. Imaging*, 2017, **45**, 635–645.
- J. Jose, A. Peter, K. Y. Thajudeen, M. Gomes Pereira, V. P. Athira, S. G. Bhat and H. Michel, *Results Eng.*, 2024, **22**, 102060.

- 31 J. Li, C. Wu, P. K. Chu and M. Gelinsky, *Mater. Sci. Eng., R*, 2020, **140**, 100543.
- 32 M. P. Sekar, H. Budharaju, A. Zennifer, S. Sethuraman, N. Vermeulen, D. Sundaramurthi and D. M. Kalaskar, *J. Tissue Eng.*, 2021, **12**, 204173142110276.
- 33 V. S. Telang, R. Pemmada, V. Thomas, S. Ramakrishna, P. Tandon and H. S. Nanda, *Curr. Opin. Biomed. Eng.*, 2021, **17**, 100264.
- 34 S. V. Murphy and A. Atala, *Nat. Biotechnol.*, 2014, **32**, 773–785.
- 35 A. Rossi, T. Pescara, A. M. Gambelli, F. Gaggia, A. Asthana, Q. Perrier, G. Basta, M. Moretti, N. Senin, F. Rossi, G. Orlando and R. Calafiore, *Front. Bioeng. Biotechnol.*, 2024, **12**, DOI: [10.3389/fbioe.2024.1393641](https://doi.org/10.3389/fbioe.2024.1393641).
- 36 N. Guan, Z. Liu, Y. Zhao, Q. Li and Y. Wang, *Drug Delivery*, 2020, **27**, 1438–1451.
- 37 M. A. A. Ansari, A. A. Golebiowska, M. Dash, P. Kumar, P. K. Jain, S. P. Nukavarapu, S. Ramakrishna and H. S. Nanda, *Biomater. Sci.*, 2022, **10**, 2789–2816.
- 38 M. Kuss and B. Duan, in *Biofabrication and 3D Tissue Modeling*, The Royal Society of Chemistry, 2019, pp. 22–48.
- 39 S. Boularaoui, G. Al Hussein, K. A. Khan, N. Christoforou and C. Stefanini, *Bioprinting*, 2020, **20**, e00093.
- 40 C. Q. Zhao, W. G. Liu, Z. Y. Xu, J. G. Li, T. T. Huang, Y. J. Lu, H. G. Huang and J. X. Lin, *Carbohydr. Polym.*, 2020, **236**, 116058.
- 41 H. S. Kim, S. G. Kumbar and S. P. Nukavarapu, *Curr. Opin. Biomed. Eng.*, 2021, **17**, 100260.
- 42 Y. J. Tan, X. Tan, W. Y. Yeong and S. B. Tor, *Sci. Rep.*, 2016, **6**, 1–13.
- 43 S. Xin, K. A. Deo, J. Dai, N. K. R. Pandian, D. Chimene, R. M. Moebius, A. Jain, A. Han, A. K. Gaharwar and D. L. Alge, *Sci. Adv.*, 2021, **7**, eabk3087.
- 44 X. Cui, J. Li, Y. Hartanto, M. Durham, J. Tang, H. Zhang, G. Hooper, K. Lim and T. Woodfield, *Adv. Healthcare Mater.*, 2020, **9**, 1901648.
- 45 P. Chansoria, R. Rizzo, D. Rüttsche, H. Liu, P. Delrot and M. Zenobi-Wong, *Chem. Rev.*, 2024, **124**, 8787–8822.
- 46 C. Bai, X. Yang, D. Hu, P. Jiang and X. Wang, in *Vat Photopolymerization Additive Manufacturing*, Elsevier, 2024, pp. 439–494.
- 47 Y. Li, X. Zhang, X. Zhang, Y. Zhang and D. Hou, *Polymers*, 2023, **15**, 3940.
- 48 J. Shao, Y. Liu, Y. Li, Y. Wang, R. Li, L. Yao, Y. Chen, Y. Fei, J. Wang and A. Zhao, *Mater. Today Commun.*, 2024, **40**, 109645.
- 49 C. E. Garciamendez-Mijares, F. J. Aguilar, P. Hernandez, X. Kuang, M. Gonzalez, V. Ortiz, R. A. Riesgo, D. S. R. Ruiz, V. A. M. Rivera, J. C. Rodriguez, F. L. Mestre, P. C. Castillo, A. Perez, L. M. Cruz, K. S. Lim and Y. S. Zhang, *Appl. Phys. Rev.*, 2024, **11**, DOI: [10.1063/5.0187558](https://doi.org/10.1063/5.0187558).
- 50 O. Guillaume, M. A. Geven, D. W. Grijpma, T. T. Tang, L. Qin, Y. X. Lai, H. Yuan, R. G. Richards and D. Eglin, *Polym. Adv. Technol.*, 2017, **28**, 1219–1225.
- 51 X. Ma, X. Qu, W. Zhu, Y.-S. Li, S. Yuan, H. Zhang, J. Liu, P. Wang, C. S. E. Lai, F. Zanella, G.-S. Feng, F. Sheikh, S. Chien and S. Chen, *Proc. Natl. Acad. Sci. U. S. A.*, 2016, **113**, 2206–2211.
- 52 U. Shaukat, E. Rossegger and S. Schlögl, *Polymers*, 2022, **14**, 2449.
- 53 W. L. Ng, J. M. Lee, M. Zhou, Y.-W. Chen, K.-X. A. Lee, W. Y. Yeong and Y.-F. Shen, *Biofabrication*, 2020, **12**, 022001.
- 54 V. Keriquel, H. Oliveira, M. Rémy, S. Ziane, S. Delmond, B. Rousseau, S. Rey, S. Catros, J. Amédée, F. Guillemot and J. C. Fricain, *Sci. Rep.*, 2017, **7**, 1–10.
- 55 V. Keriquel, H. Oliveira, M. Rémy, S. Ziane, S. Delmond, B. Rousseau, S. Rey, S. Catros, J. Amédée, F. Guillemot and J.-C. Fricain, *Sci. Rep.*, 2017, **7**, 1778.
- 56 M. Alonzo, S. AnilKumar, B. Roman, N. Tasnim and B. Joddar, *Transl. Res.*, 2019, **211**, 64–83.
- 57 T. Salih, M. Caputo and M. T. Ghorbel, *Biomolecules*, 2024, **14**, 861.
- 58 H.-Q. Xu, J.-C. Liu, Z.-Y. Zhang and C.-X. Xu, *Mil. Med. Res.*, 2022, **9**, 70.
- 59 G. Huang, Y. Zhao, D. Chen, L. Wei, Z. Hu, J. Li, X. Zhou, B. Yang and Z. Chen, *Biomater. Sci.*, 2024, **12**, 1425–1448.
- 60 L. Koch, M. Gruene, C. Unger and B. Chichkov, *Curr. Pharm. Biotechnol.*, 2013, **14**, 91–97.
- 61 D. Song, Y. Xu, S. Liu, L. Wen and X. Wang, *Polymers*, 2021, **13**, 1–32.
- 62 P. S. Gungor-Ozkerim, I. Inci, Y. S. Zhang, A. Khademhosseini and M. R. Dokmeci, *Biomater. Sci.*, 2018, **6**, 915–946.
- 63 A. Sorkio, L. Koch, L. Koivusalo, A. Deiwick, S. Miettinen, B. Chichkov and H. Skottman, *Biomaterials*, 2018, **171**, 57–71.
- 64 C. Dou, V. Perez, J. Qu, A. Tsin, B. Xu and J. Li, *ChemBioEng Rev.*, 2021, **8**, 517–534.
- 65 O. Kédan, D. Hakobyan, M. Rémy, S. Ziane, N. Dusserre, J. C. Fricain, S. Delmond, N. B. Thébaud and R. Devillard, *Biofabrication*, 2019, **11**, 045002.
- 66 D. Hakobyan, C. Médina, N. Dusserre, M. L. Stachowicz, C. Handschin, J. C. Fricain, J. Guillermet-Guibert and H. Oliveira, *Biofabrication*, 2020, **12**, 035001.
- 67 B. Guillotin, A. Souquet, S. Catros, M. Duocastella, B. Pippenger, S. Bellance, R. Bareille, M. Rémy, L. Bordenave, J. Amédée and F. Guillemot, *Biomaterials*, 2010, **31**, 7250–7256.
- 68 S. Michael, H. Sorg, C. T. Peck, L. Koch, A. Deiwick, B. Chichkov, P. M. Vogt and K. Reimers, *PLoS One*, 2013, **8**, e57741.
- 69 S. Catros, J. C. Fricain, B. Guillotin, B. Pippenger, R. Bareille, M. Remy, E. Lebraud, B. Desbat, J. Amédée and F. Guillemot, *Biofabrication*, 2011, **3**, 025001.
- 70 S. Ruiz-Alonso, I. Villate-Beitia, I. Gallego, M. Lafuente-Merchan, G. Puras, L. Saenz-del-Burgo and J. L. Pedraz, *Pharmaceutics*, 2021, **13**, 308.
- 71 X. Li, B. Liu, B. Pei, J. Chen, D. Zhou, J. Peng, X. Zhang, W. Jia and T. Xu, *Chem. Rev.*, 2020, **120**, 10793–10833.
- 72 W. L. Ng, H. Xi, V. Shkolnikov, G. L. Goh, R. Suntornnond and W. Y. Yeong, *Int. J. Bioprint.*, 2021, **8**, 424.

- 73 V. V. Nayak, V. Sanjairaj, R. K. Behera, J. E. Smay, N. Gupta, P. G. Coelho and L. Witek, *J. Biomed. Mater. Res., Part B*, 2024, **112**, e35402.
- 74 D. Kang, J. A. Park, W. Kim, S. Kim, H. Lee, W. Kim, J. Yoo and S. Jung, *Adv. Sci.*, 2021, **8**, 2004990.
- 75 W. L. Ng and V. Shkolnikov, *Int. J. Bioprint.*, 2024, 2135.
- 76 I. Angelopoulos, M. C. Allenby, M. Lim and M. Zamorano, *Biotechnol. Bioeng.*, 2020, **117**, 272–284.
- 77 W. L. Ng, X. Huang, V. Shkolnikov, G. L. Goh, R. Suntornnond and W. Y. Yeong, *Int. J. Bioprint.*, 2022, **8**, 1–17.
- 78 W. L. Ng, J. M. Lee, W. Y. Yeong and M. Win Naing, *Biomater. Sci.*, 2017, **5**, 632–647.
- 79 J. Dudman, A. M. Ferreira, P. Gentile, X. Wang and K. Dalgarno, *Cells*, 2021, **10**, 3329.
- 80 R. Nasehi, S. Aveic and H. Fischer, *Int. J. Bioprint.*, 2023, **9**, 743.
- 81 N. Okubo, A. J. Qureshi, K. Dalgarno, K. L. Goh and S. Derebail, *Bioprinting*, 2019, **13**, e00043.
- 82 H. Lee, S. H. Kim, J. S. Lee, Y. J. Lee, O. J. Lee, O. Ajiteru, M. T. Sultan, S. W. Lee and C. H. Park, *Adv. Healthcare Mater.*, 2023, **12**, 2202664.
- 83 L. Horváth, Y. Umehara, C. Jud, F. Blank, A. Petri-Fink and B. Rothen-Rutishauser, *Sci. Rep.*, 2015, **5**, 7974.
- 84 S. Rahmani Dabbagh, M. Rezapour Sarabi, M. T. Birtek, N. Mustafaoglu, Y. S. Zhang and S. Tasoglu, *Aggregate*, 2023, **4**, e197.
- 85 X. Zhu, Q. Xu, H. Li, M. Liu, Z. Li, K. Yang, J. Zhao, L. Qian, Z. Peng, G. Zhang, J. Yang, F. Wang, D. Li and H. Lan, *Adv. Mater.*, 2019, **31**, 1902479.
- 86 Z. Gu, J. Fu, H. Lin and Y. He, *Asian J. Pharm. Sci.*, 2020, **15**, 529–557.
- 87 J. He, B. Zhang, Z. Li, M. Mao, J. Li, K. Han and D. Li, *Biofabrication*, 2020, **12**, 042002.
- 88 T. G. Papaioannou, D. Manolesou, E. Dimakakos, G. Tsoucalas, M. Vavuranakis and D. Tousoulis, *Acta Cardiol. Sin.*, 2019, **35**, 284–289.
- 89 M. Kuzucu, G. Vera, M. Beaumont, S. Fischer, P. Wei, V. P. Shastri and A. Forget, *ACS Biomater. Sci. Eng.*, 2021, **7**, 2192–2197.
- 90 L. Gasperini, D. Maniglio, A. Motta and C. Migliaresi, *Tissue Eng., Part C*, 2015, **21**, 123–132.
- 91 Q. Gao, P. Zhao, R. Zhou, P. Wang, J. Fu and Y. He, *Bio-Des. Manuf.*, 2019, **2**, 1–9.
- 92 B. Brenken, E. Barocio, A. Favalaro, V. Kunc and R. B. Pipes, *Addit. Manuf.*, 2018, **21**, 1–16.
- 93 J. Vajda, M. Milojević, U. Maver and B. Vihar, *Biomedicines*, 2021, **9**, 1–27.
- 94 H. Liang, J. He, J. Chang, B. Zhang and D. Li, *Int. J. Bioprint.*, 2018, **4**, 1–8.
- 95 E. Altun, N. Ekren, S. E. Kuruca and O. Gunduz, *Mater. Lett.*, 2019, **234**, 163–167.
- 96 S. Vijayavenkataraman, S. Zhang, W. F. Lu and J. Y. H. Fuh, *J. Mater. Res.*, 2018, **33**, 1999–2011.
- 97 J. He, F. Xu, R. Dong, B. Guo and D. Li, *Biofabrication*, 2017, **9**, 015007.
- 98 Y. E. Choe and G. H. Kim, *Virtual Phys. Prototyp.*, 2020, **15**, 403–416.
- 99 Z. Qiu, H. Zhu, Y. Wang, A. Kasimu, D. Li and J. He, *Bio-Des. Manuf.*, 2023, **6**, 136–149.
- 100 N. Mkhize and H. Bhaskaran, *Small Sci.*, 2022, **2**, 2100073.
- 101 A. Reizabal, B. Tandon, S. Lanceros-Méndez and P. D. Dalton, *Small*, 2023, **19**, 2205255.
- 102 M. Mao, H. Liang, J. He, A. Kasimu, Y. Zhang, L. Wang, X. Li and D. Li, *Int. J. Bioprint.*, 1970, **7**, 362.
- 103 G. Gillispie, P. Prim, J. Copus, J. Fisher, A. G. Mikos, J. J. Yoo, A. Atala and S. J. Lee, *Biofabrication*, 2020, **12**, 022003.
- 104 M. Petretta, G. Desando, B. Grigolo and L. Roseti, *Materials*, 2021, **14**, 3528.
- 105 L. Tytgat, L. Van Damme, M. Ortega Arevalo, H. Declercq, H. Thienpont, H. Otteveare, P. Blondeel, P. Dubruel and S. Van Vlierberghe, *Int. J. Biol. Macromol.*, 2019, **140**, 929–938.
- 106 Y. Wang, X. Yuan, B. Yao, S. Zhu, P. Zhu and S. Huang, *Bioact. Mater.*, 2022, **17**, 178–194.
- 107 N. Khoshnood and A. Zamanian, *Bioprinting*, 2020, **19**, e00088.
- 108 S. Agarwal, S. Saha, V. K. Balla, A. Pal, A. Barui and S. Bodhak, *Front. Mech. Eng.*, 2020, **6**, 589171.
- 109 R. D. Ventura, *Med. Lasers*, 2021, **10**, 76–81.
- 110 M. Gruene, M. Pflaum, A. Deiwick, L. Koch, S. Schlie, C. Unger, M. Wilhelmi, A. Haverich and B. N. Chichkov, *Biofabrication*, 2011, **3**, 015005.
- 111 M. Gruene, M. Pflaum, C. Hess, S. Diamantouros, S. Schlie, A. Deiwick, L. Koch, M. Wilhelmi, S. Jockenhoewel, A. Haverich and B. Chichkov, *Tissue Eng., Part C*, 2011, **17**, 973–982.
- 112 R. Gaebel, N. Ma, J. Liu, J. Guan, L. Koch, C. Klopsch, M. Gruene, A. Toelk, W. Wang, P. Mark, F. Wang, B. Chichkov, W. Li and G. Steinhoff, *Biomaterials*, 2011, **32**, 9218–9230.
- 113 C. Cong, X. Li, W. Xiao, J. Li, M. Jin, S. H. Kim and P. Zhang, *Nanotechnol. Rev.*, 2022, **11**, 3305–3334.
- 114 Y. Wu, *Acta Biomater.*, 2021, **128**, 21–41.
- 115 S. H. Ahn, H. J. Lee and G. H. Kim, *Biomacromolecules*, 2011, **12**, 4256–4263.
- 116 T. Jungst, I. Pennings, M. Schmitz, A. J. W. P. Rosenberg, J. Groll and D. Gawlitta, *Adv. Funct. Mater.*, 2019, **29**, 1905987.
- 117 B. Kong, Y. Chen, R. Liu, X. Liu, C. Liu, Z. Shao, L. Xiong, X. Liu, W. Sun and S. Mi, *Nat. Commun.*, 2020, **11**, 1435.
- 118 J. L. Li, Y. L. Cai, Y. L. Guo, J. Y. H. Fuh, J. Sun, G. S. Hong, R. N. Lam, Y. S. Wong, W. Wang, B. Y. Tay and E. S. Thian, *J. Biomed. Mater. Res., Part B*, 2014, **102**, 651–658.
- 119 M. Mao, J. He, Z. Li, K. Han and D. Li, *Acta Biomater.*, 2020, **101**, 141–151.
- 120 Y. Liu, T. Huang, N. A. Yap, K. Lim and L. A. Ju, *Bioact. Mater.*, 2024, **42**, 328–344.
- 121 M. Abellan Lopez, L. Hutter, E. Pagin, M. Véliér, J. Véran, L. Giraud, C. Dumoulin, L. Arnaud, N. Macagno,

- R. Appay, L. Daniel, B. Guillet, L. Balasse, H. Caso, D. Casanova, B. Bertrand, F. Dignat, L. Hermant, H. Riesterer, F. Guillemot, F. Sabatier and J. Magalon, *Front. Bioeng. Biotechnol.*, 2023, **11**, 1217655.
- 122 S. A. Oluwole, W. D. Weldu, K. Jayaraman, K. A. Barnard and C. Agatemor, 2024Article number: 4c00537, *ACS Appl. Bio Mater.*, 2024, 4c00537, DOI: [10.1021/acsabm.4c00537](https://doi.org/10.1021/acsabm.4c00537).
- 123 R. Byrne, A. Carrico, M. Lettieri, A. K. Rajan, R. J. Forster and L. R. Cumba, *Mater. Today Bio*, 2024, **28**, 101185.
- 124 S. Naghieh and X. Chen, *J. Pharm. Anal.*, 2021, **11**, 564–579.
- 125 A. Schwab, R. Levato, M. D'Este, S. Piluso, D. Eglin and J. Malda, *Chem. Rev.*, 2020, **120**, 11028–11055.
- 126 W. L. Ng and V. Shkolnikov, *Bio-Des. Manuf.*, 2024, **7**, 771–799.
- 127 T. D. Ngo, A. Kashani, G. Imbalzano, K. T. Q. Nguyen and D. Hui, *Composites, Part B*, 2018, **143**, 172–196.
- 128 A. Habib, R. Sarah, S. Tuladhar, B. Khoda and S. M. Limon, *Bioprinting*, 2024, **38**, e00332.
- 129 J. Park and D. Kim, *Adv. Healthcare Mater.*, 2024, 2304496, DOI: [10.1002/adhm.202304496](https://doi.org/10.1002/adhm.202304496).
- 130 H. Liu, Y. Gong, K. Zhang, S. Ke, Y. Wang, J. Wang and H. Wang, *Gels*, 2023, **9**, 195.
- 131 D. Gogoi, M. Kumar and J. Singh, *Ann. 3D Print. Med.*, 2024, **15**, 100159.
- 132 W. Liu, M. A. Heinrich, Y. Zhou, A. Akpek, N. Hu, X. Liu, X. Guan, Z. Zhong, X. Jin, A. Khademhosseini and Y. S. Zhang, *Adv. Healthcare Mater.*, 2017, **6**, 1601451.
- 133 S. H. Moon, T. Y. Park, H. J. Cha and Y. J. Yang, *Mater. Today Bio*, 2024, **25**, 100973.
- 134 M. A. Habib and B. Khoda, *J. Manuf. Process.*, 2022, **76**, 708–718.
- 135 D. Venkata Krishna and M. Ravi Sankar, *Eng. Regen.*, 2022, **76**, 708–718.
- 136 X. B. Chen, A. Fazel Anvari-Yazdi, X. Duan, A. Zimmerling, R. Gharraei, N. K. Sharma, S. Sweilem and L. Ning, *Bioact. Mater.*, 2023, **28**, 511–536.
- 137 S. Tavakoli, N. Krishnan, H. Mokhtari, O. P. Oommen and O. P. Varghese, *Adv. Funct. Mater.*, 2024, **34**, 2307040.
- 138 X. Li, F. Zheng, X. Wang, X. Geng, S. Zhao, H. Liu, D. Dou, Y. Leng, L. Wang and Y. Fan, *Int. J. Bioprint.*, 2022, **9**, 649.
- 139 Z. Ahmad, S. Salman, S. A. Khan, A. Amin, Z. U. Rahman, Y. O. Al-Ghamdi, K. Akhtar, E. M. Bakhsh and S. B. Khan, *Gels*, 2022, **8**, 167.
- 140 K. K. Moncal, V. Ozbolat, P. Datta, D. N. Heo and I. T. Ozbolat, *J. Mater. Sci. Mater. Med.*, 2019, **30**, 55.
- 141 F. You, B. F. Eames and X. Chen, *Int. J. Mol. Sci.*, 2017, **18**, 1597.
- 142 M. Hovakimyan, R. F. Guthoff and O. Stachs, *J. Ophthalmol.*, 2012, **2012**, 1–12.
- 143 Y. Yu, K. K. Moncal, J. Li, W. Peng, I. Rivero, J. A. Martin and I. T. Ozbolat, *Sci. Rep.*, 2016, **6**, 28714.
- 144 R. Sridharan, A. R. Cameron, D. J. Kelly, C. J. Kearney and F. J. O'Brien, *Mater. Today*, 2015, **18**, 313–325.
- 145 G. H. McKinley and M. Renardy, *Phys. Fluids*, 2011, **23**, 127101.
- 146 B. Derby, *Annu. Rev. Mater. Res.*, 2010, **40**, 395–414.
- 147 T. C. de Goede, N. Laan, K. G. de Bruin and D. Bonn, *Langmuir*, 2018, **34**, 5163–5168.
- 148 J. Eggers and E. Villermaux, *Rep. Prog. Phys.*, 2008, **71**, 036601.
- 149 D. Jang, D. Kim and J. Moon, *Langmuir*, 2009, **25**, 2629–2635.
- 150 H. Wee, C. R. Anthony and O. A. Basaran, *Phys. Rev. Fluids.*, 2022, **7**, L112001.
- 151 A. Goswami and Y. Hardalupas, *J. Fluid Mech.*, 2023, **961**, A17.
- 152 Z. Lu, W. Gao, F. Liu, J. Cui, S. Feng, C. Liang, Y. Guo, Z. Wang, Z. Mao and B. Zhang, *Addit. Manuf.*, 2024, **94**, 104443.
- 153 S. K. Paral, D.-Z. Lin, Y.-L. Cheng, S.-C. Lin and J.-Y. Jeng, *Polymers*, 2023, **15**, 2716.
- 154 T. Aziz, F. Haq, A. Farid, L. Cheng, L. F. Chuah, A. Bokhari, M. Mubashir, D. Y. Y. Tang and P. L. Show, *Carbon Lett.*, 2024, **34**, 477–494.
- 155 R. H. Bean, G. Nayyar, M. K. Brown, J. Wen, Y. Fu, K. I. Winey, C. B. Williams and T. E. Long, *Addit. Manuf.*, 2024, **92**, 104391.
- 156 W. Li, L. S. Mille, J. A. Robledo, T. Uribe, V. Huerta and Y. S. Zhang, 2020Volume: 9Article number: 2000156, *Adv. Healthcare Mater.*, 2020, **9**, 2000156.
- 157 M. Shah, A. Ullah, K. Azher, A. U. Rehman, W. Juan, N. Aktürk, C. S. Tüfekci and M. U. Salamci, *RSC Adv.*, 2023, **13**, 1456–1496.
- 158 C. D. O'Connell, C. Onofrillo, S. Duchi, X. Li, Y. Zhang, P. Tian, L. Lu, A. Trengove, A. Quigley, S. Gambhir, A. Khansari, T. Mladenovska, A. O'Connor, C. Di Bella, P. F. Choong and G. G. Wallace, *Biofabrication*, 2019, **11**, 035003.
- 159 A. Machado, I. Pereira, F. Costa, A. Brandão, J. E. Pereira, A. C. Mauricio, J. D. Santos, I. Amaro, R. Falacho, R. Coelho, N. Cruz and M. Gama, *Clin. Oral Investig.*, 2023, **27**, 979–994.
- 160 A. Bernhardt, M. Wehrli, B. Paul, T. Hochmuth, M. Schumacher, K. Schütz and M. Gelinsky, *PLoS One*, 2015, **10**, e0129205.
- 161 M. Rizwan, S. W. Chan, P. A. Comeau, T. L. Willett and E. K. F. Yim, *Biomed. Mater.*, 2020, **15**, 065017.
- 162 E. Hodder, S. Duin, D. Kilian, T. Ahlfeld, J. Seidel, C. Nachtigall, P. Bush, D. Covill, M. Gelinsky and A. Lode, *J. Mater. Sci. Mater. Med.*, 2019, **30**, 10.
- 163 Y. Gu, A. Forget and V. P. Shastri, *Adv. Sci.*, 2022, **9**, 2103469.
- 164 M. Gomez-Florit, A. Pardo, R. M. A. Domingues, A. L. Graça, P. S. Babo, R. L. Reis and M. E. Gomes, *Molecules*, 2020, **25**, 5858.
- 165 E. O. Osidak, V. I. Kozhukhov, M. S. Osidak and S. P. Domogatsky, *Int. J. Bioprint.*, 2024, **6**, 270.
- 166 Y. S. Kim and F. Guilak, *Int. J. Mol. Sci.*, 2022, **23**, 8662.
- 167 I. Lukin, I. Erezuma, L. Maeso, J. Zarate, M. F. Desimone, T. H. Al-Tel, A. Dolatshahi-Pirouz and G. Orive, *Pharmaceutics*, 2022, **14**, 1–19.

- 168 A. Fatimi, O. V. Okoro, D. Podstawczyk, J. Siminska-Stanny and A. Shavandi, *Gels*, 2022, **8**, 179.
- 169 S. Vanaei, M. S. Parizi, S. Vanaei, F. Saleemizadehparizi and H. R. Vanaei, *Eng. Regen.*, 2021, **2**, 1–18.
- 170 C. I. Idumah, *Int. J. Polym. Mater. Polym. Biomater.*, 2024, 1–30.
- 171 T. Insperger and G. Stépán, *Appl. Math. Sci.*, 2011, **178**, 93–149.
- 172 F. Liu and X. Wang, *Polymers*, 2020, **12**, 1765.
- 173 M. Gharibshahian, M. Salehi, N. Beheshtizadeh, M. Kamalabadi-Farahani, A. Atashi, M.-S. Nourbakhsh and M. Alizadeh, *Front. Bioeng. Biotechnol.*, 2023, **11**, 1168504.
- 174 A. Schwab, R. Levato, M. D'Este, S. Piluso, D. Eglin and J. Malda, *Chem. Rev.*, 2020, **120**, 11028–11055.
- 175 A. L. Rutz, K. E. Hyland, A. E. Jakus, W. R. Burghardt and R. N. Shah, *Adv. Mater.*, 2015, **27**, 1607–1614.
- 176 B. A. G. de Melo, Y. A. Jodat, E. M. Cruz, J. C. Benincasa, S. R. Shin and M. A. Porcionatto, *Acta Biomater.*, 2020, **117**, 60–76.
- 177 H. Rastin, R. T. Ormsby, G. J. Atkins and D. Losic, *ACS Appl. Bio Mater.*, 2020, **3**, 1815–1826.
- 178 D. Petta, U. D'Amora, L. Ambrosio, D. W. Grijpma, D. Eglin and M. D'Este, *Biofabrication*, 2020, **12**, 032001.
- 179 C. B. Rodell, C. B. Highley, M. H. Chen, N. N. Dusaj, C. Wang, L. Han and J. A. Burdick, *Soft Matter*, 2016, **12**, 7839–7847.
- 180 L. Ouyang, C. B. Highley, C. B. Rodell, W. Sun and J. A. Burdick, *ACS Biomater. Sci. Eng.*, 2016, **2**, 1743–1751.
- 181 S. Hong, D. Sycks, H. F. Chan, S. Lin, G. P. Lopez, F. Guilak, K. W. Leong and X. Zhao, *Adv. Mater.*, 2015, **27**, 4035–4040.
- 182 N. K. Simha, C. S. Carlson and J. L. Lewis, *J. Mater. Sci. Mater. Med.*, 2004, **15**, 631–639.
- 183 G. Ying, N. Jiang, S. Maharjan, Y. Yin, R. Chai, X. Cao, J. Yang, A. K. Miri, S. Hassan and Y. S. Zhang, *Adv. Mater.*, 2018, **30**, 1805460.
- 184 B. Raphael, T. Khalil, V. L. Workman, A. Smith, C. P. Brown, C. Streuli, A. Saiani and M. Domingos, *Mater. Lett.*, 2017, **190**, 103–106.
- 185 K. Pataky, T. Braschler, A. Negro, P. Renaud, M. P. Lutolf and J. Brugger, *Adv. Mater.*, 2012, **24**, 391–396.
- 186 P. A. Amorim, M. A. d'Ávila, R. Anand, P. Moldenaers, P. Van Puyvelde and V. Bloemen, *Bioprinting*, 2021, **22**, e00129.
- 187 N. Cui, C.-Y. Dai, X. Mao, X. Lv, Y. Gu, E.-S. Lee, H.-B. Jiang and Y. Sun, *Gels*, 2022, **8**, 360.
- 188 M. Müller, J. Becher, M. Schnabelrauch and M. Zenobi-Wong, *Biofabrication*, 2015, **7**, 35006.
- 189 P. Ramiah, L. C. du Toit, Y. E. Choonara, P. P. D. Kondiah and V. Pillay, *Front. Mater.*, 2020, **7**, 00076.
- 190 B. S. Kim, H. Kim, G. Gao, J. Jang and D.-W. Cho, *Biofabrication*, 2017, **9**, 034104.
- 191 S. P. Tarassoli, Z. M. Jessop, A. Al-Sabah, N. Gao, S. Whitaker, S. Doak and I. S. Whitaker, *J. Plast. Reconstr. Aesthet. Surg.*, 2018, **71**, 615–623.
- 192 G. K. Menon and A. M. Kligman, *Skin Pharmacol. Physiol.*, 2009, **22**, 178–189.
- 193 N. Bhardwaj, D. Chouhan and B. B. Mandal, *Curr. Pharm. Des.*, 2017, **23**, 3455–3482.
- 194 F. P. W. Mamsen, C. H. Kiilerich, J. Hesselfeldt-Nielsen, I. Saltvig, C. L.-N. Remvig, H. Trøstrup and V.-J. Schmidt, *J. Pers. Med.*, 2022, **12**, 2067.
- 195 T. Hodgkinson and A. Bayat, *Arch. Dermatol. Res.*, 2011, **303**, 301–315.
- 196 M. Sheikholeslam, M. E. E. Wright, M. G. Jeschke and S. Amini-Nik, *Adv. Healthcare Mater.*, 2018, **7**, 1700897.
- 197 K. Vig, A. Chaudhari, S. Tripathi, S. Dixit, R. Sahu, S. Pillai, V. A. Dennis and S. R. Singh, *Int. J. Mol. Sci.*, 2017, **18**, 789.
- 198 B. S. Kim, Y. W. Kwon, J. S. Kong, G. T. Park, G. Gao, W. Han, M. B. Kim, H. Lee, J. H. Kim and D. W. Cho, *Biomaterials*, 2018, **168**, 38–53.
- 199 K.-S. Jang, S.-J. Park, J.-J. Choi, H.-N. Kim, K.-M. Shim, M.-J. Kim, I.-H. Jang, S.-W. Jin, S.-S. Kang, S.-E. Kim and S.-H. Moon, *Materials*, 2021, **14**, 5177.
- 200 S. J. Lee, J. H. Lee, J. Park, W. D. Kim and S. A. Park, *Materials*, 2020, **13**, 3522.
- 201 R. Ramakrishnan, N. Kasoju, R. Raju, R. Geevarghese, A. Gauthaman and A. Bhatt, *Carbohydr. Polym. Technol. Appl.*, 2022, **3**, 100184.
- 202 W. L. Ng, S. Wang, W. Y. Yeong and M. W. Naing, *Trends Biotechnol.*, 2016, **34**, 689–699.
- 203 R. D. Abbott and D. L. Kaplan, *Trends Biotechnol.*, 2015, **33**, 401–407.
- 204 J. Zhang, S. Yun, A. Karami, B. Jing, A. Zannettino, Y. Du and H. Zhang, *Bioprinting*, 2020, **19**, e00089.
- 205 S. J. Lee, J. H. Lee, J. Park, W. D. Kim and S. A. Park, *Materials*, 2020, **13**, 1–9.
- 206 S. van de Vijfeijken, T. Munker, R. Spijker, L. Karssemakers, W. Vandertop, A. Becking, D. Ubbink, A. Becking, L. Dubois, L. Karssemakers, D. Milstein, S. van de Vijfeijken, P. Depauw, F. Hoefnagels, W. Vandertop, C. Kleverlaan, T. Munker, T. Maal, E. Nout, M. Riool, and S. Zaat, *World Neurosurg.*, 2018, **117**, 443–452.
- 207 L. Vidal, C. Kamplaitner, M. Á. Brennan, A. Hoornaert and P. Layrolle, *Front. Bioeng. Biotechnol.*, 2020, **8**, 00061.
- 208 H. Qu, H. Fu, Z. Han and Y. Sun, *RSC Adv.*, 2019, **9**, 26252–26262.
- 209 B. Dalisson, B. Charbonnier, A. Aoude, M. Gilardino, E. Harvey, N. Makhoul and J. Barralet, *Acta Biomater.*, 2021, **136**, 37–55.
- 210 P. Baldwin, D. J. Li, D. A. Auston, H. S. Mir, R. S. Yoon and K. J. Koval, *J. Orthop. Traumatol.*, 2019, **33**, 203–213.
- 211 E. Capuana, F. Lopresti, F. Carfi Pavia, V. Brucato and V. La Carrubba, *Polymers*, 2021, **13**, 2041.
- 212 S. Anjum, F. Rahman, P. Pandey, D. K. Arya, M. Alam, P. S. Rajinikanth and Q. Ao, *Int. J. Mol. Sci.*, 2022, **23**, 9206.
- 213 D. Y. Kwon, J. Y. Park, B. Y. Lee and M. S. Kim, *Polymers*, 2020, **12**, 2210.
- 214 M. Kamaraj, G. Sreevani, G. Prabusankar and S. N. Rath, *Mater. Sci. Eng., C*, 2021, **131**, 112478.

- 215 C. Li and W. Cui, *Eng. Regen.*, 2021, **2**, 195–205.
- 216 Q. Yan, H. Dong, J. Su, J. Han, B. Song, Q. Wei and Y. Shi, *Engineering*, 2018, **4**, 729–742.
- 217 M. Nabiyouni, T. Brückner, H. Zhou, U. Gbureck and S. B. Bhaduri, *Acta Biomater.*, 2018, **66**, 23–43.
- 218 N. Dubey, J. A. Ferreira, J. Malda, S. B. Bhaduri and M. C. Bottino, *ACS Appl. Mater. Interfaces*, 2020, **12**, 23752–23763.
- 219 D. Chimene, L. Miller, L. M. Cross, M. K. Jaiswal, I. Singh and A. K. Gaharwar, *ACS Appl. Mater. Interfaces*, 2020, **12**, 15976–15988.
- 220 J. Lee, J. Hong, W. J. Kim and G. H. Kim, *Carbohydr. Polym.*, 2020, **250**, 116914.
- 221 W. Kim and G. Kim, *Biofabrication*, 2019, 0–31.
- 222 A. J. Sophia Fox, A. Bedi and S. A. Rodeo, *Sports Health*, 2009, **1**, 461–468.
- 223 T. Stampoultzis, P. Karami and D. P. Pioletti, *Curr. Res. Transl. Med.*, 2021, **69**, 103299.
- 224 X. Yang, Z. Lu, H. Wu, W. Li, L. Zheng and J. Zhao, *Mater. Sci. Eng., C*, 2018, **83**, 195–201.
- 225 C. Antich, J. de Vicente, G. Jiménez, C. Chocarro, E. Carrillo, E. Montañez, P. Gálvez-Martín and J. A. Marchal, *Acta Biomater.*, 2020, **106**, 114–123.
- 226 L. Roseti, C. Cavallo, G. Desando, V. Parisi, M. Petretta, I. Bartolotti and B. Grigolo, *Materials*, 2018, **11**, 1749.
- 227 Y. P. Singh, A. Bandyopadhyay and B. B. Mandal, *ACS Appl. Mater. Interfaces*, 2019, **11**, 33684–33696.
- 228 S. Rathan, L. Dejob, R. Schipani, B. Haffner, M. E. Möbius and D. J. Kelly, *Adv. Healthcare Mater.*, 2019, **8**, 1–11.
- 229 H. Kang, Y. Zeng and S. Varghese, *Acta Biomater.*, 2018, **78**, 365–377.
- 230 C. J. Little, N. K. Bawolin and X. Chen, *Tissue Eng., Part B*, 2011, **17**, 213–227.
- 231 V. K. A Devi, R. Shyam, A. Palaniappan, A. K. Jaiswal, T.-H. Oh and A. J. Nathanael, *Polymers*, 2021, **13**, 3782.
- 232 Z. Zhang and L. Schon, *Cartilage*, 2022, **13**, 194760352210930.
- 233 Y. Cen, G. Lou, J. Qi, M. Zheng and Y. Liu, *Cell Commun. Signaling*, 2023, **21**, 214.
- 234 Y.-M. Wang, K. Li, X.-G. Dou, H. Bai, X.-P. Zhao, X. Ma, L.-J. Li, Z.-S. Chen and Y.-C. Huang, in *Acute Exacerbation of Chronic Hepatitis B*, Springer Netherlands, Dordrecht, 2019, pp. 273–370.
- 235 P. A. Cortesi, S. Conti, L. Scalone, A. Jaffe, A. Ciaccio, S. Okolicsanyi, M. Rota, L. Fabris, M. Colledan, S. Fagioli, L. S. Belli, G. Cesana, M. Strazzabosco and L. G. Mantovani, *Liver Int.*, 2020, **40**, 2630–2642.
- 236 H. B. El-Serag, *Gastroenterology*, 2012, **142**, 1264–1273.
- 237 D. (Danielle) Huang, S. B. Gibeley, C. Xu, Y. Xiao, O. Celik, H. N. Ginsberg and K. W. Leong, *Adv. Funct. Mater.*, 2020, **30**, 1909553.
- 238 N. Badwei, *World J. Transplant.*, 2024, **14**, 96637.
- 239 Q. Wang, Y. Feng, A. Wang, Y. Hu, Y. Cao, J. Zheng, Y. Le and J. Liu, *iLIVER*, 2024, **3**, 100080.
- 240 C. Benwood, J. Chrenek, R. L. Kirsch, N. Z. Masri, H. Richards, K. Teetzen and S. M. Willerth, *Bioengineering*, 2021, **8**, 1–19.
- 241 H. Lee, W. Han, H. Kim, D. H. Ha, J. Jang, B. S. Kim and D. W. Cho, *Biomacromolecules*, 2017, **18**, 1229–1237.
- 242 F. Al-Hakim Khalak, F. García-Villén, S. Ruiz-Alonso, J. L. Pedraz and L. Saenz-del-Burgo, *Int. J. Mol. Sci.*, 2022, **23**, 12930.
- 243 M. K. Kim, W. Jeong and H.-W. Kang, *J. Funct. Biomater.*, 2023, **14**, 417.
- 244 M. K. Kim, W. Jeong, S. M. Lee, J. B. Kim, S. Jin and H. W. Kang, *Biofabrication*, 2020, **12**, 025003.
- 245 A. Abaci and M. Guvendiren, *Adv. Healthcare Mater.*, 2020, **9**, 2000734.
- 246 N. Ashammakhi, S. Ahadian, C. Xu, H. Montazerian, H. Ko, R. Nasiri, N. Barros and A. Khademhosseini, *Mater. Today Bio*, 2019, **1**, 100008.
- 247 R. El Assal, S. Guven, U. A. Gurkan, I. Gozen, H. Shafiee, S. Dalbeyler, N. Abdalla, G. Thomas, W. Fuld, B. M. W. Illigens, J. Estanislau, J. Khoory, R. Kaufman, C. Zylberberg, N. Lindeman, Q. Wen, I. Ghiran and U. Demirci, *Adv. Mater.*, 2014, **26**, 5815–5822.
- 248 Ö. Yildirim and A. Arslan-Yildiz, *Biomater. Sci.*, 2022, **10**, 6707–6717.
- 249 R. U. Hassan, S. M. Khalil, S. A. Khan, S. Ali, J. Moon, D.-H. Cho and D. Byun, *Polymers*, 2022, **14**, 4373.
- 250 A. Skardal, J. Aleman, S. Forsythe, S. Rajan, S. Murphy, M. Devarasetty, N. Pourhabibi Zarandi, G. Nzou, R. Wicks, H. Sadri-Ardekani, C. Bishop, S. Soker, A. Hall, T. Shupe and A. Atala, *Biofabrication*, 2020, **12**, 025017.
- 251 Y. Meng, J. Cao, Y. Chen, Y. Yu and L. Ye, *J. Mater. Chem. B*, 2020, **8**, 677–690.
- 252 N. Dubey, J. A. Ferreira, J. Malda, S. B. Bhaduri and M. C. Bottino, *ACS Appl. Mater. Interfaces*, 2020, **12**, 23752–23763.
- 253 C.-T. Huang, L. Kumar Shrestha, K. Ariga and S. Hsu, *J. Mater. Chem. B*, 2017, **5**, 8854–8864.
- 254 M. T. Poldervaart, H. Gremmels, K. van Deventer, J. O. Fledderus, F. C. Öner, M. C. Verhaar, W. J. A. Dhert and J. Alblas, *J. Controlled Release*, 2014, **184**, 58–66.
- 255 H. Kim, B. Kang, X. Cui, S. Lee, K. Lee, D. Cho, W. Hwang, T. B. F. Woodfield, K. S. Lim and J. Jang, *Adv. Funct. Mater.*, 2021, **31**, 2011252.
- 256 J. Zheng, Y. Liu, C. Hou, Z. Li, S. Yang, X. Liang, L. Zhou, J. Guo, J. Zhang and X. Huang, *Int. J. Bioprint.*, 2022, **8**, 597.
- 257 Q. Mao, Y. Wang, Y. Li, S. Juengpanich, W. Li, M. Chen, J. Yin, J. Fu and X. Cai, *Mater. Sci. Eng., C*, 2020, **109**, 110625.
- 258 X. Zhang, Y. Liu, C. Luo, C. Zhai, Z. Li, Y. Zhang, T. Yuan, S. Dong, J. Zhang and W. Fan, *Mater. Sci. Eng., C*, 2021, **118**, 111388.
- 259 D. Wang, Y. Guo, J. Zhu, F. Liu, Y. Xue, Y. Huang, B. Zhu, D. Wu, H. Pan, T. Gong, Y. Lu, Y. Yang and Z. Wang, *Acta Biomater.*, 2023, **165**, 86–101.
- 260 J. Hauptstein, T. Böck, M. Bartolf-Kopp, L. Forster, P. Stahlhut, A. Nadernezhad, G. Blahetek, A. Zerneckemadsen, R. Detsch, T. Jüngst, J. Groll, J. Teßmar and T. Blunk, *Adv. Healthcare Mater.*, 2020, **9**, 2000737.

- 261 X. Cui and T. Boland, *Biomaterials*, 2009, **30**, 6221–6227.
- 262 M. Nakamura, S. Iwanaga, C. Henmi, K. Arai and Y. Nishiyama, *Biofabrication*, 2010, **2**, 014110.
- 263 B. Duan, L. A. Hockaday, K. H. Kang and J. T. Butcher, *J. Biomed. Mater. Res., Part A*, 2013, **101A**, 1255–1264.
- 264 L. Koch, A. Deiwick, S. Schlie, S. Michael, M. Gruene, V. Cogger, D. Zychlinski, A. Schambach, K. Reimers, P. M. Vogt and B. Chichkov, *Biotechnol. Bioeng.*, 2012, **109**, 1855–1863.
- 265 S. Ramesh, O. L. A. Harrysson, P. K. Rao, A. Tamayol, D. R. Cormier, Y. Zhang and I. V. Rivero, *Bioprinting*, 2021, **21**, e00116.
- 266 J. Shi, B. Wu, S. Li, J. Song, B. Song and W. F. Lu, *Biomed. Phys. Eng. Express*, 2018, **4**, 045028.
- 267 P. He, Y. Liu and R. Qiao, *Microfluid. Nanofluid.*, 2015, **18**, 569–585.
- 268 K. H. K. Wong, J. M. Chan, R. D. Kamm and J. Tien, *Annu. Rev. Biomed. Eng.*, 2012, **14**, 205–230.
- 269 K. M. Kim, Y. J. Choi, J.-H. Hwang, A. R. Kim, H. J. Cho, E. S. Hwang, J. Y. Park, S.-H. Lee and J.-H. Hong, *PLoS One*, 2014, **9**, e92427.
- 270 Y. Koo and G. Kim, *Biofabrication*, 2016, **8**, 025010.
- 271 R. Levato, T. Jungst, R. G. Scheuring, T. Blunk, J. Groll and J. Malda, *Adv. Mater.*, 2020, **32**, 1906423.
- 272 C. Du, W. Huang and Y. Lei, *Int. J. Bioprint.*, 2023, **9**, 753.
- 273 M. Sreepadmanabh, A. B. Arun and T. Bhattacharjee, *Biophys. Rev.*, 2024, **5**, 021304.
- 274 K. Wang, Z. Wang, H. Hu and C. Gao, *Supramol. Mater.*, 2022, **1**, 100006.
- 275 T. Kamperman, S. Henke, C. W. Visser, M. Karperien and J. Leijten, *Small*, 2017, **13**, 1603711.
- 276 L. S. Moreira Teixeira, J. Feijen, C. A. van Blitterswijk, P. J. Dijkstra and M. Karperien, *Biomaterials*, 2012, **33**, 1281–1290.
- 277 X. Lin, X. Li and X. Lin, *Molecules*, 2020, **25**, 1375.
- 278 A. Neagu, *J. 3D Print. Med.*, 2017, **1**, 103–121.
- 279 R. Naranjo-Alcazar, S. Bendix, T. Groth and G. Gallego Ferrer, *Gels*, 2023, **9**, 230.
- 280 J. Sun, Y. Gong, M. Xu, H. Chen, H. Shao and R. Zhou, *Micromachines*, 2024, **15**, 463.
- 281 J. Göhl, K. Markstedt, A. Mark, K. Håkansson, P. Gatenholm and F. Edelvik, *Biofabrication*, 2018, **10**, 034105.
- 282 R. Choe, E. Devoy, B. Kuzemchak, M. Sherry, E. Jabari, J. D. Packer and J. P. Fisher, *Biofabrication*, 2022, **14**, 025015.
- 283 A. Blaeser, D. F. Duarte Campos, U. Puster, W. Richtering, M. M. Stevens and H. Fischer, *Adv. Healthcare Mater.*, 2016, **5**, 326–333.
- 284 J. C. Gómez-Blanco, E. Mancha-Sánchez, A. C. Marcos, M. Matamoros, A. Díaz-Parralejo and J. B. Pagador, *Processes*, 2020, **8**, 865.
- 285 M. Nooranidoost, D. Izbassarov, S. Tasoglu and M. Muradoglu, *Phys. Fluids*, 2019, **31**, 081901.
- 286 J. C. Gómez-Blanco, J. B. Pagador, V. P. Galván-Chacón, L. F. Sánchez-Peralta, M. Matamoros, A. Marcos and F. M. Sánchez-Margallo, *Int. J. Bioprint.*, 2023, **9**, 730.
- 287 G. Decante, J. B. Costa, J. Silva-Correia, M. N. Collins, R. L. Reis and J. M. Oliveira, *Biofabrication*, 2021, **13**, 032001.
- 288 J. Karvinen and M. Kellomäki, *Bioprinting*, 2023, **32**, e00274.
- 289 T. A. Mappa, C.-M. Liu, C.-C. Tseng, M. Ruslin, J.-H. Cheng, W.-C. Lan, B.-H. Huang, Y.-C. Cho, C.-C. Hsieh, H.-H. Kuo, C.-H. Tsou and Y.-K. Shen, *Polymers*, 2023, **15**, 3223.
- 290 S. Freeman, S. Calabro, R. Williams, S. Jin and K. Ye, *Front. Bioeng. Biotechnol.*, 2022, **10**, DOI: [10.3389/fbioe.2022.913579](https://doi.org/10.3389/fbioe.2022.913579).
- 291 C. Bailey, S. Stoyanov, H. Lu, T. Tilford, C. Yin and N. Strusevich, in *Nanopackaging*, Springer International Publishing, Cham, 2018, pp. 45–82.
- 292 C. Yu and J. Jiang, *Int. J. Bioprint.*, 2020, **6**, 253.
- 293 J. Lee, S. J. Oh, S. H. An, W.-D. Kim and S.-H. Kim, *Biofabrication*, 2020, **12**, 035018.
- 294 S. Tian, R. Stevens, B. McInnes and N. Lewinski, *Micromachines*, 2021, **12**, 780.
- 295 H. Zhang and S. K. Moon, *ACS Appl. Mater. Interfaces*, 2021, **13**, 53323–53345.
- 296 P. I. Frazier and J. Wang, 2016, *Bayesian Optimization for Materials Design*, pp. 45–75.
- 297 A. Hashemi, M. Ezati, I. Zumberg, T. Vicar, L. Chmelikova, V. Cmiel and V. Provaznik, *Mater. Today Commun.*, 2024, **40**, 109777.
- 298 J. Sun, K. Yao, J. An, L. Jing, K. Huang and D. Huang, *Int. J. Bioprint.*, 2024, **9**, 717.
- 299 L. Jin, X. Zhai, K. Wang, K. Zhang, D. Wu, A. Nazir, J. Jiang and W.-H. Liao, *Mater. Des.*, 2024, **244**, 113086.
- 300 K. S. Kaswan, J. S. Dhatwal, R. Batra, B. Balusamy and E. Gangadevi, in *Computational Intelligence in Bioprinting*, Wiley, 2024, pp. 303–321.
- 301 R. Chang, J. Nam and W. Sun, *Tissue Eng., Part A*, 2008, **14**, 41–48.
- 302 A. D. Graham, S. N. Olof, M. J. Burke, J. P. K. Armstrong, E. A. Mikhailova, J. G. Nicholson, S. J. Box, F. G. Szele, A. W. Perriman and H. Bayley, *Sci. Rep.*, 2017, **7**, 7004.
- 303 Y. Yonemoto, K. Tashiro, K. Shimizu and T. Kunugi, *Sci. Rep.*, 2022, **12**, 5093.
- 304 J. Adhikari, A. Roy, A. Das, M. Ghosh, S. Thomas, A. Sinha, J. Kim and P. Saha, *Macromol. Biosci.*, 2021, **21**, e2000179.
- 305 H. Mao, L. Yang, H. Zhu, L. Wu, P. Ji, J. Yang and Z. Gu, *Prog. Nat. Sci.: Mater. Int.*, 2020, **30**, 618–634.
- 306 Z. Chen, C. Du, S. Liu, J. Liu, Y. Yang, L. Dong, W. Zhao, W. Huang and Y. Lei, *Giant*, 2024, **19**, 100323.
- 307 A. A. Golebiowska, J. T. Intravaia, V. M. Sathe, S. G. Kumbar and S. P. Nukavarapu, *Bioact. Mater.*, 2024, **32**, 98–123.
- 308 D. E. Godar, C. Gurunathan and I. Ilev, *Photochem. Photobiol.*, 2019, **95**, 581–586.
- 309 M. de Villiers and L. H. Du Plessis, *Biomed. Mater.*, 2023, **18**, 045031.

- 310 X. Sun and P. D. Kaufman, *Chromosoma*, 2018, **127**, 175–186.
- 311 B. Parisi, M. Sünnen, R. Chippalkatti and D. K. Abankwa, *STAR Protoc.*, 2023, **4**, 102637.
- 312 M. Alonzo, R. El Khoury, N. Nagiah, V. Thakur, M. Chattopadhyay and B. Joddar, *ACS Appl. Mater. Interfaces*, 2022, **14**, 21800–21813.
- 313 K. Zheng, M. Chai, B. Luo, K. Cheng, Z. Wang, N. Li and X. Shi, *Smart Mater. Med.*, 2024, **5**, 183–195.
- 314 D. P. Forrestal, T. J. Klein and M. A. Woodruff, *Biotechnol. Bioeng.*, 2017, **114**, 1129–1139.
- 315 A. Tocchio, M. Tamplenizza, F. Martello, I. Gerges, E. Rossi, S. Argentiore, S. Rodighiero, W. Zhao, P. Milani and C. Lenardi, *Biomaterials*, 2015, **45**, 124–131.
- 316 Y. Kim, Y. W. Kim, S. B. Lee, K. Kang, S. Yoon, D. Choi, S.-H. Park and J. Jeong, *Biomaterials*, 2021, **274**, 120899.
- 317 C. Kengla, E. Renteria, C. Wivell, A. Atala, J. J. Yoo and S. J. Lee, *3D Print. Addit. Manuf.*, 2017, **4**, 239–247.
- 318 L. Xiao, Y. Sun, L. Liao and X. Su, *J. Mater. Chem. B*, 2023, **11**, 2550–2567.
- 319 K. Loukelis, Z. A. Helal, A. G. Mikos and M. Chatzinikolaidou, *Gels*, 2023, **9**, 103.
- 320 S. V. Murphy, P. De Coppi and A. Atala, *Nat. Biomed. Eng.*, 2019, **4**, 370–380.
- 321 S. Bonamici, *H.R.34–21st Century Cures Act*, 2016.
- 322 V. Mansouri, N. Beheshtizadeh, M. Gharibshahian, L. Sabouri, M. Varzandeh and N. Rezaei, *Biomed. Pharmacother.*, 2021, **141**, 111875.
- 323 Guidance for Industry and Food and Drug Administration Staff, Technical Considerations for Additive Manufactured Medical Devices.
- 324 J. G. Hunsberger, S. Goel, J. Allickson and A. Atala, *Curr. Stem Cell Rep.*, 2017, **3**, 77–82.
- 325 R. Genç, *Tohoku J. Exp. Med.*, 2008, **216**, 287–296.
- 326 A. M. Compaan, K. Christensen and Y. Huang, *ACS Biomater. Sci. Eng.*, 2017, **3**, 1519–1526.